12-2014

Cellular-based Brain Pathology in the Anterior Cingulate Cortex of Males with Autism Spectrum Disorder

Jessica D. Crawford
East Tennessee State University

Cellular-based Brain Pathology in the Anterior Cingulate Cortex of Males with Autism Spectrum Disorder

---

A dissertation

presented to

the faculty of the Department of Biomedical Sciences

East Tennessee State University

In partial fulfillment

of the requirements for the degree

Doctor of Philosophy in Biomedical Sciences

---

by

Jessica D. Crawford

December 2014

Gregory A. Ordway, Ph.D., Chair

Scott Champney, Ph.D.

Donald Hoover, Ph.D.

Michael Kruppa, Ph.D.

Meng-Yang Zhu, Ph.D.

Keywords: autism spectrum disorder, laser capture microdissection, postmortem brain tissue

ABSTRACT

Cellular-based Brain Pathology in the Anterior Cingulate Cortex of Males with Autism Spectrum Disorder

by

Jessica D. Crawford

Autism spectrum disorder (ASD) now affects 1 in 68 children in the United States. Disorders within this spectrum share hallmark deficits in verbal and nonverbal communication, repetitive behavior, and social interaction. The cause of ASD is still unknown. Even though hundreds of genetic abnormalities have been identified in ASD, these markers account for less than 1% of all ASD cases. Researchers continue to search for pathological markers common to all or most cases of ASD. The research presented in this dissertation used a novel combination of state-of-the-art methods to investigate brain pathology in ASD. Postmortem anterior cingulate cortex (ACC) from ASD and typically developing brain donors was obtained from 2 national brain banks. The ACC was chosen for study because of its documented role in influencing behaviors characteristically disrupted in ASD. An initial study revealed elevated glial fibrillary acidic protein (GFAP) in ACC white matter from ASD brain donors compared to typically developing control donors. Laser capture microdissection was then employed to isolate specific cell populations from the ACC from ASD and control brain donors. Captured cells were used to interrogate potential gene expression abnormalities that may underlie biological mechanisms that contribute behavioral abnormalities of ASD. The expression of 4 genes associated with synaptic function, *NTRK2*, *GRM8*, *SLC1A1*, and *GRIP1*, were found to be significantly lower in ACC pyramidal neurons from ASD donors when

compared to control donors. These expression abnormalities were not observed in ACC glia. Given robust evidence of neuronal and glial pathology in the ACC in ASD, a novel method for whole transcriptome analysis in single cell populations was developed to permit an unbiased analysis of brain cellular pathology in ASD. A list of genes that were differentially expressed, comparing ASD to control donors, was produced for both white matter and pyramidal neuron samples. By examining the ASD brain at the level of its most basic component, the cell, methods were developed that should allow future research to identify common cellular-based pathology of the ASD brain. Such research will increase the likelihood of future development of novel pharmacotherapy for ASD patients.

TABLE OF CONTENTS

Page

LIST OF TABLES

Table Page

LIST OF FIGURES

Figure Page

CHAPTER 1

INTRODUCTION

Autism Spectrum Disorder

Autism spectrum disorder (ASD) is a collection of development disorders that affect social interaction, verbal and nonverbal communication, and repetitive behaviors. Based on new diagnostic guidelines released in the Diagnostic and Statistical Manual of Mental Disorders V (DSM-V) (American Psychiatric Association, 2013), the spectrum now includes autistic disorder, pervasive developmental disorder not otherwise specified (PDD-NOS), and Asperger's syndrome. The world prevalence of ASD is 1% (Kim et al., 2011). Children with ASD can be found in countries throughout the world, but the greatest number of affected individuals occurs in the United States. There has been a 78% increase in the number of ASD cases since 2002. The disorder now affects 1 in 68 in the United States with a male to female ratio of 5:1 (Baio, 2014). A more age-targeted report from the Centers for Disease Control (CDC) found that as many as 1 in 50 school-age children in the United States could be affected (Blumberg et al., 2013).

With the worldwide increase in the number of cases per year, many countries including the United States and France have designated this disorder as a national concern and in response have increased funds for services and research. Currently ASD is costing the United States $250 billion per year (Buescher, Cidav, Knapp, & Mandell, 2014). Despite the increase in awareness and efforts to impede the rise in this disorder, the social burden will only grow in the coming years. In the next 10 years it is

projected that the cost for the United States could reach $400 billion per year (Buescher et al., 2014). In additional to the cost associated with caring for any child, families of ASD individuals will spend an addition $35,000 per year for care and services (Horlin, Falkmer, Parsons, Albrecht, & Falkmer, 2014). This cost typically increases after age 18 when school-related services end. The root of cost stems from the nature of the disorder. ASD is diagnosed very early in life and is a life-long disorder. It does not change the life expectancy of individuals meaning that services are need for 60 plus years. Other comorbidities, especially intellectual disabilities, only add to the cost and amount of services needed for the individual. The fact that no effective treatments exist to prevent, slow the progress, or cure this disorder increases the urgency for understanding the pathobiological development and progression of this disease.

Diagnostic Methods

Due to the nature of a spectrum disorder, the presentation of signs and symptoms is extremely heterogeneous throughout the population. Researchers and clinicians believe that the broad variability in ASD presentation might shed light on the etiology of the disorder, which has yet to be discovered. However, the lack of information about the pathophysiology of ASD translates to a purely behavioral diagnosis. The most common diagnostic technique employs a standardized assessment called the Autism Diagnostic Interview Revised (ADI-R) (Le Couteur, Haden, Hammal, & McConachie, 2008). Children are generally diagnosed around 18 months to 2 years of age. Due to a push for early intervention, emerging diagnostic tests have allowed for a diagnosis to be made prior to a child's second birthday based

on review of home videos and parental reporting (Adrien et al., 1991, 1992; Baranek, 1999; Maestro, Casella, Milone, Muratori, & Palacio-Espasa, 1999; Mars, Mauk, & Dowrick, 1998; Massie, 1978; Osterling & Dawson, 1994; Rosenthal, Massie, & Wulff, 1980; Werner, Dawson, Osterling, & Dinno, 2000; Zakian, Malvy, Desombre, Roux, & Lenoir, 2000; Zwaigenbaum et al., 2005). Early intervention is one of the top concerns for clinicians. It is a well-accepted theory that the earlier behavioral therapy and intervention can take place in a patient's life, the better the overall prognosis will be for that individual. Individuals are more likely to live independently and be employed as adults. In addition to a better outcome, the cost of lifetime care and services can be reduced by as much as two thirds if intervention is started early (Buescher et al., 2014).

Current Treatments

Current treatment paradigms include drugs that offer symptomatic relief paired with behavioral modification therapy. Currently there are only two drugs that have been approved by the Food and Drug Administration (FDA) for the treatment of behaviors associated with ASD. These drugs are the atypical antipsychotics risperidone and aripiprazole, which are approved to treat irritability in 6-17 year old children with ASD (Blankenship, Erickson, Stigler, Posey, & McDougle, 2010; Kirino, 2012; Wink, Erickson, & McDougle, 2010). Despite the wide use of these drugs in the ASD patient population, they are not targeted at the core symptoms of ASD. Many drugs, including antidepressants and anticonvulsants, are prescribed for "off-label" use in hopes of managing other aspects of the disease such as hyperactive and self-harming behaviors or common comorbidities (Lofthouse, Hendren, Hurt, Arnold, & Butter, 2012).

Despite the emphasis on the core behavioral deficits, physiological symptoms are also present. ASD patients display symptoms ranging from seizures to gastrointestinal abnormalities (Kral, Eriksen, Souders, & Pinto-Martin, 2013; Robinson, 2012). Due to the lack of treatment options available, many parents have turned to alternative medicines and treatments such as dietary restriction or various vitamin regimens in hopes of alleviating symptoms (Levenson, 2013; Lofthouse et al., 2012). One of the most popular of these treatments remains the gluten-free, casein-free diet (Whiteley et al., 2012). The popularity of this treatment still holds despite reports that it has no effect of the symptoms of ASD (Marí-Bauset, Zazpe, Mari-Sanchis, Llopis-González, & Morales-Suárez-Varela, 2014). Because reasonable treatment options are not available to significantly enhance outcomes, reverse the disease, or arrest its progress, parents and clinicians are turning to treatment options that do little to improve the quality of life for these patients. Sadly, these nonevidence based and alternative treatments increase the cost of the disorder in the face of little benefit to the ASD patient.

Etiology of ASD

As discussed above, there are no effective treatments for ASD mainly due to the lack of an identifiable cause. The increase in research over the last decade has produced many clues to guide researchers. As with any spectrum disorder, it could be hypothesized that the heterogeneity of symptom presentation could represent different underlying causes. For ASD these causes can be divided into three categories. There are a percentage of ASD cases that can be linked to other neurological disorders such

as tuberous sclerosis (Barton & Volkmar, 1998; Wassink, Brzustowicz, Bartlett, & Szatmari, 2004). Chromosomal abnormalities can also account for a small percentage of ASD cases (Bruining et al., 2014; Devlin & Scherer, 2012; Konstantareas & Homatidis, 1999; Liao et al., 2013). However, these associations with ASD only account for about 10% of the population of ASD patients. The remaining 90% of cases, which are categorized as idiopathic autism, have an unknown origin. A variety of factors including environmental exposures and genetic abnormalities have been linked to idiopathic autism (Blake, Hoyme, & Crotwell, 2013).

Role of Genetics

A vast amount of the current research in ASD is based on patient genetics. Research on the genetics of ASD has identified over 100 mutations thought to contribute to the development of ASD (Betancur, 2011). These mutations include chromosomal alterations, copy number variations, and single gene mutations. Some of the major mutated genes of interest that are worth noting are *PTEN*, the *SHANK* family, and the *NLGN* family. The majority of these genes are neurological based with a great number of them encoding synapse-related proteins. Some of these known gene and chromosomal mutations also play a role in other neuropsychiatric and autism-related disorders where the genetic based etiology of the disease is more certain, such as Fragile X and Angelmann syndromes. A unifying genetic or biochemical basis of ASD might be hard to elucidate due to the prevalence of comorbidities in ASD patients. In this patient population 70% of individuals have at least one other diagnosed psychiatric disorder with over 40% have two or more comorbid disorders (Simonoff et al., 2008).

The identification and treatment of these other disorders are so essential that diagnostic tools have been developed to screen for these psychiatric disorders with the presence of ASD behavioral symptoms (Leyfer et al., 2006; Leyfer, Tager-Flusberg, Dowd, Tomblin, & Folstein, 2008).

Regardless of the complexity of the disorder, there is little doubt that genetics play a role in the etiology of autism, but there is equal evidence to show that genetics is not the only factor. The strongest evidence comes from twin studies of autism concordance. Twin studies show that genes play some role in the development of the disease but are not the only factors at work. The prevalence of ASD among monozygotic twins is 35% to 90% (Ronald & Hoekstra, 2011). However, as a spectrum disorder symptoms are highly variable even between monozygotic twins resulting in differential placement on the ASD spectrum. These findings suggest that environmental factors affect underlying genetic variation to promote ASD onset.

One of the most recent twin studies was performed on a population in California in 2011. Based of the findings of this study, gene mutations are likely to account for roughly 55% of the cases of autism (Hallmayer et al., 2011). This is much lower than previously reported rates. There are several possible reasons for the outcome of this study. One is the inclusion of a boarder population of twins that represented a variety of socioeconomic groups. Most previous twin studies were on smaller, more homogenous populations. Another reason affecting the lower gene contribution to ASD risk could be related to changes in diagnostic criteria over time. By 2011 the DSM IV was using the spectrum-based diagnostic criteria. Moving forward with the newest diagnostic criteria release in the DSM V, this study best describes the current population of ASD patients.

However, with only half of the cases of idiopathic ASD accounted for, researchers must look to other factors to fully understand this group of disorders.

Environmental Factors

An increase in the human ingestion of synthetic chemicals and compounds has paralleled the increase in ASD rates. Both pregnant women and children are being exposed to these chemicals on a daily basis and strikingly only a small percentage have been researched to determine what potential harmful effects could be produced in susceptible populations. Because gene mutations only account for some of the cases of ASD, researchers are also interested in the role of environmental factors in the pathology of ASD. These factors not only include the outdoor environment such as external pollutants and heavy metals (Bjorklund, 2013) but also prenatal environmental factors such as maternal antibodies, infection, and inflammation.

There has been a controversial debate about the link between autism and vaccines. In the late 1990s the issue first received attention after a publication in the Lancet claimed that the measles-mumps-rubella (MMR) vaccination could cause autism (Wakefield et al., 1998). The number of parents vaccinating their children dropped in response to the article. Even though the article was later retracted due to falsified data, the issue is still debated and the number of children receiving vaccinations is still down. Since the initial publication, researchers have been trying to reassure the public about the safety and positive benefits of vaccinating children (Godlee, Smith, & Marcovitch, 2011; Savoy, 2014; Taylor, Swerdfeger, & Eslick, 2014).

ASD is considered a developmental disease because symptoms emerge at the

same time the brain is undergoing major growth and changes. Researchers have been trying to identify at what point (prenatal or postnatal) development is affected and ASD occurs. There is strong evidence to suggest that a maternal infection or an active immune response during pregnancy increases the chance of delivering a child with ASD (Lee et al., 2014; Zerbo et al., 2013). Maternal antibodies and other diffusible factors of the immune response cross the placenta and may alter the undeveloped immune system of the fetus (Poletaev et al., 2014). Some of these antibodies have been classified as anti-brain and are associated with severe cognitive dysfunction (Piras et al., 2014).

Maternal antibodies are not the only substances that can cross the placental barrier. There is also evidence that the medications used during pregnancy can increase the risk of ASD. Not all prescription drug use is associated with ASD. Drugs such as steroids and cardiovascular drugs were not found to increase the risk of ASD in children (Gardener, Spiegelman, & Buka, 2009). The largest risk is linked to the use of psychoactive drugs, in particular antidepressants (Gidaya et al., 2014; Harrington, Lee, Crum, Zimmerman, & Hertz-Picciotto, 2013). More research is needed to see the effects of these drugs in a larger population and determine if the mother's need for treatment outweighs the risk to the child.

Brain Pathology

Despite autism first being observed in 1940s (Kanner, 1943), it was not until the 1980s that researchers started to uncover the underlying neuropathology. One of the first anatomical features of ASD to be noted was an increase in head size. Brain

imaging data supports that a similar increase in brain growth occurs in 90% of autistic males under the age of 4 (Courchesne et al., 2001). It is not clearly understood if this overall increase in brain size remains through adulthood. This is mostly due to the lack of adult population studies. To date, there have not been any reliable correlations found between an increase in brain size and key behavioral traits associated with ASD. With the advent of new imaging technologies that allow for the division of specific brain structure volumes to be measure separately, behavior specific correlation could begin to be discovered with focus on the regions thought to modulate those behaviors.

The brain consists of two matter types. Gray matter is comprised of the neuronal cell bodies and various glial cell types including protoplasmic astrocytes, oligodendrocytes, and microglia. As the neuronal axons leave the gray matter to make connections to other brain areas, the axons pass into white matter. Within white matter, the axons are covered by oligodendrocytes creating the myelin sheath and supported by other glial cell types including fibrous astrocytes and microglia. Brain imaging studies have found that these two matter types do not undergo the same growth pattern in the ASD brain. Evidence suggests that white matter show a greater enlargement in the ASD brain during early childhood than gray matter (Courchesne et al., 2001; Hazlett et al., 2005; Herbert et al., 2003). However, gray matter overgrowth changes have been found to last into adulthood, whereas white matter alterations are transient and only seen in young children (Hazlett, Poe, Gerig, Smith, & Piven, 2006).

The white and gray matter changes mentioned above are most likely the result of underlying cellular changes. The variation in growth pattern between the two matter types could be attributed to the differing cell populations in each matter type. Within the

cortical gray matter, there are microstructural changes observed in the ASD brain. Cortical tissue contains a vast amount of minicolumns, which are functional units that contain both excitatory and inhibitory neurons working together to maintain brain homeostasis. In the ASD brain there is an imbalance in these minicolumns due to disruptions in the inhibitory force (Casanova, Buxhoeveden, Switala, & Roy, 2002; Casanova & Trippe, 2009). Cellular dysfunction has also been noted in white matter where an excess of interstitial space has been attributed to the pathology of a yet unknown cell type found in white matter (Groen, Buitelaar, van der Gaag, & Zwiers, 2011).

Methods for Researching ASD Pathology

In addition to the genetics data produced by using patient's blood samples discussed above, the other main research methodologies used to study ASD are brain imaging in living subjects, modeling ASD using laboratory animals, and pathology studies using human postmortem tissue from ASD brain donors. Each of these methods provides unique information to our understanding of ASD. A relatively recent introduction of animal models and patient tissue samples into ASD research has opened the door to the application of molecular and cellular techniques to determine the underlying pathology of ASD. Brain imaging was discussed in a previous section in regards to brain structure studies. The other two methodologies are reviewed below.

Animal Models of ASD

In the efforts to create a dynamic model of the disorder researchers have turned

to animal models. A wealth of genetic data already exists from ASD patients that provide numerous genes of interests for the creation of models. One downside to this approach is the hypothesis that it takes several gene abnormalities occurring together in order to produced the disease. When researchers create a knockout mouse for one of the major genes associated with ASD, the animal only presents with one or two of the behavioral core symptoms but not all three of them. Even though these animals are not used for comprehensive studies of ASD, the models have produced information about what genes are important for specific behaviors and brain development. For example, the *PTEN* knockout mouse shows deficits in social interaction and an increase in repetitive behavior but shows no change in communication. However, these changes seems to be associated with alternation of synaptic signaling (Lugo et al., 2014).

Another criticism of current animal models is the lack of anatomical pathology. The disorder is diagnosis solely on behavior and the current models do well in modeling the behavioral features of autism. Most validation studies for these models do not examine the underlying brain pathology along with behavior. Those studies that have taken the step to include anatomical validation have yielded very few models that show the brain abnormalities seen in patients with autism.

The mouse model that has been most accepted and researched in regards to ASD is the BTBR T^{+}*tf*/J mouse. This mouse is an inbred strain that exhibits all three of the hallmark behaviors of ASD. These behavioral traits have been tested using multiple behavioral methods for the measurement of social interaction, communication, and repetitive behaviors (Bolivar, Walters, & Phoenix, 2007; McFarlane et al., 2008; Meyza et al., 2012). This model also displays neuroanatomical changes as well. Some of the

more notable brain changes are the absence of the corpus callosum and size alteration in the hippocampus. These structural changes have been found in a small number of ASD patients but are not widespread in the population. This model was created using a forward genetic model system where researchers create a model that exhibits the characteristics of a disorder and then find the genes responsible for the changes. This could prove to be a better approach than reverse genetic model creation because multiple gene abnormalities are required for ASD to occur.

Use of Postmortem Tissue in ASD Research

The use of postmortem brain tissue from autistic donors allows researchers to interrogate molecular and cellular pathology underlying brain abnormalities discovered using *in vivo* imaging techniques. However, there are several limitations to the use of postmortem tissue as there is with any research methodology. A large downside is the variation found in human subject studies. Unlike animal or cell culture models, subject to subject variability is a consideration that has to be taken into account during the planning phase of any postmortem experiment or project. Factors such as tissue quality, age, sex, postmortem interval time, medical history, and toxicology could influence findings. In the studies presented here our lab has controlled for as many of these factors as was possible by matching control and ASD cases by the potentially confounding variable. For those variables that could not be matched across control and ASD cases, statistical methods were used to evaluate the potential effect of the variable on experimental outcomes.

Another limitation is the static nature of a tissue sample. Postmortem tissue

allows for the investigation of a disease state at one time point. This type of sample lends itself well to studies designed to measure expression levels of various genes and proteins or even structural and morphometric analysis. However, the tissue sample cannot be manipulated biochemically to investigate mechanisms by which pathology is initiated or induced. Once data are collected from postmortem tissue, the research approach must then move to an appropriate model of the disease that allows for a dynamic environment, i.e. reverse translational research.

Despite the drawbacks of human postmortem brain research, the use of these tissues allows for a detailed examination of the biological and molecular processes associated with the disease state in the human subject. In an editorial from Autism Research, the official journal of the International Society for Autism Research, the editor-in-chief. Anthony Bailey addressed the need for ASD research using postmortem tissues stating that the field could only move forward by uncovering the molecular pathology that postmortem tissue can provide (Bailey, 2008). A growing group of ASD researchers agree with. Bailey's understanding of the importance of postmortem studies. This has prompted the worldwide campaign, It Takes Brains, to increase brain donations and provide support for postmortem researchers. Even with the increased interest in ASD postmortem research, the field is still alarmingly behind that of other brain disorders. Not only are there a small number of ASD brains available, but proper typically developing age matched controls are also needed. Typically developing controls are defined as individuals who do not have any diagnosis classified as a developmental disorder as well as other diagnosed medical disorders. These controls are important because they allow for the comparison of brain pathology in the presence

and absence of ASD at a given age point.

The use of ASD postmortem tissue has so far been limited to stereology and homogenate sample-based protein studies. While these studies have been paramount in introducing the use of postmortem tissue into ASD research, the resolution of these experiments has not been high enough to truly identify underlying molecular pathways or cellular changes associated with ASD. The brain is a very complex organ made up of highly specialized areas communicating within and between each other to function properly. At the core of this organization are numerous cell types that play a role in this overall structure and function. Currently, ASD postmortem studies have focused on these areas as whole entities despite the underlying cellular complexity. This could be one reason that past postmortem studies have done little in the way of producing answers about the cellular basis of ASD.

Overview of Experiments

This dissertation presents a set of studies that systematically increase the resolution of analysis of ASD pathology, i.e. interrogating potential gene expression abnormalities in specific brain regions, brain matter types, and then cell types. By combining both molecular approaches and postmortem brain tissue, a better understanding of pathology should be achieved. My research was focused specifically on ASD brain pathology, but the methods used could be applied to study any neurological or psychiatric disease. The pathways and genes found to be altered in these studies could also serve as a starting point for the investigation of other diseases or could be employed in animal models using transgenic technology.

Chapter 2 begins with the investigation of cell specific protein markers within gray and white matter regions of Brodmann area 24 (BA24) and Brodmann area 10 (BA10). As discussed above, ASD postmortem brain research had not investigated brain pathology within a specific brain region at a tissue or cellular level. By simply dividing the brain regions by the matter types (white versus gray), we start to reduce the number of different cell types present in the experimental sample. This study directed my single cell studies to identify specific cell populations that could contribute to pathology.

Chapter 3 used laser capture microdissection to examine the glutamate signaling pathway that is critical to brain function and that is thought to be disrupted in ASD. Data from functional imaging and genetics studies support the theory that there is an imbalance in the excitatory/inhibitory system of the brain of ASD patients (Pizzarelli & Cherubini, 2011; Snijders, Milivojevic, & Kemner, 2013; Tebartz van Elst et al., 2014). This study analyzed the expression of key glutamate receptor and transporter genes as well as neurotrophic pathways in laser captured neurons and astrocytes from typically developing and ASD brains. The results of this study further emphasize the need for cell population based studies of brain pathology. The neuronal, but not glial, cell population exhibited significant differences in the expression of several genes comparing control and ASD brains. The expression of these genes was also investigated in homogenate punched-dissected samples, which are gray matter samples that are dissected using a 3.5 mm trephine punch and contained all gray matter cell types. However, these changes were not found in homogenate punch-dissected samples from the same subjects. This illustrates that the presence of multiple cell populations in the experimental sample can present an inaccurate picture of brain

pathology.

The gene and protein expression alterations discovered in the previously discussed studies compelled our lab to ask how much could be learned about the regulation of gene expression in a single cell population. With little to no data about the potential molecular mechanism(s) underlying ASD brain pathology, we wanted to find other gene or pathway alterations that could help us further understand the cell specific data we produced. Chapter 4 discusses the development of a method to fully characterize the transcriptional footprint of a specific cell type and what differences exist comparing brains of control and ASD donors. This method was based on RNA-Seq, which provides in-depth analysis of the transcriptome. This sequencing method produces vast amounts of data including transcript copy number, differential expression genes, rare isoforms, splicing variants, transcriptional start points, and identification of 5' and 3' ends of transcripts. Because the main objective was to determine feasibility of this method, my research focused on identifying differentially expressed genes in single populations of cells comparing ASD and typically developing control donors. My research did not dismiss the other forms of data that RNA-Seq provides, but studies investigating rare isoforms or alternative transcriptional regulators that are identified by RNA-Seq are currently beyond the resources of our lab due to the small number of pairs we currently have in our brain bank. We could be capable of performing this type of analysis in the future through collaboration or addition of tissue to our bank. However, these types of studies are beyond the scope of the current project.

Other methods could be used to examine differential expression, such as microarrays and RT-qPCR. However, these methods only provide relative

quantification of changes in transcription. RNA-Seq's absolute quantification of transcript through sequencing permits a more advance analysis than data collected using microarrays. As our brain bank grows in number, absolute quantification allows for the addition of pairs in separate analyses. Hence, over time we can analyze additional pairs and add to our existing database. Also in future studies others can retrospectively mine the database sequence information that is being created.

As more and more researchers adopt next generation sequencing techniques, RNA-Seq is becoming a commonly used technique for transcriptional analysis, almost replacing microarrays. However, herein we pushed the limits of this technology by analyzing laser captured single cell populations. The nature of LCM samples makes experimentation difficult because of the small amount of sample collected for analysis and because of RNA degradation issues. Chapter 4 discusses the experimental considerations and limitations of using LCM samples as well as advances in RNA-based methods that allows for low input sequencing.

The CDC reports that there has been a 78% increase in autism over the last decade (Baio, 2014). Despite advances in the understanding of ASD, there is currently no known cause. As presented in this dissertation, we examine ASD brain pathology at the single cell level in order to identify molecular pathologies that could reveal targets for the future development of treatments for ASD. In addition, LCM and RNA-Seq technologies were paired to identify gene expression abnormalities in specific cell types, a pairing that has not been successfully employed by other laboratories to date. ASD research is thereby moved forward by developing methods to identify key molecular and cellular pathways involved in the pathology of this disease.

CHAPTER 2

ELEVATED GFAP PROTEIN IN ANTERIOR CINGULATE CORTICAL WHITE MATTER IN MALES WITH AUTISM SPECTRUM DISORDER

INTRODUCTION

Autism spectrum disorder (ASD) is a developmental disorder characterized by disruption of social interaction behaviors, reduced verbal and non-verbal communication, and the presence of repetitive behaviors. The reported prevalence of this disorder has grown rapidly with the current estimate of affected children to be 1 in 68 (Blumberg et al., 2013). A variety of factors including environmental exposures and genetic abnormalities have been linked to ASD (Blake et al., 2013). Besides behavioral deficits, ASD patients suffer from other comorbidities including seizures and gastrointestinal abnormalities (Kral et al., 2013; Robinson, 2012). Current treatment paradigms include drugs that offer individual symptomatic relief paired with behavioral modification therapy. Reasonable treatment options are not available to significantly improve quality of life, reverse the disorder, or arrest its progress. Thus, the need for understanding the neuropathology of this disorder is crucial.

In addition to the behavioral deficits mentioned above, ASD patients display anatomical brain abnormalities when compared to typically developing control subjects. ASD brain pathology has been described using imaging methods such as fMRI and brain volumetric analysis. Both developmental and structural changes have been found in brain regions subserving behaviors that are affected in ASD. There is an aggressive overgrowth in brain volume in ASD in both the cerebrum and cerebellum between ages

two and four when compared to age-matched control subjects. By middle to late childhood, ASD and age-matched control brains are similar in size (Courchesne et al., 2011). White and gray matter in the brain do not undergo the same pathological changes in size and development and it is unclear if gross brain abnormalities are linked to specific cellular alterations and dysfunction (as reviewed by Amaral et al., 2008).

A consistent pathological finding in the ASD brain is abnormal white matter. Diffusion tensor imaging (DTI) studies have been used to investigate white matter pathology by measuring the amount of diffusion through brain matter. White matter is more restrictive to the movement of water molecules than gray matter resulting in decreased diffusion relative to gray matter. Increased diffusion of water in white matter has been observed in ASD as compared to typically developing subjects, possibly resulting from excess interstitial space in ASD (Groen et al., 2011). Several studies of this nature have shown an overall increase in white matter size and a decrease in structural integrity in ASD, further suggesting that cells within the white matter are dysfunctional and/or structural changes exist in axons passing through white matter (Groen et al., 2011; Ingalhalikar et al., 2011; Noriuchi et al., 2010; Radua et al., 2010; Sundaram et al., 2008). The specific types of cells that contribute to these white matter abnormalities in ASD are unknown. Macroglial cells, specifically astrocytes and oligodendrocytes, are found abundantly in white matter tracts, whereas there are few neuron cell bodies. Hence, it seems reasonable to speculate that dysfunction in macroglia accounts for at least part of the ASD-associated deficits in white matter integrity.

The purpose of this study was to examine the levels of two proteins expressed

abundantly by brain astrocytes and oligodendrocytes in ASD. Glial fibrillary protein (GFAP) is considered a marker of astrocytes. GFAP is up-regulated following an insult or injury to the brain, additionally making it an indicator of CNS pathology (Sofroniew & Vinters, 2010). Myelin oligodendrocyte glycoprotein (MOG) is marker protein for mature myelin-producing oligodendrocytes. Since the myelin sheath has an integral role in neurotransmission, myelin abnormalities could result in dysfunction of neuronal conduction along axons in ASD. This study investigated GFAP and MOG protein expression in white and gray matter from the ventral anterior cingulate cortex (Brodmann area 24; BA24) and the anterior prefrontal cortex (BA10) using postmortem brain tissues from age-matched typically developed control and ASD donors. These brain areas were selected for their documented role in influencing behaviors characteristically disrupted in ASD such as social interaction and repetitive behaviors. Findings here show elevated GFAP immunoreactivity (ir) in ASD that is both matter and brain area specific. The specificity of these findings guide future studies to elucidate the cellular pathology associated with ASD.

Methods

Brain Tissues

Frozen tissue blocks containing BA24 and BA10 from 14 ASD donors and 14 typically developed control donors were obtained from Autism Tissue Program, Harvard Brain Tissue Resource Center (Belmont, MA) and NICHD Brain and Tissue Bank for Developmental Disorders (Baltimore, MD) (Table 2.1). This study was reviewed and approved for exemption by the Institutional Review Board of East Tennessee State

University under the Department of Health and Human Services exemption 45 CFR 46.101(b) relating to the use of publicly available unidentifiable pathology specimens. ASD and control donors were matched prior to experimentation as closely as possible by age primarily, but also by RNA quality (Table 2.1), to reduce the impact of these factors on protein and mRNA data from the two groups. ASD donors met diagnostic criteria outlined in the Diagnostic and Statistical Manual (DSM) IV for autistic disorder. The Autism Diagnostic Interview-Revised (ADI-R) and other medical records were also used to confirm diagnoses. Causes of death and comorbidities are not included in Table 2.1 to protect the identities of the decedents. Cause of death for typically developed control donors included asphyxia (3), drowning (3), motor vehicle accident (2), heart attack (2), dilated cardiomyopathy (1), pneumonia (1), commotio cordis (1), and an unknown cause (1). Cause of death for ASD donors included asphyxia (2), heart attack (1), cardiac arrhythmia (1), congestive heart failure (1), cardiopulmonary arrest (1), motor vehicle accident (1), acute respiratory distress syndrome (1), stopped breathing (1), skull fracture (1), subdural he9morrhage (1), cancer (1), diabetic ketoacidosis (1), and bowel obstruction (1).

Table 2.1. Subject demographic information.

Pair	ID	Age	Gender	RIN[a]	PMI (hours)[b]	Toxicology	Assays	Tissue
	Controls							
1	AN14757	24	M	7.8	21.33	No drugs reported	LCM[c], qPCR[d], WB[e]	BA24, BA10
2	AN07176	21	M	8	29.91	No drugs reported	LCM, qPCR, WB	BA24, BA10
3	AN07444	17	M	7.5	30.75	Sertraline	LCM, qPCR, WB	BA24, BA10
4	5408	6	M	7	16	No drugs reported	LCM, qPCR, WB	BA24, BA10
5	4848	16	M	7.6	15	No drugs reported	LCM, qPCR, WB	BA24, BA10
6	5342	22	M	8.1	14	No drugs reported	LCM, qPCR, WB	BA24, BA10
7	5079	33	M	7.3	16	Ethanol	LCM, qPCR, WB	BA24, BA10
8	M3231M	37	M	7.4	24	No drugs reported	LCM, qPCR, WB	BA24, BA10
9	AN12137	31	M	7.3	32.92	No drugs reported	qPCR, WB	BA24, BA10
10	AN03217	19	M	7.6	18.58	No drugs reported	qPCR, WB	BA24, BA10
11	AN00544	17	M	7.8	28.92	No drugs reported	qPCR, WB	BA24, BA10
12	AN17425	16	M	7.5	26.16	No drugs reported	qPCR, WB	BA24, BA10
13	4590	20	M	7.6	19	No drugs reported	qPCR, WB	BA24, BA10
14	4670	4	M	7	17	No drugs reported	WB	BA10
	MEAN	**20.21**		**7.54**	**22.11**			
	SEM	**2.46**		**0.09**	**1.75**			
	ASD							
1	AN04166	24	M	8.1	18.51	No drugs reported	LCM, qPCR, WB	BA24, BA10
2	AN03935	20	M	8.6	28	No drugs reported	LCM, qPCR, WB	BA24, BA10
3	AN02987	15	M	6.5	30.83	No drugs reported	LCM, qPCR, WB	BA24, BA10
4	5144	7	M	8	3	No drugs reported	LCM, qPCR, WB	BA24, BA10
5	5302	16	M	6.6	20	Risperidone, Fluvoxamine, Clonidine, Insulin	LCM, qPCR, WB	BA24, BA10
6	5176	22	M	7.1	18	Risperidone	LCM, qPCR, WB	BA24, BA10
7	5297	33	M	7.1	50	Quetiapine, Fluoxetine, Valproate, Ziprasidone	LCM, qPCR, WB	BA24, BA10
8	5027	37	M	7.7	26	Risperidone, Fluvoxamine	LCM, qPCR, WB	BA24, BA10
9	AN11989	30	M	7.7	16.06	Sertraline, Clomipramine, others for pain management and CHF[f]	qPCR, WB	BA24, BA10
10	AN07817	19	M	7.2	14.83	No drugs reported	qPCR, WB	BA24, BA10
11	AN00764	20	M	8	23.66	Minocycline	qPCR, WB	BA24, BA10
12	AN04682	15	M	7.6	23.23	No drugs reported	qPCR, WB	BA24, BA10
13	4999	20	M	7	14	No drugs reported	qPCR, WB	BA24, BA10
14	5308	4	M	6.5	21	No drugs reported	WB	BA10
	MEAN	**20.14**		**7.41**	**21.94**			
	SEM	**2.42**		**0.17**	**2.84**			
	P value[g]	**0.98**		**0.51**	**0.96**			

[a] RNA integrity number (index of RNA quality)
[b] Postmortem interval
[c] Laser capture microdissection
[d] Quantitative polymerase chain reaction
[e] Western blotting
[f] Congestive heart failure
[g] Results of an independent t-test comparing control and ASD groups.

Tissue Preparation and Sectioning

Frozen tissue sections (50 μm) of BA24 and BA10 were cut using a cryostat microtome (Leica CM3050S) and tissue samples were punch-dissected from sections using a disposable 3.5 mm trephine. White and gray matter samples were separately collected for each brain area (Fig 2.1A). Frozen tissue sections (10 μm) cut using the same microtome were prepared as previously described for laser capture microdissection (LCM) (Ordway, Szebeni, Duffourc, Dessus-Babus, & Szebeni, 2009).

Western Blotting

Protein from punch-dissected samples was isolated using ice-cold Tris-EDTA buffer with a protease inhibitor cocktail (Thermo Scientific, Rockford, IL) and sonication for 20 sec. Equal amounts of protein (10 μg per lane; Micro BCA Protein Assay Kit; Thermo Scientific, Rockford, IL) per sample were diluted 1:1 in SDS sample buffer and separated by electrophoresis using pre-cast Tris-Glycine gels (NuSep, Bogart, GA). Subsequently, resolved proteins were transferred onto nitrocellulose membranes. Membranes were incubated with 5% milk-based blocking agent (Bio-Rad, Hercules, CA), and then incubated with primary antibody overnight at 4^{o} C. Primary antibodies included GFAP (1:500, Sigma-Aldrich, St. Louis, MO), MOG (1:1500, Abcam, Cambridge, MA), and glyceraldehyde-3-phosphate dehydrogenase (GAPDH; control for loading; 1:1000, EMD Millipore, Billerica, MA). Membranes were washed with TBS-Tween (0.5%) buffer (Boston BioProducts, Ashland, MA) three times for 10 min, incubated with anti-mouse (1:5000) and anti-rabbit (1:20,000) secondary antibody for one h at 22^{o} C and washed again three times for 10 min with TBS-Tween (0.5%) buffer (Boston BioProducts, Ashland, MA). Immunochemically identified bands were detected

using horseradish peroxidase conjugated secondary antibodies reacted with the chemiluminescent substrate, Amersham ECL Prime Western Blotting Detection Reagent (GE Healthcare, Piscataway, NJ). Bands were visualized and analyzed using a G:Box imager (Syngene, Frederick, MD). Paired ASD and typically developed control samples were run on the same gel in triplicate along with a set of protein standards. Data were normalized to GAPDH-ir measured on the same blot, after stripping GFAP and MOG antibodies. Band densities were measured using GeneTool software (Syngene, Frederick, MD).

Laser Capture Microdissection

Laser capture of astrocytes identified using a rapid immunohistochemical stain for GFAP (Fig. 2.1B-D) was performed on an Arcturus XT (Life Technologies, Grand Island, NY) as previously described (Ordway et al. 2009).

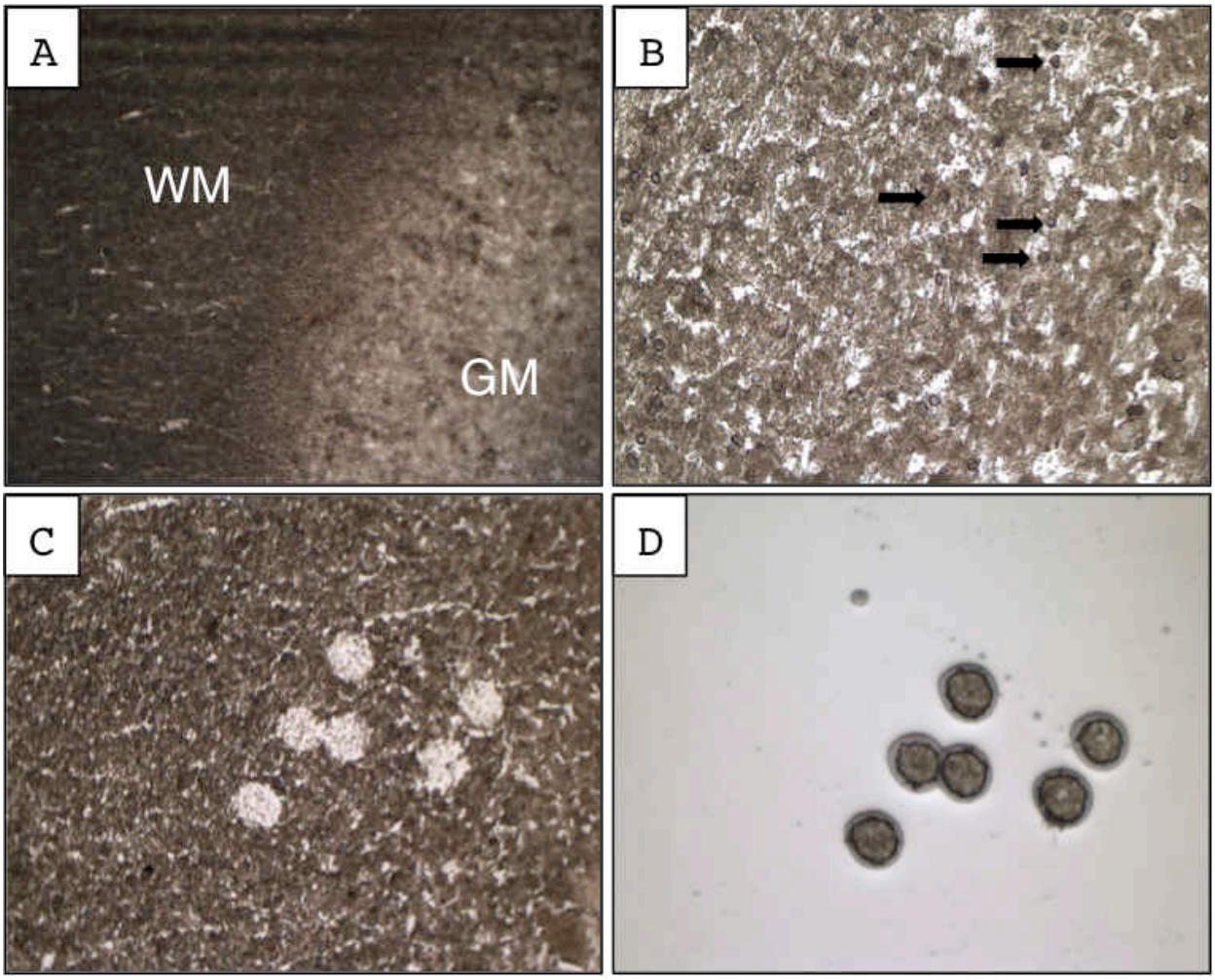

Figure 2.1. Tissue collection of white and gray matter and laser capture microdissection of astrocytes. Panel A shows gray and white matter regions in BA24 identified with GFAP immunostaining (2x magnification). Panel B shows GFAP immunostained cells (individuals cell indicated by arrows) in white matter (40x magnification). Shown in panel C is the absence of laser captured cells in the tissue section following capture (20x magnification). Panel D shows the GFAP immunoreactive cells adhered to the polymer cap (20x magnification).

Quantitative Polymerase Chain Reactions

Total RNA was isolated from tissue samples using the Maxwell simplyRNA LEV kit (Promega, Madison, WI). The quality of RNA extracted from brain tissue samples was assessed using the Bioanalyzer RNA 6000 Nano chip (Agilent Technologies, Santa Carla, CA) and all samples had RNA integrity number (RIN) values of ≥ 6.5. RNA was converted to double-stranded cDNA using Superscript III reverse transcriptase kit (Invitrogen, Carlsbad, CA) according to the manufacturer's protocol. Quantitative real-time PCR (qPCR) was performed using cDNA template, 2x Platinum PCR quantitative supermix-UDG (Invitrogen, Grand Island, NY), 10 μM fluorogenic probe, and 250 nM gene specific primers on the Stratagene MX3000P (Agilent Technologies, Santa Carla, CA). Intron-spanning primers were designed using PrimerQuest software (Integrated DNA Technologies, Coralville, IA) in a region of the target gene containing no secondary structure as determined by mFold3 (Zuker, 2003) shown in Appendix B. For some genes, primers were obtained from Qiagen (Valencia, CA). Each sample was analyzed in triplicate. A five point standard curve on each plate was used to determine reaction efficiency and copy number of amplicons. Gene expression data were normalized to the geometric mean of three housekeeping genes, *GAPDH*, T*BP*, and *Ribo18S1.* Fold-differences in gene expression between control and ASD groups were determined using the $2^{-\Delta\Delta CT}$ method (Livak & Schmittgen, 2001). To quantify RNA levels from laser captured astrocytes, a semi-quantitative end-point PCR method was used as described previously (Ordway et al., 2009), wherein target genes were normalized with the average of two reference genes, *GAPDH* and *Ribo18S1*.

Statistical Analysis

A Grubb's test was used or remove outliers in data sets (Grubbs, 1950). Data from ASD and typically developed control donors were statistically compared using the Student's t-test for independent measures. As an additional check (see Results), data were also analyzed using the t-test for paired measures and the statistical findings for these paired tests are included in supplementary materials. Differences were considered statistically significant at $p < 0.05$. Pearson's correlation analysis was used to determine possible effects of age, RIN, and postmortem interval (PMI) on dependent variables. Because many correlations were examined, a $p < 0.01$ was chosen *a priori* to reduce the risk of type I errors. Statistical analysis was performed using SPSS (version 21, IBM, New York, NY) and graphed using Prism (version 5.0b, GraphPad Software, La Jolla, CA).

RESULTS

Donors and tissues.

Careful pairing of ASD and typically developed control donors was performed prior to the initiation of experiments as described in the Methods. As a result, there were no statistically significant differences between the two groups of donors when comparing ages, RINs or PMIs (Table 2.1).

Western blot analysis of white and gray matter GFAP and MOG

Levels of GFAP-ir and MOG-ir were measured in four brain regions, including white and gray matter areas of both BA10 and BA24. Except for BA10 gray matter ($r^2=0.68$; $p=0.001$) from ASD donors only, there were not significant correlations

between age and levels of GFAP-ir or MOG-ir in any of the brain regions (Table 2.2). This lack of correlation was observed whether examining potential age effects in control and ASD separately, or when examining age versus protein levels for all subjects from both groups. Likewise, levels of GFAP-ir and MOG-ir did not significantly correlate with either RIN or PMI in any brain region (Table 2.2).

Table 2.2. Pearson's correlation analysis of GFAP-ir and MOG-ir for BA24 and BA10 white (WM) and gray (GM) matter versus age, RIN, and PMI.

All Subjects

		Age		RIN		PMI	
		r^2	p value	r^2	p value	r^2	p value
BA24	WM GFAP	0.03	0.45	0.00	0.97	0.04	0.35
	WM MOG	0.00	0.81	0.04	0.34	0.08	0.19
	GM GFAP	0.06	0.25	0.01	0.70	0.08	0.18
	GM MOG	0.00	0.89	0.00	0.93	0.00	0.93
BA10	WM GFAP	0.03	0.03	0.03	0.54	0.01	0.71
	WM MOG	0.05	0.40	0.00	0.89	0.00	0.98
	GM GFAP	0.20	0.03	0.00	0.92	0.07	0.25
	GM MOG	0.20	0.03	0.02	0.49	0.10	0.15

Control Subjects Only

		Age		RIN		PMI	
		r^2	p value	r^2	p value	r^2	p value
BA24	WM GFAP	0.15	0.24	0.02	0.65	0.03	0.57
	WM MOG	0.05	0.48	0.13	0.25	0.17	0.18
	GM GFAP	0.04	0.52	0.31	0.05	0.13	0.22
	GM MOG	0.14	0.23	0.01	0.81	0.08	0.38
BA10	WM GFAP	0.46	0.07	0.10	0.44	0.01	0.82
	WM MOG	0.28	0.18	0.05	0.58	0.00	0.91
	GM GFAP	0.18	0.19	0.07	0.42	0.03	0.61
	GM MOG	0.03	0.62	0.04	0.53	0.08	0.40

ASD Subjects Only

		Age		RIN		PMI	
		r^2	p value	r^2	p value	r^2	p value
BA24	WM GFAP	0.02	0.68	0.01	0.75	0.08	0.38
	WM MOG	0.02	0.69	0.02	0.66	0.05	0.53
	GM GFAP	0.17	0.19	0.02	0.65	0.06	0.45
	GM MOG	0.04	0.53	0.01	0.78	0.00	0.87
BA10	WM GFAP	0.32	0.15	0.33	0.14	0.08	0.49
	WM MOG	0.08	0.51	0.00	0.87	0.02	0.71
	GM GFAP	0.68	0.001	0.00	0.94	0.38	0.04
	GM MOG	0.06	0.46	0.01	0.82	0.21	0.16

Age was the primary criteria for matching control and ASD donors. Given the lack of consistent effects of age on GFAP-ir levels, further statistical analyses of Western blot data utilized a t-test for independent measures. Significantly elevated levels of GFAP-ir were observed in BA24 white matter of ASD donors as compared to control donors (Fig. 2.2A; $p=0.008$). In contrast, MOG-ir levels were similar in these same tissues from control and ASD donors (Fig. 2.2A; $p=0.85$). Furthermore, no significant differences were observed for GFAP-ir or MOG-ir levels comparing control and ASD donors for BA24 gray matter (Fig. 2.2B; GFAP $p=0.88$; MOG $p=0.67$), BA10 white matter (Fig. 2.2C; GFAP $p=0.13$; MOG $p=0.17$), or BA10 gray matter (Fig. 2.2D; GFAP $p=0.50$; MOG $p=0.94$). Since the study was originally set up and performed in a matched pair design (see Methods), we also examined the data using a paired t-test, which yielded very similar results (Table 2.3).

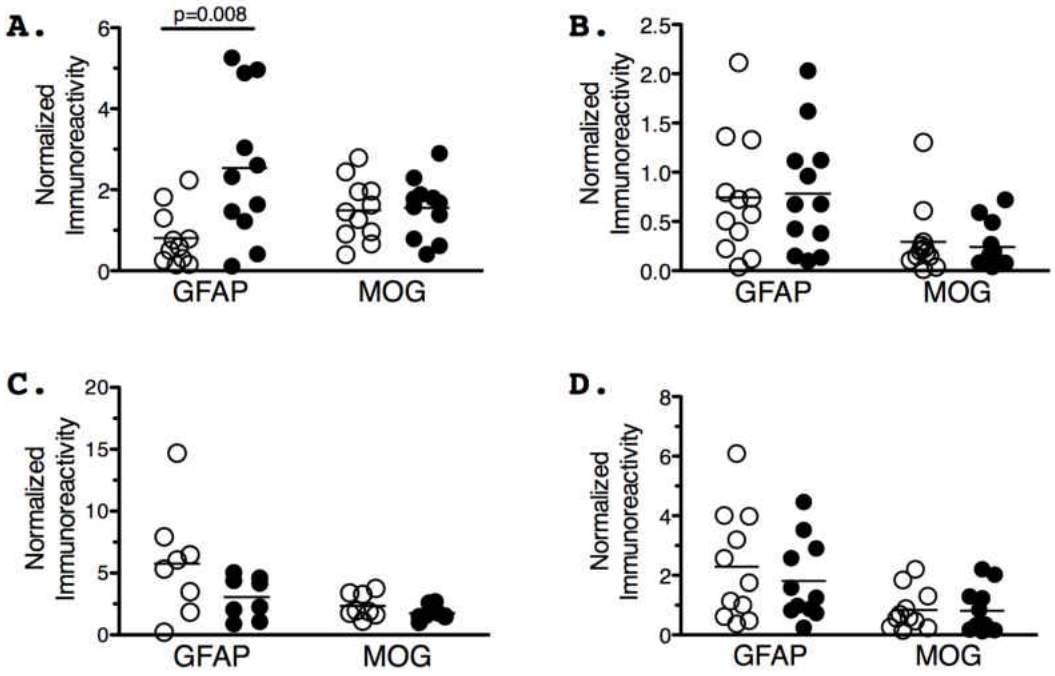

Figure 2.2. Western blot analysis of GFAP-ir and MOG-ir in punch-dissected white and gray matter from BA24 and BA10 of typically developing control donors (open symbols) and ASD donors (closed symbols). Immunoreactivity levels are normalized to GAPDH-ir determined on the same blot. (A) BA24 white matter; (B) BA24 gray matter; (C) BA10 white matter; (D) BA10 gray matter. Statistical significance is noted in the horizontal bar above the data points.

Table 2.3. Paired Student's t-test analysis of GFAP-ir and MOG-ir for BA24 and BA10 white and gray matter.

	BA24		**BA10**	
	WM	**GM**	**WM**	**GM**
GFAP	p=0.006	p=0.85	p=0.10	p=0.39
MOG	p=0.64	p=0.54	p=0.21	p=0.87

qPCR analysis of GFAP and MOG expression

Because ASD was associated with elevated GFAP protein levels in BA24, we examined gene expression levels of glial markers using RNA isolated from homogenates of white or gray matter from ASD and control donors. There were no significant correlations between age or PMI with levels of GFAP or MOG gene expression. RIN significantly correlated with levels of *GFAP* expression (p=0.003) only in BA24 white matter and only in control subjects (Table 2.4). No significant differences in the levels of expression of either *GFAP* (Fig. 2.3A; p=0.61) or *MOG* (Fig 2.3A; p=0.20) were observed comparing control and ASD donors. Comparison of gene expression levels in BA24 white matter of control and ASD donors using a paired t-test yielded similar results (Table 2.5). Likewise, gene expression for *GFAP* and *MOG* in gray matter was not different comparing control and ASD donors as assessed using an independent (Fig. 2.3B; *GFAP*, p=0.52; *MOG*, p=0.95) or a paired t-test (Table 2.5).

Table 2.4. Pearson's correlations analysis of *GFAP* and *MOG* expression for BA24 white (WM) and gray (GM) matter and BA24 white and gray matter laser captured astrocytes versus age, RIN, and PMI.

All Subjects

		Age		RIN		PMI	
		r^2	p value	r^2	p value	r^2	p value
WM	GFAP	0.00	0.79	0.01	0.72	0.01	0.58
	MOG	0.12	0.10	0.06	0.22	0.02	0.56
	LCM GFAP	0.13	0.21	0.43	0.01	0.02	0.64
GM	GFAP	0.00	0.78	0.04	0.41	0.02	0.55
	MOG	0.00	0.77	0.01	0.73	0.18	0.048
	LCM GFAP	0.07	0.32	0.12	0.19	0.25	0.051

Control Subjects Only

		Age		RIN		PMI	
		r^2	p value	r^2	p value	r^2	p value
WM	GFAP	0.00	0.99	0.56	0.003	0.00	0.98
	MOG	0.27	0.07	0.03	0.55	0.00	1.00
	LCM GFAP	0.25	0.25	0.34	0.17	0.15	0.39
GM	GFAP	0.00	0.94	0.21	0.18	0.07	0.46
	MOG	0.06	0.45	0.00	0.85	0.01	0.79
	LCM GFAP	0.28	0.18	0.10	0.45	0.25	0.21

ASD Subjects Only

		Age		RIN		PMI	
		r^2	p value	r^2	p value	r^2	p value
WM	GFAP	0.02	0.62	0.15	0.19	0.05	0.45
	MOG	0.01	0.74	0.13	0.25	0.07	0.40
	LCM GFAP	0.06	0.59	0.50	0.08	0.50	0.08
GM	GFAP	0.01	0.73	0.15	0.24	0.01	0.76
	MOG	0.01	0.73	0.01	0.79	0.48	0.02
	LCM GFAP	0.01	0.82	0.26	0.19	0.26	0.19

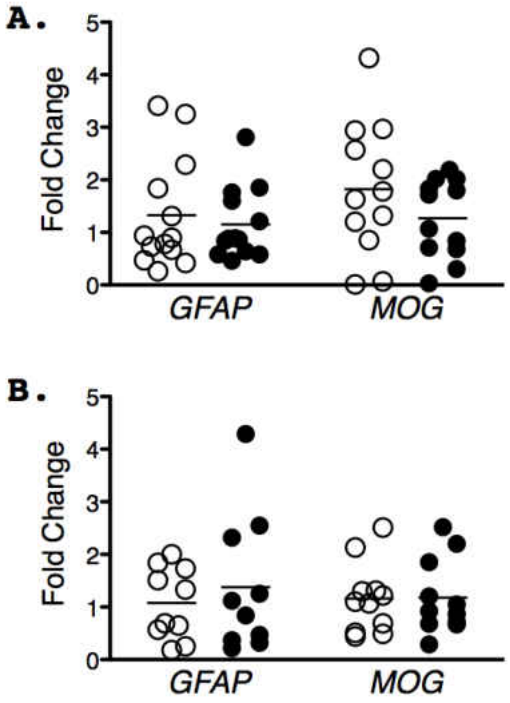

Figure 2.3. Levels of expression of *GFAP* and *MOG* in punch-dissected white (A) and gray (B) matter from BA24 of typically developing control donors (open symbols) and ASD donors (closed symbols). Gene expression levels are normalized to the geometric mean of stable references genes (*GAPDH*, *TBP*, and *Ribo18S1)*. No statistically significant differences were observed.

Table 2.5. Paired Student's t-test analysis of *GFAP* and *MOG* expression for BA24 white and gray matter and BA24 white and gray matter laser captured astrocytes.

	BA24			
	WM Punch	**GM Punch**	**WM LCM**	**GM LCM**
GFAP	p=0.67	p=0.58	p=0.82	p=0.15
MOG	p=0.18	p=0.96		

Laser-captured BA24 astrocyte PCR analysis for GFAP expression

We considered the possibility that the use of LCM to specifically capture GFAP-immunoreactive astrocytes for PCR analysis of GFAP gene expression might yield a more accurate analysis of astrocyte GFAP gene expression levels than measuring gene

expression in mRNA isolated from homogenates of cortical tissue. Hence, LCM collected GFAP-immunoreactive astrocytes from both BA24 gray and white matter from eight of the control-ASD donor pairs used for protein studies above. There were no significant correlations between age or PMI with levels of GFAP or MOG gene expression. RIN significantly correlated with levels of *GFAP* expression (p=0.01) only in BA24 white matter and only when all subjects from both groups were combined (Table 2.4). Levels of *GFAP* expression were not different comparing control and ASD donors, in both white (p=0.93;) and gray matter (p=0.11) cell populations analyzed using independent t-test (Fig. 2.4) or a paired t-test (Table 2.5).

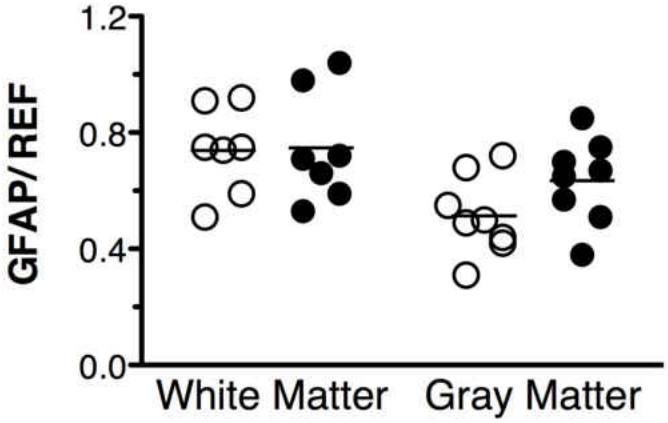

Figure 2.4. Levels of expression of *GFAP* in laser captured astrocytes from BA24 white and gray matter of typically developing control donors (open symbols) and ASD donors (closed symbols). Gene expression levels are normalized to the average of levels of expression of references genes (*GAPDH* and *Ribo18S1*).

DISCUSSION

Autism has been considered a disorder of aberrant connections between and within brain regions. This theory of disrupted connectivity is supported by findings of reduced axon thickness and neuronal disorganization (Courchesne et al., 2007; Minshew & Williams, 2007; Zikopoulos & Barbas, 2010). Most ASD research to date has focused on pathology of neurons with little regard to the other major cell types of the brain. Physiologically, glia assist neurons in a variety of ways including protecting neurons from cytotoxic glutamate exposure, providing vital growth factors essential for neuronal survival, and providing support for electrical conduction along axons. Pathology of glia could lead to the aberrant functioning of neurons and could account for imaging abnormalities seen in ASD white matter (Zeidán-Chuliá et al., 2014), making it imperative to determine the possible contributory role of glial to the etiology of this disease.

Within the ASD field, protein expression studies utilizing postmortem brain tissues have been mostly limited to the examination of brain areas, as whole entities, with little regard for differences between white and gray matter. Glial cells occur in both gray and white matter. However, the function and types of glia differ between these types of brain tissue. For example, protoplasmic astrocytes are found in gray matter, whereas fibrous astrocytes are present in white matter. Each of these astrocytes types have their own function and structure (Kimelberg, 2010). Increases in GFAP-ir have been observed in the frontal and parietal cortices, cerebellum, and the anterior cingulate gyrus of autistic subjects when compared to age-matched controls, suggesting the presence of reactive astrogliosis (Laurence et al., 2005; Vargas et al., 2005). These

studies used homogenized brain tissues without anatomically distinguishing between white and gray matter or cell types within these brain regions. The present study is the first to evaluate two glial cell markers separately in gray and white matter. The results of this study demonstrate elevated levels of the astrocyte marker, GFAP, specifically in white matter in BA24 of the ventral anterior cingulate cortex from ASD donors as compared to matched typically developing control donors.

Astrocytes compose the bulk of activated glial cells in ASD, although microglia are also activated (Vargas et al., 2005). Viral and inflammatory processes as well as direct brain trauma can increase astrocyte reactivity (Sofroniew & Vinters, 2010). Many cytokines and inflammatory factors are up-regulated in the ASD brain (Pardo, Vargas, & Zimmerman, 2005), factors that may mediate glial activation and subsequent increases in GFAP expression in ASD. Glia activation is a phasic process that involves many different biochemical pathways. Based on the type of insult, astrocytes can return to a non-reactive state, trigger cellular mechanisms of defense, and/or induce astrocytic proliferation aimed at remodeling the affected brain area (Pekny, Wilhelmsson, & Pekna, 2014). The phasic nature of GFAP regulation might explain the large range of GFAP-ir levels observed in white and gray matter of all subjects in the present study.

GFAP expression in BA24 white matter was similar comparing ASD and control donors, despite a difference in GFAP protein levels. Others have noted a different response pattern in translational and transcriptional regulation of *GFAP* as well as a biphasic expression of *GFAP* in activated cells (Tawfik, LaCroix-Fralish, Nutile-McMenemy, & DeLeo, 2005) which could account for the apparent discrepancy in the present study. We also considered that homogenate tissue samples contain a variety of

cells that could make it difficult to distinguish the cellular source of pathology. Therefore, potential gene expression differences were also interrogated in laser captured astrocytes. However, no change in the gene expression of glial markers was found in laser captured astrocyte populations from control and ASD brains. It is also possible that GFAP protein increases are occurring in other glial cell types that also express GFAP, such as microglia, which were not studied here. Neurons and other glial cell types can release diffusible factors during cellular stress that can cause cellular activation to occur (Sofroniew & Vinters, 2010). Future studies are needed to determine the specific mechanism and cellular source of white matter GFAP activation in ASD.

Previous research has implicated a role of oligodendrocyte pathology in ASD. Increases in myelin density around the corpus callosum in the ASD brain has been demonstrated using magnetization transfer imaging (MTI), a method used to visualize myelin in the brain (Gozzi et al., 2012). The myelin increase may result from aberrant signaling by growth factors that mediate myelination in the white matter (Zaccaria, Lagace, Eisch, & McCasland, 2010; Zikopoulos & Barbas, 2013). Oligodendrocytes are also very sensitive to metabolic changes that can be produced by various pathologies (Butts, Houde, & Mehmet, 2008). Oxidative stress and pro-inflammatory events in ASD could also contribute to pathology in this cell type (Angelidou et al., 2012; Ghanizadeh et al., 2012). In the present study, no differences in MOG protein levels or gene expression were observed comparing control and ASD donors. Since *MOG* is expressed in mature myelinating oligodendrocytes, it remains possible that oligodendrocytes at earlier stages of differentiation may be selectively or preferentially affected in ASD due to the above-mentioned evidence of aberrant signaling during the

cell maturation process. Further study measuring proteins that are specifically expressed by immature oligodendrocytes is warranted.

We found that elevated GFAP protein levels in ASD were not only specific to white matter relative to gray matter, but also occurred in BA24 but not in BA10. Among many attributes of BA24, it mediates behaviors related to social interaction (Gariépy et al., 2014), deficits of which are hallmark behavioral traits of ASD. Numerous previous studies have demonstrated pathology in BA24. Imaging and immunohistochemical studies have shown significant differences in BA24 between ASD and control brains including early developmental brain overgrowth in ASD (Minshew & Williams, 2007) as well as prominent glial activation in ASD (Vargas et al., 2005). BA24 also receives direct inputs from the limbic system, an area of the brain that modulates social and emotional behaviors and that also displays prominent ASD pathology (Devinsky, Morrell, & Vogt, 1995).

Limitations

While white and gray matter were dissected and analyzed separately, these samples still included a variety of cell types found within each type of tissue. The availability of postmortem tissue itself is a severe limitation in current and previous ASD studies. Available brain specimens are not only few in number, but also those available are from donors who were exposed to a number of medications that could influence experimental outcomes. In selecting and pairing study subjects, we used exclusion criteria to narrow down the study population to reduce variation in experimental data. Subjects with any co-morbidity, including epilepsy, were excluded. One ASD subject did have a seizure prior to death but had no reported history of seizure disorders.

Because of the selection criteria of this study, it is important to note that our data reflects pathology in a specific subset (no seizure disorders) of the ASD population.

CONCLUSION AND FUTURE DIRECTION

This is the first study that demonstrates distinct protein expression abnormalities in white matter not gray matter from BA24 brain tissue in humans. This finding suggests a very distinct cellular response to pathology in this brain region that did not extend to the other cortical region in this study. While this study is important in moving the field toward the identification of a pathological target, it lacks the clarity and depth needed to identify a distinct cellular source or pathophysiological mechanism. ASD patients symptomatically present with vast differences in abnormal behaviors. Using an approach targeted at molecular pathology within a single cell population, a common cellular dysfunction may be found that could unify our conceptualization of ASD brain pathology throughout the spectrum. In addition, identification of key cellular abnormalities could result in the development of novel targeted treatments for ASD.

CHAPTER 3

NTRK2 EXPRESSION DEFICIT IN LASER CAPTURED PYRAMIDAL NEURONS FROM THE ANTERIOR CINGULATE CORTEX IN MALES WITH AUTISM SPECTRUM DISORDER

Background

Autism spectrum disorder (ASD) is a neurodevelopmental disorder that includes repetitive behaviors and impairments in social communication and interaction (American Psychological Association, 2013). In recent years, ASD and disorders with associated autism behaviors have largely been attributed to genetic etiology in the literature (as reviewed by Jeste & Geschwind, 2014). However, it is likely that the heterogeneity of ASD results from a complex interplay of inherited genetics and developmental influences that result in abnormal intercellular communication in the brain. It is anticipated that areas of the brain that modulate the behaviors that are disrupted in ASD are particularly vulnerable to the cellular pathobiology of ASD likely includes disrupted connectivity between discrete areas of the brain that modulate behaviors that are abnormal from infancy.

The anterior cingulate cortex (ACC), an area of the brain that is involved in social and repetitive behaviors (Amaral et al., 2008), has consistently displayed abnormalities in ASD as revealed through imaging and neuroanatomical studies. Functional MRI was used to demonstrate hypoactivation of the anterior cingulate cortical activity between subjects with ASD and unaffected control subjects when conducting social tasks (as reviewed by Di Martino et al., 2009). However, resting-state differences have also been

identified in the ACC, suggesting that this brain area may display inherent alterations that are task-independent, but may substantially augment functional connectivity disassociations (Kennedy & Courchesne, 2008). Alternative methods including SPECT (Sasaki et al., 2010), EEG (Santesso et al., 2010; Sokhadze et al., 2010; Vlamings, Jonkman, Hoeksma, van Engeland, & Kemner, 2008), PET (Buchsbaum et al., 2001; Hall, Szechtman, & Nahmias, 2003; Nakamura et al., 2010), and fractional anisotropy (Thakkar et al., 2008) have also demonstrated abnormalities in the cingulate cortex in ASD.

The few postmortem studies that have focused on the anterior cingulate cortex have identified molecular and anatomical differences between ASD and developmentally normal control brain tissue. Stereology studies using the neocortex of the anterior cingulate indicated that neurons were smaller and demonstrated increased cell packing density (Simms, Kemper, Timbie, Bauman, & Blatt, 2009). Reductions in both mRNA and protein levels of the axonal guidance proteins plexinA4 and roundabout 2 were identified in tissue homogenates of ACC from ASD donors (Suda et al., 2011), as well as alterations in serotonin (Thanseem et al., 2010) and GABA (Oblak, Gibbs, & Blatt, 2009, 2010) related genes. Interestingly, increased gene expression in the transcriptional control factor, *Sp1*, was found in postmortem ACC from ASD donors, which could have wide spread implications and contribute to the complexity of ASD. Collectively, these studies demonstrate that pathology in the ACC exists in autism. However, little is known about what types of cells in the ACC are affected.

Pyramidal neurons in layer III of the neocortex are key cellular mediators of neural output of the anterior cingulate cortex. These pyramidal cells are excitatory

glutamatergic neurons that have a complex synaptic relationship with many other cell types in other neocortical layers of the ACC, including inhibitory neurons, glia, and long-range projecting glutamate neurons of layer 5. The current study was undertaken to investigate specific cellular pathology of pyramidal cells in layer III of the ACC from ASD donors. The levels of expression of several glutamate-related genes were measured specifically in pyramidal neurons captured by laser microdissection from layer III of the ACC from postmortem brain tissue from ASD donor and developmentally normal control subject brain tissue. The glutamate-related genes chosen for study were those associated with ASD identified in gene association, laboratory animal, and/or postmortem pathology studies (Barnby et al., 2005; Dölen et al., 2007; Jamain et al., 2002; Pinto et al., 2010; Purcell, Jeon, Zimmerman, Blue, & Pevsner, 2001; Rainey & van der Walt, 1998) and/or because of their strong association with glutamatergic neurotransmission. Additionally, two neurotrophic factor genes (*BDNF* and *NTRK2*) were studied because of the link between glutamatergic transmission and BDNF signaling (Browne & Lucki, 2013) and the association of BDNF and *NTRK2* pathology in ASD (Correia et al., 2010). The findings of this study demonstrate that ACC in ASD is associated with abnormal levels of expression of several genes related to glutamate neurotransmission, with the most striking finding being a robust reduction of NTRK2 gene expression.

Methods

Brain Tissue

Brain tissues for ASD and control donors were provided by the National Institutes

for Child Health and Development (NICHD) Brain and Tissue Bank (Baltimore, MD) and the Autism Tissue Program (Belmont, MA). In total, brain tissue from 12 developmentally normal control donors and 12 ASD donors were used for the different experiments (see Table 3.1). Comorbidities and causes of death were not included in the table in order to protect donor identities. However, control donors died by drowning (3 donors), heart condition (3 donors), trauma (3 donors), asphyxia (1 subject), pneumonia (1 subject), and unknown cause (1 subject). It should be mentioned that one control subject was diagnosed with depressive disorders and died by suicide. The ASD donors died by trauma (3 donors), asphyxia (3 donors), acute respiratory distress syndrome (1 subject), cardiopulmonary arrest (1 subject), cancer (1 subject), ketoacidosis (1 subject), bowel obstruction (1 subject), and cardiac arrhythmia (1 subject). The ASD group had one subject that the ASD diagnosis could not be medically confirmed after death and one subject that had a single seizure episode but did not have a medical diagnosis of seizure disorder. The samples were closely matched by gender and age. Additionally, we analyzed RNA integrity values (RIN, index of RNA quality) in matched pairs of donors prior to experimentation to be sure these were closely matched for the paired analyses (Auer et al., 2003).

Table 3.1. Subject demographic information.

Pair	ID	Age	Gender	RIN[a]	PMI (hours)[b]	Toxicology	Assays	Tissue
Control Donors								
1	AN14757	24	M	7.8	21.33	No drugs reported	LCM[c], qPCR[d]	BA24, BA10
2	AN07176	21	M	8	29.91	No drugs reported	LCM, qPCR	BA24, BA10
3	AN07444	17	M	7.5	30.75	Sertraline	LCM, qPCR	BA24
4	5408	6	M	7	16	No drugs reported	LCM, qPCR	BA24, BA10
5	4848	16	M	7.6	15	No drugs reported	LCM, qPCR	BA24, BA10
6	5342	22	M	8.1	14	No drugs reported	LCM, qPCR	BA24, BA10
7	5079	33	M	7.3	16	Ethanol	LCM, qPCR	BA24, BA10
8	M3231M	37	M	7.4	24	No drugs reported	LCM, qPCR	BA24, BA10
9	4590	20	M	7.6	19	No drugs reported	LCM, qPCR	BA10
Mean ± SEM (BA24 donors)		**22.0 ±3.4**		**7.59 ±0.13**	**20.9 ±2.4**			
Mean ± SEM (BA10 donors)		**22.4 ±3.4**		**7.60 ±0.13**	**19.4 ±1.9**			
ASD Donors								
1	AN04166	24	M	8.1	18.51	No drugs reported	LCM, qPCR	BA24, BA10
2	AN03935	20	M	8.6	28	No drugs reported	LCM, qPCR	BA24, BA10
3	AN02987	15	M	6.5	30.83	No drugs reported	LCM, qPCR	BA24
4	5144	7	M	8.0	3	No drugs reported	LCM, qPCR	BA24, BA10
5	5302	16	M	6.6	20	Risperidone, Fluvoxamine, Clonidine, Insulin	LCM, qPCR	BA24, BA10
6	5176	22	M	7.1	18	Risperidone	LCM, qPCR	BA24, BA10
7	5297	33	M	7.1	50	Quetiapine, Fluoxetine, Valproate, Ziprasidone	LCM, qPCR	BA24, BA10
8	5027	37	M	7.7	26	Risperidone, Fluvoxamine	LCM, qPCR	BA24, BA10
9	4999	20	M	7.0	14	No drugs reported	LCM, qPCR	BA10
Mean ± SEM (BA24 donors)		**21.6 ±3.4**		**7.46 ±0.27**	**24.3 ±4.8**			
Mean ± SEM (BA10 donors)		**22.2 ±3.3**		**7.53 ±0.24**	**23.4 ±5.4**			
P value[g] (BA 24)		**0.94**		**0.68**	**0.53**			
P value[g] (BA10)		**0.98**		**0.79**	**0.60**			

[a] RNA integrity number (index of RNA quality)
[b] Postmortem interval
[c] Endpoint PCR analysis of reversed transcribed RNA isolated from cells collected by laser capture microdissection
[d] Quantitative polymerase chain reaction of reverse transcribed RNA isolated from punch-dissected tissues
[g] Results of a two-tailed independent t-test comparing control and ASD groups.

Tissue preparation

Blocks of tissue containing ACC, specifically Brodmann area 24 (BA24), and prefrontal cortex Brodmann area 10 (BA10) were received and stored at -80^{o}C. All brain tissues were obtained from the left hemispheric side except AN03935. Tissue homogenates used for quantitative PCR were obtained using a 3 mm trephine to punch-dissect a 50 µm section of gray matter from the anterior cingulate that contained all 6 neocortical layers. A cryostat microtome was used to section tissue blocks for laser capture microdissection (LCM). Tissue from the cortex was sectioned at -20^{o}C and 10 µm sections were mounted slides that were immediately placed in a chilled microslide on ice. Between each tissue block, all physical elements of cryosectioning were thoroughly cleaned with 100% ethanol to avoid any cross contamination. Sectioned tissue was desiccated at room temperature for 5 minutes and stored at -80^{o}C until use. All subject tissue pairs were sectioned or punch-dissected on the same day to ensure storage time is identical for all tissue pairs.

Laser capture microdissection

Neurons were visualized by staining frozen 10 µm thick sections with the Histogene staining kit (Life Technologies; Grand Island, NY) according to manufacturer's instructions. In short, the protocol used a cresyl violet stain on an ethanol fixed slide followed by a series of dehydration steps. Stained slides were placed in a vacuum chamber until ready for LCM. Astrocytes were identified using a modified glial fibrillary acidic protein (GFAP) rapid immunohistochemistry protocol as previously described (Chandley et al., 2012; Ordway et al., 2009). Briefly, 10 µm slides

were fixed in acetone (5 min), blocked in horse serum (10 min), incubated with GFAP antibody (10 min; ThermoFisher, Pittsburgh, PA) anti-mouse antibody (5 min; Vectastain, Burlingame, CA), and avidin-biotinylated horseradish peroxidase (5 min; Jackson ImmunoResearch, West Grove, PA). The GFAP stain was visualized using diaminobenzidine (Sigma; St. Louis, MO) with ammonium nickel sulfate (Sigma; St. Louis, MO) for 5 min, then for an additional 5 min with 0.1% H_2O_2. Afterwards, the slide was ethanol dehydrated with 5 min incubation in xylene. The slide is kept in a vacuum chamber for 10 min prior to LCM.

LCM was performed using an Arcturus XT (Life Technologies) instrument. Neurons were extracted onto CapSure macrocaps using a 25 μm spot size that is first cut by a ultraviolet (UV) laser and then placed onto the cap by infrared (IR) laser spotting. Neurons were morphologically identified in layer III of the neocortex at 40X magnification (Figure 3.1C-D). Astrocytes were captured using an Arcturus Veritas (Life Technologies; Grand Island, NY) instrument. Astrocytes were morphologically identified at 60X magnification and placed onto caps by IR laser only using a 10 μm spot size (Figure 3.1E-F). Cells were removed from cap using lysis buffer incubation at 42^{o}C.

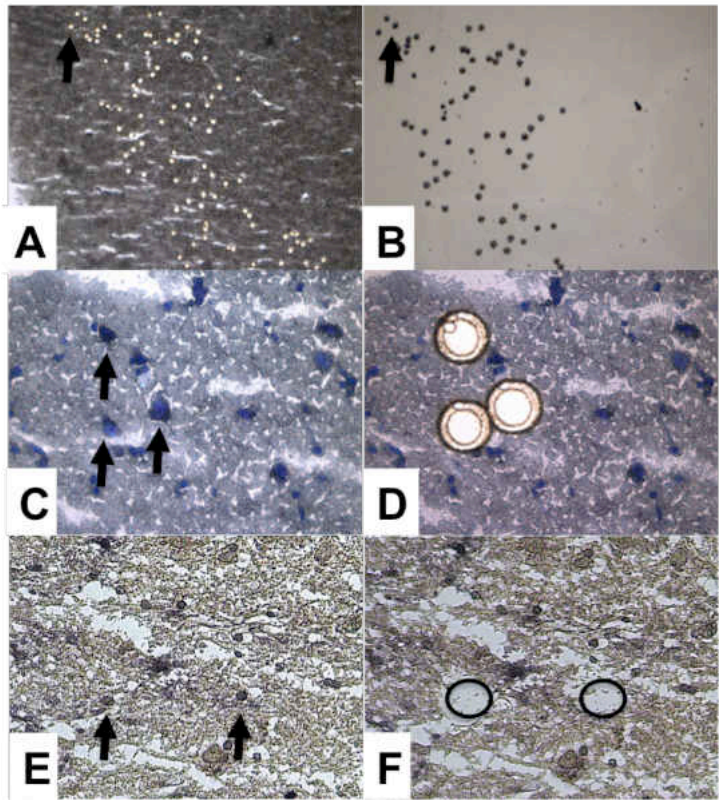

Figure 3.1. Laser capture microdissection of pyramidal neurons and astrocytes.

Shown in Panel A is the absence of laser captured nissl-stained pyramidal neurons from cortical layer 3 in BA24 gray matter tissue following capture (20x magnification). Panel B shows those cells adhered to the polymer cap (20x magnification). Panel C and D illustrate the before (C) and after (D) capture images for nissl-stained BA24 pyramidal neurons (40x magnification). Panel E and F shows the same laser capture process for GFAP immunostained astrocytes in BA24 gray matter (60x magnification).

RNA preparation and reverse transcriptase

Total RNA was extracted from tissue homogenates using the Maxwell simplyRNA LEV kit (Promega, Madison, WI). Laser captured cells using the

RNAqueous Micro kit with DNase treatment (Life Technologies; Grand Island, NY). RNA quality was assessed by measuring RIN values obtained using the Agilent 2100 Bioanalyzer (Agilent Technologies; Santa Clara, CA). RNA samples were reverse transcribed into cDNA using the Superscript III kit (Life Technologies; Grand Island, NY) that contained oligodT and random hexamer primers.

Quantitative polymerase chain reaction

Gene specific primers were either designed using Mfold web server software (Zuker, 2003) and primer quest design software (IDT; Coralville, IA) to generate 100 base-pair amplicons to span exon junctions. Some primers were purchased from a vendor (Qiagen; Valencia, CA). Gene primer sequences are shown in Appendix B. To quantify transcripts, endpoint PCR was used for RNA isolated from laser captured cells and real-time quantitative PCR (qPCR) was used for RNA isolated from tissue homogenates as previously described (Ordway et al., 2009; Xiang et al., 2008). For PCR reactions (*BDNF*, *GRIN2D*, *GRIN2B*, and *GRM8*) that were initially problematic using 5Prime Hot Master Mix Taq polymerase (5Prime; Gaithersburg, MA), a modified polymerase from Qiagen (Valencia, CA) was employed using the same reaction parameters.

Statistical analysis

Calculations for qPCR data involved converting cycle threshold (Ct) values to fold-change between control and autism donors using the $2^{-\Delta\Delta CT}$ method by Livak and Schmittgen (Livak & Schmittgen, 2001). Endpoint PCR data was computed as relative

values generated from the ratios of amounts of target gene expression to the average of two reference gene expressions. Afterwards, both data from qPCR and endpoint PCR were analyzed by the paired Student t-test. Statistical results are reported before and after Holm's Bonferroni correction (Gaetano, 2014; Holm, 1979) for the number of comparisons as noted in the results below. Pearson's correlation was used to determine possible effects of postmortem variables (age, RIN, and PMI) on the expression of each gene. Given the number of correlation tests, a $p<0.01$ was chosen *a priori* to indicate statistical significance in order to reduce type I errors.

Results

Glutamate-related gene expression.

The levels of expression of 7 ionotropic glutamate receptor subunit genes (*GRIN1*, *GRIN2A*, *GRIN2B*, *GRIN2C*, *GRIN2D*, *GRIK2*, *GRIA1*) and two metabotropic glutamate receptor genes (*GRM5*, *GRM8*) were measured in BA24 pyramidal neurons and surrounding astrocytes from ASD and age-matched control donors. *GRM8* expression was not detectable in astrocytes. Levels of *GRM8* expression were modestly lower in pyramidal neurons from ASD donors compared to matched control donors ($t=2.89$; $p=0.034$), but statistical significance was lost when the p value was corrected for the number of matched pair comparisons of gene expressions in neurons (Table 3.2). No other differences in the levels of expression of any glutamate receptor gene were observed in either pyramidal neurons or astrocytes comparing ASD to control donors (Figure 3.2).

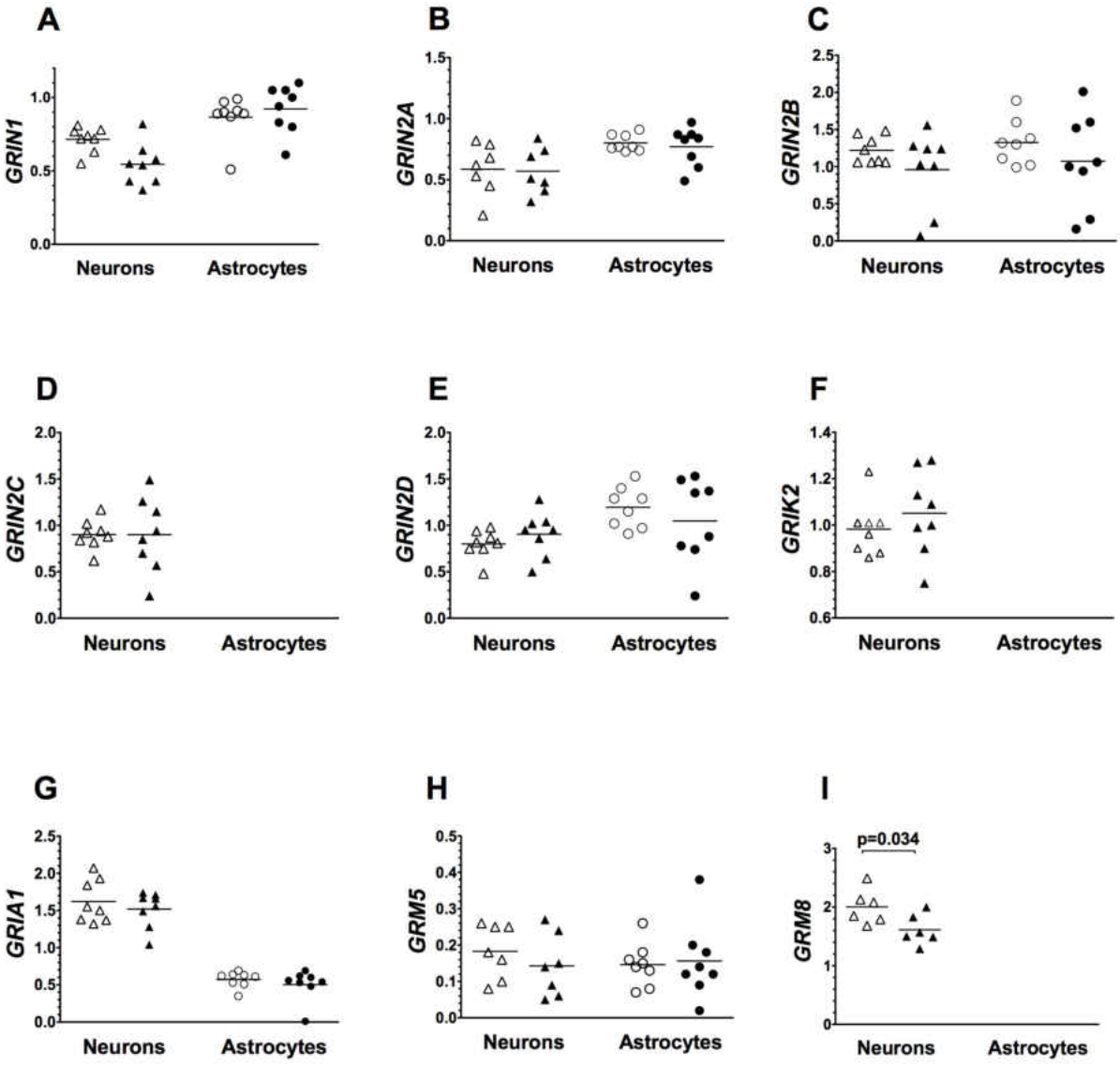

Figure 3.2. Levels of expression of ionotropic glutamate receptor subunits and metabotropic glutamate receptors.

Expression of glutamate receptors and receptor subunits was measured in laser captured BA24 pyramidal neurons and separately in surrounding astrocytes of typically developing control donors (open symbols) and ASD donors (closed symbols). Gene expression levels are normalized to the averaged levels of expression of references genes (*GAPDH* and *Ribo18S1*). Mean values are noted by horizontal lines and

statistical significance (uncorrected for the number of comparisons) is noted above the data points.

Table 3.2. Results of Holm-Bonferroni Sequential Correction of multiple paired Student's t-tests of gene expression data from BA24 neurons.

Gene (protein)	P value from Paired t-test	P' from correction[a]	Significance?
RNA18S1 / GAPDH	0.3774	1.000	No
GRIN1 (NR1)	0.0533	0.583	No
GRIN2A (NR2A)	0.9051	1.000	No
GRIN2B (NR2B)	0.1160	1.000	No
GRIN2C (NR2C)	0.9924	1.000	No
GRIN2D (NR2D)	0.1146	1.000	No
GRIA1 (GluR-1)	0.2424	1.000	No
GRIK2 (GRIK2, GluK2)	0.3793	1.000	No
GRM5 (mGluR5)	0.1061	1.000	No
GRM8 (mGluR8)	0.0340	0.408	No
SLC1A1 (EAAT3)	0.0235	0.312	No
SLC17A7 (VGlut1)	0.5034	1.000	No
GRIP1 (GRIP1)	0.0064	0.090	No
BDNF (BDNF)	0.4846	1.000	No
NTRK2 (NTRK2,TrkB)	0.0006	0.009	Yes

[a] Holm-Bonferroni corrected p value

Additional genes associated with glutamatergic neurotransmission were interrogated in BA24 pyramidal neurons and astrocytes, including glutamate transporter genes, *SLC1A1*, *SLC1A2*, *SLC1A3*, *SLC17A7*, and the glutamate receptor interacting gene, *GRIP1*. Of these genes, the expression of astrocyte-associated transporter genes *SLC1A2* and *SLC1A3* was not measured in neurons and the neuronal glutamate transporter gene *SLC1A1* was not measured in astrocytes. Levels of *SLC1A1* (t= 2.88;

p=0.024) and *GRIP1* (t=3.84; p =0.006) gene expression were lower in pyramidal neurons captured from ASD donors as compared to matched control donors (Figure 3.33). However, statistical significance was lost when p values were corrected for the number of matched pair comparisons (Table 3.2). No significant differences in the levels of expression of any of the glutamate-related genes, *SLC1A2*, *SLC17A7,* and *GRIP1*, were observed in astrocytes comparing ASD to matched control donors (Figure 3.3).

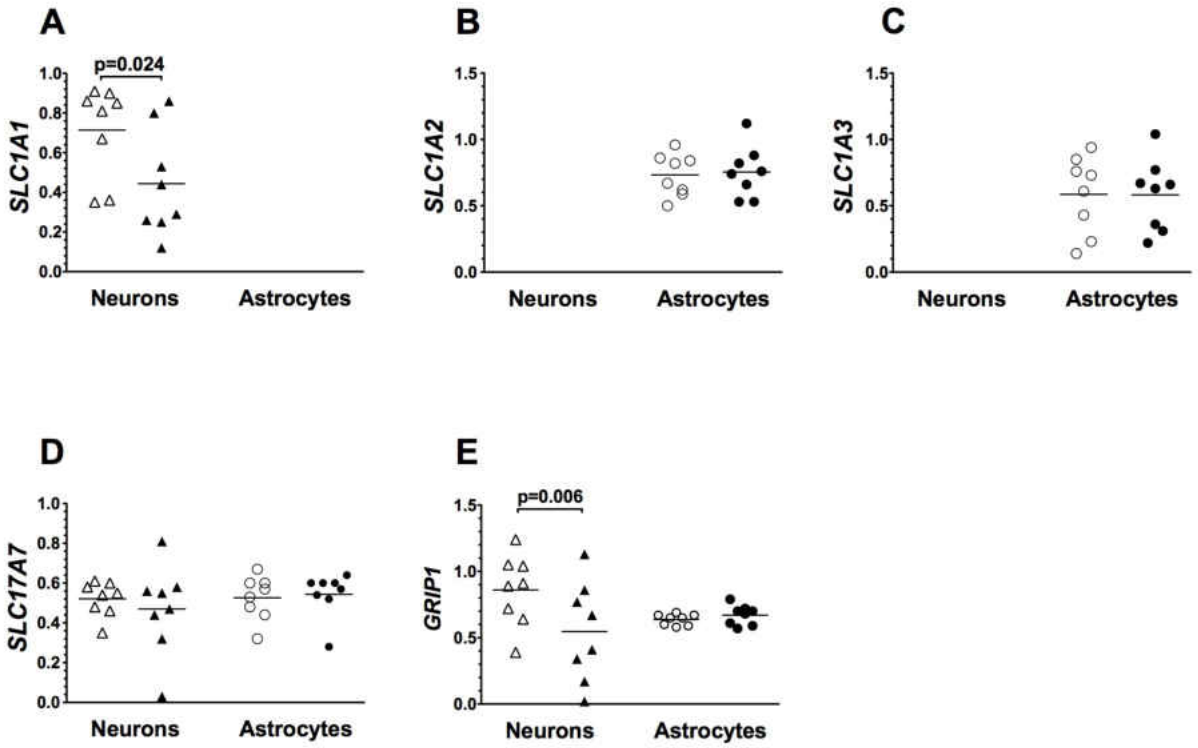

Figure 3.3. Levels of expression of glutamate transporter genes and a glutamate receptor interacting gene.

Gene expression was measured in laser captured BA24 pyramidal neurons and separately in surrounding astrocytes of typically developing control donors (open

symbols) and ASD donors (closed symbols). Gene expression levels are normalized to the averaged levels of expression of references genes (*GAPDH* and *Ribo18S1*). Mean values are noted by horizontal lines and statistical significance (uncorrected for the number of comparisons) is noted above the data points.

BDNF/NTRK2.

Levels of expression the neurotrophic factor gene *BDNF* and its receptor gene *NTRK2* were measured in pyramidal neurons and astrocytes from BA24 (Figure 3.4). *BDNF* expression in both neurons and astrocytes was similar comparing ASD to matched control donors. However, *NTRK2* expression levels were robustly lower in pyramidal neurons (t=5.87; p=0.0006), but not astrocytes, from ASD donors as compared to control donors. The difference in *NTRK2* expression levels between ASD and control donors remained statistically significant after correction for the number of matched comparisons (Table 3.2).

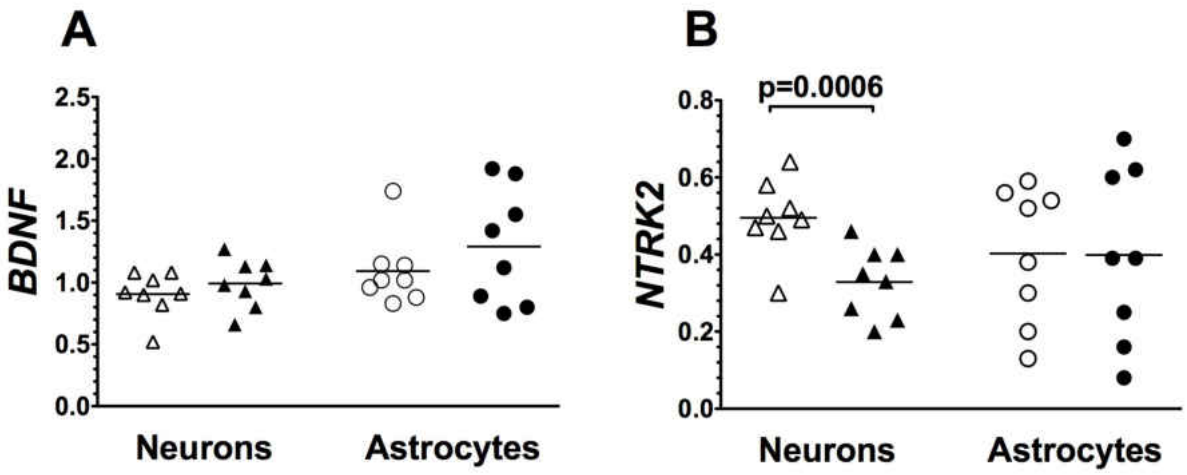

Figure 3.4. Levels of expression of *BDNF* and its receptor gene *NTRK2*.
Gene expression was measured in laser captured BA24 pyramidal neurons and separately in surrounding astrocytes of typically developing control donors (open symbols) and ASD donors (closed symbols). Gene expression levels are normalized to the averaged levels of expression of references genes (*GAPDH* and *Ribo18S1*). Mean values are noted by horizontal lines and statistical significance (uncorrected for the number of comparisons) is noted above the data points.

Expression of selected genes in BA10.

The expression levels of four genes were studied in BA10 pyramidal neurons from ASD and control donors. Chosen for study were those genes analyzed in BA24 pyramidal neurons that demonstrated either no difference (*GRM5*), marginal or modest differences (*GRIN1*, *SLC1A1*) or highly significant differences (*NTRK2*) comparing ASD to control donors as noted above. In this set of experiments, BA10 tissue from one age-matched pair of donors used in the BA24 studies above was not available; BA10 tissue from one different age-matched pair of donors was substituted as noted in Table 3.1. The expression levels of each of these four genes in laser captured pyramidal neurons from BA10 were similar in ASD and matched controls (Figure 3.5; *GRIN1* t=0.74, p=0.49; *GRM5* t=0.90, p=0.40; *SLC1A1* t=0.26, p=0.80; *NTRK2* t=0.03, p=0.97).

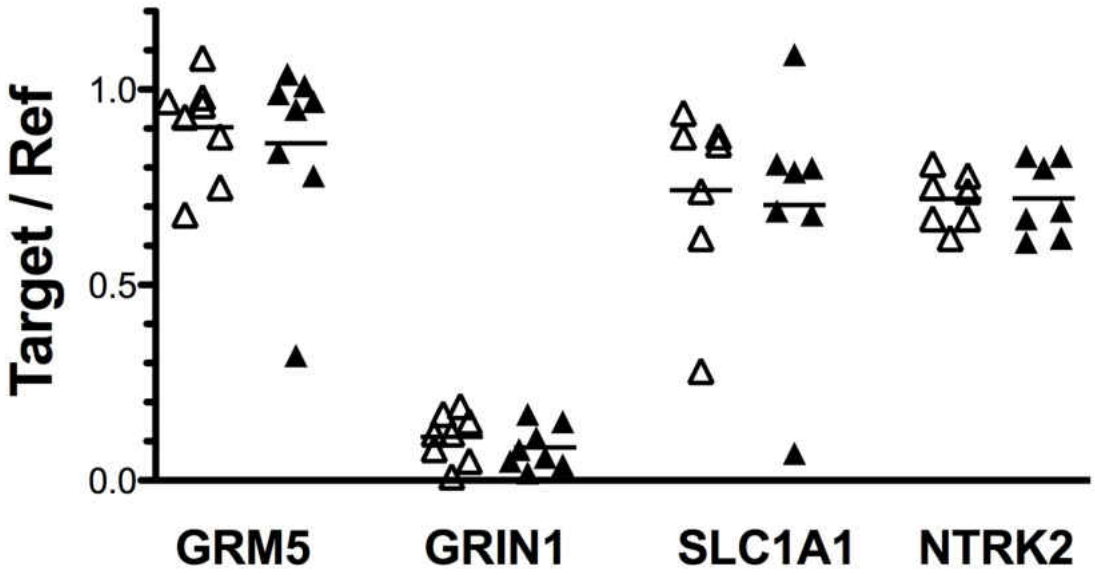

Figure 3.5. Levels of expression of *GRM5, GRIN1, SLC1A1,* and *NTRK2* in pyramidal neurons of BA10.

Gene expression was measured in laser captured BA10 pyramidal neurons from typically developing control donors (open symbols) and ASD donors (closed symbols). Gene expression levels are normalized to the averaged levels of expression of references genes (*GAPDH* and *Ribo18S1*). Mean values are noted by horizontal lines. No statistically significant differences were observed.

Demographic variables, reference genes, and tissue factors.

There were no statistical differences between ASD and matched control donors of BA24 tissue regarding age, RIN, or PMI values (Table 3.1). Likewise, there were no differences in these variables comparing groups of donors of BA10 tissue (Table 3.1). There were no significant correlations between age or PMI and any of the 15 gene

expressions measured in BA24 pyramidal neurons (Table 3.3). There was a significant correlation between levels of *GRIN2C* expression and RIN values, but there were no other correlations between RIN and the levels of any mRNA that was studied in BA24 pyramidal neurons. In BA24 astrocytes, age correlated significantly with *NTRK2* gene expression levels ($p=0.002$), but not with levels of any other gene (Table 3.4). RIN did not significantly correlate with expression levels of any gene in BA24 astrocytes, while PMI correlated with only *SLC17A7* gene expression in BA24 astrocytes (Table 3.4). In BA10 pyramidal neurons, there were no significant correlations between age, RIN, or PMI and the levels of expression of any of the target or reference genes (Table 3.5).

Table 3.3. Pearson's correlation analyses for possible relationships between gene expression levels in BA24 neurons and age, RNA quality (RIN) and postmortem interval (PMI).

Gene[a] (protein[b])	Statistic	Age	RIN	PMI
RNA18S1 / GAPDH[c]	Pearson Correlation Sig. (2-tailed) N	-.309 .243 16	.043 .875 16	-.250 .350 16
GRIN1 (NR1)	Pearson Correlation Sig. (2-tailed) N	.050 .855 16	.318 .231 16	-.226 .400 16
GRIN2A (NR2A)	Pearson Correlation Sig. (2-tailed) N	-.055 .851 14	.531 .051 14	.176 .548 14
GRIN2B (NR2B)	Pearson Correlation Sig. (2-tailed) N	.109 .687 16	.579 .019 16	-.250 .351 16
GRIN2C (NR2C)	Pearson Correlation Sig. (2-tailed) N	.229 .394 16	.642[d] .007 16	-.091 .737 16
GRIN2D (NR2D)	Pearson Correlation Sig. (2-tailed) N	.322 .224 16	.082 .763 16	.203 .452 16
GRIA1 (GluR-1)	Pearson Correlation Sig. (2-tailed) N	-.374 .154 16	.213 .429 16	-.012 .966 16
GRIK2 (GRIK2, GluK2)	Pearson Correlation Sig. (2-tailed) N	-.316 .233 16	.250 .350 16	-.346 .189 16
GRM5 (mGluR5)	Pearson Correlation Sig. (2-tailed) N	-.017 .953 15	-.117 .677 15	-.435 .105 15
GRM8 (mGluR8)	Pearson Correlation Sig. (2-tailed) N	.131 .684 12	.140 .664 12	.029 .929 12
SLC1A1 (EAAT3)	Pearson Correlation Sig. (2-tailed) N	-.191 .478 16	.285 .284 16	-.591 .016 16
SLC17A7 (VGlut1)	Pearson Correlation Sig. (2-tailed) N	.003 .991 16	.312 .240 16	-.358 .173 16
GRIP1 (GRIP1)	Pearson Correlation Sig. (2-tailed) N	-.128 .638 16	.265 .320 16	-.030 .913 16
BDNF (BDNF)	Pearson Correlation Sig. (2-tailed) N	.005 .985 16	-.084 .757 16	-.212 .430 16
NTRK2 (NTRK2,TrkB)	Pearson Correlation Sig. (2-tailed) N	.522 .038 16	.271 .310 16	-.076 .780 16

Table 3.4. Pearson's correlation analyses for possible relationships between gene expression levels in BA24 astrocytes and age, RNA quality (RIN) and postmortem interval (PMI).

Gene[a] (protein[b])	Statistic	Age	RIN	PMI
RNA18S / *GAPDH*[c]	Pearson Correlation	.074	.119	.443
	Sig. (2-tailed)	.786	.662	.085
	N	16	16	16
GRIN1 (NR1)	Pearson Correlation	.092	.133	-.003
	Sig. (2-tailed)	.736	.624	.991
	N	16	16	16
GRIN2A (NR2A)	Pearson Correlation	.282	.516	-.116
	Sig. (2-tailed)	.290	.041	.670
	N	16	16	16
GRIN2B (NR2B)	Pearson Correlation	.523	.520	-.060
	Sig. (2-tailed)	.038	.039	.826
	N	16	16	16
GRIN2D (NR2D)	Pearson Correlation	.547	.395	.227
	Sig. (2-tailed)	.028	.130	.398
	N	16	16	16
GRIA1 (GluR-1)	Pearson Correlation	-.046	.490	.009
	Sig. (2-tailed)	.865	.054	.975
	N	16	16	16
GRM5 (mGluR5)	Pearson Correlation	.577	.328	.112
	Sig. (2-tailed)	.019	.216	.679
	N	16	16	16
SLC1A3 (EAAT1)	Pearson Correlation	-.340	-.238	-.344
	Sig. (2-tailed)	.197	.375	.192
	N	16	16	16
SLC1A2 (EAAT2)	Pearson Correlation	-.101	.023	-.186
	Sig. (2-tailed)	.711	.932	.491
	N	16	16	16
SLC17A7 (vGlut1)	Pearson Correlation	-.470	.214	-.655[d]
	Sig. (2-tailed)	.066	.426	.006
	N	16	16	16
GRIP1 (GRIP1)	Pearson Correlation	-.086	-.146	.378
	Sig. (2-tailed)	.751	.590	.149
	N	16	16	16
BDNF (BDNF)	Pearson Correlation	.479	-.153	.492
	Sig. (2-tailed)	.060	.571	.053
	N	16	16	16
NTRK2 (NTRK2, TrkB)	Pearson Correlation	.711[d]	.123	.187
	Sig. (2-tailed)	.002	.649	.488
	N	16	16	16

Table 3.5. Pearson's correlation analyses for possible relationships between gene expression levels in BA10 neurons and age, RNA quality (RIN) and postmortem interval (PMI).

Gene[a] (protein[b])	Statistic	Age	RIN	PMI
RNA18S1 / GAPDH[c]	Pearson Correlation	-.122	-.407	.002
	Sig. (2-tailed)	.653	.148	.995
	N	16	14	14
GRIN1 (NR2A)	Pearson Correlation	.114	.415	.059
	Sig. (2-tailed)	.675	.140	.841
	N	16	14	14
GRM5 (mGluR5)	Pearson Correlation	.328	.228	.088
	Sig. (2-tailed)	.215	.432	.765
	N	16	16	14
SLC1A1 (EAAT3)	Pearson Correlation	-.105	.659	.282
	Sig. (2-tailed)	.722	.020	.374
	N	14	12	12
NTRK2 (NTRK2, TrkB)	Pearson Correlation	-.234	.537	-.094
	Sig. (2-tailed)	.420	.072	.773
	N	14	12	12

Reference genes were carefully chosen as those that were stable in their expression levels across the two groups of subjects. The ratios of levels of expression of *RNA18S1* and *GAPDH* were not significantly different in laser captured BA24 neurons ($t = 1.00$, $p = 0.35$), BA24 astrocytes ($t = 0.93$, $p = 0.38$), or BA10 neurons ($t = 1.82$, $p = 0.11$) comparing ASD and matched control donors (Figure 3.6).

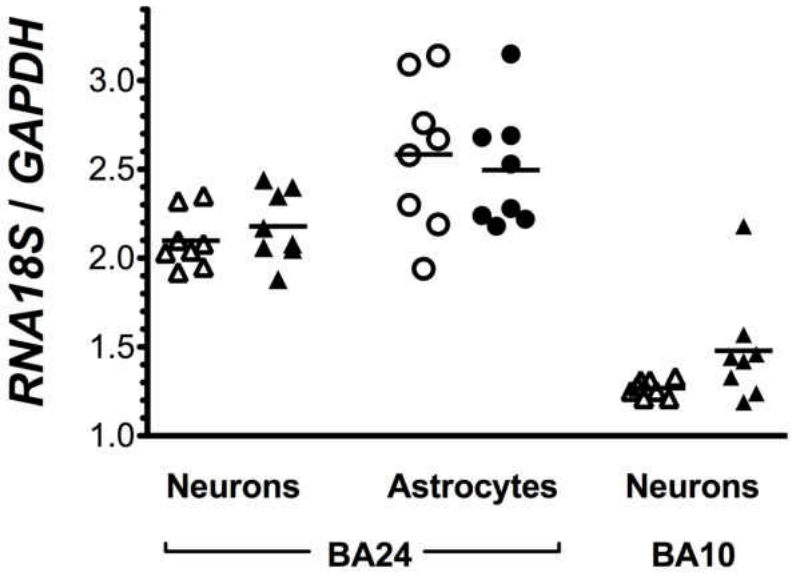

Figure 3.6. Ratio of reference gene expression levels.

Gene expression was measured for *GAPDH* and *Ribo18S1* in typically developing control donors (open symbols) and ASD donors (closed symbols). The ratio of gene expression between the two reference genes was compared for control and ASD subjects for BA24 neurons and astrocytes and BA10 neurons to ensure that the reference genes had stable expression levels between the groups. No statistically significant differences were observed.

It should be noted that we wished to screen multiple brain regions for these gene expression changes to determine the extent to which they occurred in the brain. Because LCM is time-intensive and expensive, we attempted to measure *SLC1A1*, *GRIP1*, *NTRK2* expression in RNA isolated from homogenates of ACC. However, we were unable to detect any differences in expression of these genes in RNA isolates

from homogenates of ACC, using tissues collected from seven of the eight ASD – control donor pairs that were used for the LCM study above (Figure 3.7). To verify the stability of reference gene expression levels across the two groups of subjects, the ratios of *GAPDH* and *TATA* expression were examined and were not found significantly different when comparing ASD and matched control donors (t = 0.19, p = 0.86) (Figure 3.8).

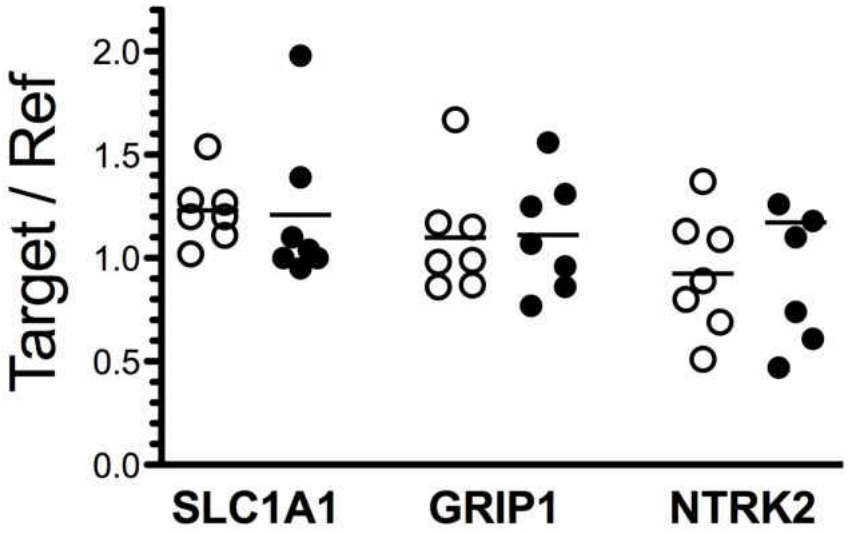

Figure 3.7. Levels of expression of *SLC1A1*, *GRIP1*, and *NTRK2* in punch-dissected BA24 gray matter.

Gene expression was measured in typically developing control donors (open symbols) and ASD donors (closed symbols) using RNA isolated from homogenates of punched-dissected gray matter rather than specific laser captured cells as shown in Figures 1-5. Gene expression levels were determined by real time PCR and are normalized to the geometric mean of stable references genes (*GAPDH and TATA)*. No statistically significant differences were observed.

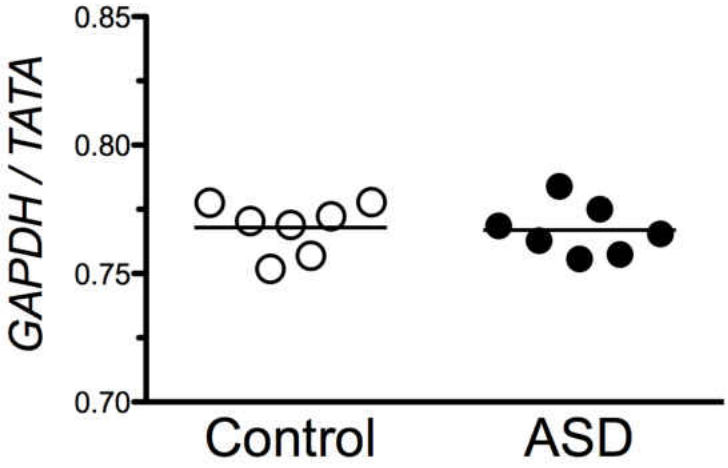

Figure 3.8. Ratio of reference gene expression levels for qPCR.

Gene expression was measured for *GAPDH* and *TATA* in typically developing control donors (open symbols) and ASD donors (closed symbols). The ratio of gene expression between the two reference genes was compared for control and ASD subjects for BA24 punch-dissected gray matter tissue samples to ensure that the reference genes had stable expression levels between the groups. No statistically significant difference was observed.

Four of the ASD donors had been prescribed psychotherapeutic medications, with three of the four receiving SSRI antidepressants and four of the four receiving antipsychotic drugs (see Table 3.1). Considering that effects of psychotherapeutic drugs might contribute to observed differences in gene expression in BA24 neurons as shown above, a comparison was made of antidepressant/antipsychotic exposed ASD donors to ASD donors not exposed to these drugs. Albeit the sample sizes of these two

groups are small and that these two subgroups were not matched for age and other demographic variables, there were no significant difference in levels of *GRM8* (unpaired t-test; t=0.17, p=0.87), *GRIP1* (0.01, p=0.99), *SLC1A1* (t=0.28, p=0.79), *NTRK2* (t=0.59, p=0.57) comparing antidepressant/antipsychotic exposed ASD donors to ASD donors without these drugs.

Discussion

This study examined the expression of genes involved in glutamatergic neurotransmission in ASD. We found modestly low levels of expression of genes encoding a glutamate receptor (*GRM8*), glutamate transporter (*SLC1A3*), and a glutamate receptor anchoring protein (*GRIP1*), and a robust reduction in expression of a neurotrophin receptor gene (*NTRK2*) in pyramidal neurons dissected by LCM from ACC tissue of donors with ASD when compared to typically developing controls. This is the first study to use LCM to isolate a specific cell population to examine the molecular pathology of ASD. The use LCM to capture distinct cell populations provided cellular resolution to the assessment of pathology, and permitted identification of gene expression changes that we were unable to detect using homogenates of the same brain region in the same subjects. The difference in the results of LCM of single cell populations versus homogenates of tissues is likely the result of overlapping gene expression in other unaffected cell types that in essence dilute cell-specific gene expression changes, as has been demonstrated in research on Alzheimer's disease (Ginsberg & Che, 2005; Ginsberg et al., 2004). The gene expression deficits identified in the present study were restricted to ACC pyramidal neurons and not found in

surrounding astrocytes in the same brain region, or in pyramidal neurons in BA10 of the prefrontal cortex, suggesting the presence of a cell- and region-specific pathology in ASD.

Cells used for this study were dissected from the neocortical layer III of the ACC where both changes in cell size and packing density have been demonstrated previously (Simms et al., 2009). Also, mini-column disturbances i.e. reduced column width and increased column number have been shown in the ACC with pyramidal neurons demonstrating misalignment (Casanova et al., 2002). An increase in spine density of pyramidal neurons in frontal, parietal and temporal lobes has been reported for ASD (Avino & Hutsler, 2010), although the ACC has not been studied to date. The present study identifies specific gene expression abnormalities in glutamatergic pyramidal cells and adds to the growing body of literature that implicates these excitatory neurons in the complex pathobiology of autism.

A recent study demonstrated that neurons, not glia, from the neocortex of multiple brain regions exhibited decreased gene expression that indicated abnormal columnar architecture within all six cortical layers that the authors referred to as “patches” (Stoner et al., 2014). The authors of these data acknowledge that they have uncovered a unique ASD cortical pathology involving several genes that are found in multiple cell types, (Stoner et al., 2014); but no mechanism of pathogenesis is known. In addition, an elevated number of neurons has been detected in layer VI of the ASD ACC indicating that incomplete migration of neurons may have occurred during development (Simms et al., 2009). Our studies have identified abnormal gene expression in pyramidal neurons, but not glia, that could contribute to abnormal

columnar structure in the neocortex in autism.

A striking finding of this study was the decreased expression of the growth factor receptor gene *NTRK2B* in ACC pyramidal neurons from ASD donors. This gene encodes the high-affinity tyrosine kinase B receptor, TrkB, the ligand for which is BDNF, NT-3 and NT-4/5 (Klein et al., 1991; Klein, Lamballe, Bryant, & Barbacid, 1992). TrkB signaling is of critical importance to cell function, with ligand-activated TrkB engaging several intracellular signaling pathways including MAPK, PI3, and ERK that are important in neurotransmission, plasticity and differentiation (Boulle et al., 2012). Several laboratories have reported elevated peripheral and central BDNF levels in ASD (Connolly et al., 2006; Correia et al., 2010; Miyazaki et al., 2004; Nelson et al., 2006; Perry et al., 2001). A genetic association between polymorphisms of *NTRK2* and ASD has also been identified (Correia et al., 2010). It seems unlikely that a functional polymorphism *NTRK2* that might account for the observed reduction in *NTRK2* expression in pyramidal cells since one would expect *NTRK2* gene expression to be similarly affected in astrocytes and pyramidal neurons in other brain regions. Of the cells that we studied, we found the reduction of *NTRK2* only in ACC pyramidal neurons. Interestingly, the most strongly associated polymorphisms in ASD were found in the intron-spanning regions of *NTRK2,* which could reflect aberrant transcriptional mechanisms under cell-specific control in ASD. Mouse knock out (KO) models indicate that *NTRK2* deficient mice die soon after birth (Klein et al., 1993; Rohrer et al., 2004). However, mice with a conditional loss of *NTRK2* expression exhibit a wide variation in behavior ranging from social deficits to antisocial behavior (as reviewed by Lindholm & Castrén, 2014). Interestingly, the TrkB receptor in BDNF conditional KO mice develop

BDNF-independent signaling mechanisms (Di Lieto et al., 2012). It is noteworthy that the BTBR mouse model for ASD exhibits reduced TrkB protein expression (Scattoni, Martire, Cartocci, Ferrante, & Ricceri, 2013). Defective TrkB signaling has been shown in Angelmann (Cao et al., 2013) and Fragile X (Uutela et al., 2014) mouse models, both of which are syndromes with a high incidence of autistic features. The present study provides further support for a role of BDNF/TrkB in ASD, specifically providing evidence of reduced *NTRK2* gene expression in ACC pyramidal neurons.

Gene expression changes in synapse-related genes have been demonstrated in disorders that have autistic features such as Angelmann Syndrome and Fragile X Syndrome (as reviewed by Ebert & Greenberg, 2013). Abnormalities in neurotransmitter signaling networks are likely to be a core component of the cellular neurobiology of ASD. We chose to interrogate potential expression changes in several genes associated with excitatory amino acid cell signaling in autism. Three of these genes, *SLC1A1, GRIP1*, and *GRM8*, demonstrated trends toward reduced expression in ACC pyramidal neurons in ASD. *SLC1A1* is responsible for glutamate uptake from the synapse by pyramidal neurons while *GRIP1* anchors AMPA receptors to the cell membrane. *GRM8* inhibits the adenylyl cyclase/cAMP pathway and decreases the likelihood of cell death associated with excess NMDA signaling (Ambrosini, Bresciani, Fracchia, Brunello, & Racagni, 1995). The decreased expression of *GRM8* receptor in ASD, if accompanied by reduced GRM8 receptor, could leave pyramidal cells susceptible to neurotoxic effects of elevated glutamate signaling through the NMDA receptor. This neurotoxic effect could be amplified further if reduced *SLC1A1* expression observed in ASD results in less glutamate transporter activity at the

glutamatergic synapse, thereby further increasing glutamate activation of NMDA receptors on these pyramidal neurons. Reduced *GRIP1* expression, as we observed in ASD, could be a compensatory mechanisms to override excess NMDA receptor activation by glutamate. Whatever the exact sequence or consequence, abnormal expression levels of these genes implies that excitatory output from the ACC via pyramidal neurons is disrupted in ASD. Because *GRIP1* and *NTRK2* is expressed by multiple cell types, it cannot be dismissed that these glutamatergic-related gene expression decreases are only found in excitatory cells. While we did not find *GRIP1* or excitatory transporter changes (*SLC1A2* and *SLC1A3*) in the glia cells studied herein, altered expression of these genes could occur in inhibitory neurons of the ACC, which were not studied. Nevertheless, any disruption of glutamate transmission and function implicates a compromise in the delicate balance of inhibitory and excitatory neuronal activity of the ACC. Future studies need to include a more detailed examination of gene expression in other cell types of the ACC.

Limitations

There were several limitations in the current study that should be taken into consideration. First, like many studies of ASD relying on postmortem brain tissue, the number of donors available was limited and reduced the power of the study. It should be noted that all donors that had a history of seizure disorder were excluded from the study to reduce experimental variability. Our laboratory has observed that the use of LCM to isolate distinct cell populations results in reduced variability of data, permitting the use of smaller sample sizes to obtain statistical significance. ASD is a highly

heterogeneous disorder and there were not enough brain donors to permit us to examine the gene expressions in subgroups of donors based on clinical presentation. Changes in gene expression do not always correlate with changes in the expression of the cognate protein, and often a change in gene expression is not temporally correlated with changes in the cognate proteins. Hence, whether reduced *NTRK2B* expression in ASD pyramidal neurons results in lower TrkB protein in these cells is not currently known. Nevertheless, altered levels of *NTRK2B* expression in ASD is highly suggestive of perturbed TrkB signaling in ASD. ASD donors used in the present study were exposed to psychotherapeutic drugs that could alter gene expression, particularly selective serotonin uptake inhibitor (SSRIs) and risperidol, an atypical antipsychotic. But, repeated administration of the antidepressants tranylcypromine, sertraline, or desipramine to rats increases *NTRK2* expression (Nibuya, Morinobu, & Duman, 1995). Hence, reduced *NTRKB* expression in the present study is unlikely to reflect previous antidepressant drug therapy. Repeated treatment of rats with ripseridol produced no change in TrkB immunoreactivity in the brain (Angelucci, Mathé, & Aloe, 2000), again suggesting that psychotherapeutic drug exposure is not a likely mediator of reduced *NTRK2* expression in ASD in the present study. Findings herein demonstrate no obvious effect of psychotherapeutic drug exposure on *NTRK2* (or *GRM8*, *GRIP1*, *SLC1A1*) expression. Tissue-related physical factors were considered as possible sources of variance in these experiments. However, there were no significant differences between ASD and control donor samples when comparing age, RNA quality (RIN), postmortem intervals (Table 3.1).

Conclusions

Multiple gene abnormalities are significantly associated with ASD (Betancur, 2011). It therefore seems likely that multiple etiologies exist that can result in ASD. Brain pathology is downstream to gene polymorphisms and etiologies, and more proximal to the pathophysiology underlying the abnormal behaviors. Hence, the neuropathology of autism may be more limited in terms of variability than the genotypes that can contribute to it, i.e. different etiologies may result in a similar structural/neurochemical abnormality that disrupts function to produce a specific set of behavioral abnormalities. The present study was designed to examine possible disruption of a key neuronal unit, the glutamatergic pyramidal neuron, of the ACC in ASD. The data presented here reveals strong evidence of disrupted neurochemistry of ACC pyramidal neurons, specifically involving glutamatergic neurotransmission and neurotrophic factor (BDNF) signaling through the TrkB receptor. It is tempting to speculate that abnormalities in ACC as revealed in imaging studies of ASD patients are at least partially the result of deficits in pyramidal neuronal function in the ACC as revealed in the present study. Pyramidal neurons in layer III of the ACC synapse with other cortical neurons including inhibitory neurons and long-range pyramidal motor neurons in layer V and the present findings suggest that neural communication with these other brain areas or pathways is altered in ASD. Interestingly, pyramidal neurons take years to reach maturity, possibly well into adolescence (Huttenlocher, 1970), indicating that normal neural development of this cell type may be especially vulnerable to deleterious environmental influences occurring early in life.

CHAPTER 4

RNA-SEQ ANALYSIS OF LASER CAPTURED SAMPLES FROM ANTERIOR CINGULATE CORTEX OF MALES WITH AUTISM SPECTRUM DISORDER

Introduction

Ginsberg et al (Ginsberg, Alldred, & Che, 2011) have shown significant disparities between gene expression differences found using homogenate brain samples versus laser captured single cell populations from the same tissues. The Ginsberg study used microarrays to examine the brains of control and Alzheimer's disease (AD) subjects. Microarray data from CA1 captured cell populations displayed a dissimilar gene expression profile compared to the data obtained from hippocampal homogenate samples. Genes found to be essential for the dysfunction of CA1 neurons in AD were not found significantly altered in the homogenate samples. We have also observed different findings depending on whether tissue contains multiple or single cell types (compare Figures 3.7 and 3.4 for *NTRK2* expression). These findings demonstrate the need to focus gene expression profiling on single cell populations in order to achieve a better understanding of the biochemical and cellular basis of pathology.

Within the ASD research field to date, molecular pathology studies used brain samples that contain multiple cell types. The results of these studies have been insufficient to formulate a theoretical etiology of the disease. ASD is a spectrum of disorders with patients exhibiting vast differences in symptom presentation. By using an approach targeted at molecular pathology within a single cell population, a common

cellular dysfunction might be found that could unify our conceptualization of ASD brain pathology throughout the spectrum. Identification of key cellular abnormalities could result in the development of novel targeted treatments for ASD. In this study, LCM was used to obtain clusters of multiple cell types and separately, selected cell populations. Using these samples, I attempted to development experimental protocols to permit gene expression profiling using RNA-Seq technology. Ultimately, I hoped to identify specific gene expression abnormalities in specific cell populations to further our understanding of ASD pathology. However, the experimental approach of combining LCM of single cell populations with RNA-Seq, was a first in the field with no published study known to us to date. Therefore, first and foremost was the determination of the feasibility of the approach.

RNA-Seq provides in-depth transcriptome analysis that cannot be achieved using methods such as microarrays, providing information regarding splicing variants, transcriptional start points, and rare RNA isoforms. RNA-Seq permits researchers to explore all levels of transcriptional regulation in the cell (Nagalakshmi, Waern, & Snyder, 2010; Wang, Gerstein, & Snyder, 2009; Wilhelm & Landry, 2009). This type of analysis has the potential to bring light to unanswered questions of ASD pathology, and also to establish a novel method to investigate the contributory roles of different brain cell types in neurological diseases. Data generated herein will be made available for mining in future studies, although it is likely that samples in addition to those that I have now analyzed will be needed to enhance the statistical power of the study.

Methods

Brain Tissue

Frozen tissue blocks containing BA24 from six ASD donors and nine typically developed control donors were obtained from Autism Tissue Program, Harvard Brain Tissue Resource Center (Belmont, MA) and NICHD Brain and Tissue Bank for Developmental Disorders (Baltimore, MD) (Table 4.1). This study was reviewed and approved for exemption by the Institutional Review Board of East Tennessee State University under the Department of Heath and Human Services exemption 45 CFR 46.101(b) relating to the use of publicly available unidentifiable pathology specimens. ASD and control donors were matched prior to experimentation as closely as possible by age primarily, but also by RNA quality (Table 4.1), to reduce the impact of these factors from the two groups. ASD donors met diagnostic criteria outlined in the Diagnostic and Statistical Manual (DSM) IV for autistic disorder. The Autism Diagnostic Interview-Revised (ADI-R) and other medical records were also used to confirm diagnoses. Causes of death and comorbidities are not included in Table 4.1 to protect the identities of the decedents. Cause of death for typically developed control donors included drowning (3 donors), motor vehicle accident (2 donors), asphyxia (1 donor), abdominal injuries (1 donor), and heart attack (1 donor). Cause of death for ASD donors included acute respiratory distress syndrome (1 donor), cancer (1 donor), drowning (1 donor), head trauma (1 donor), diabetic ketoacidosis (1 donor), and bowel obstruction (1 donor).

Table 4.1. Subject demographic information.

ID	Age	Gender	RIN[a]	PMI (hours)[b]	Toxicology	Sample
Controls						
AN14757	24	M	7.8	21.33	No drugs reported	WM[d], Neuron
AN07444	17	M	7.5	30.75	Sertraline	WM
5408	6	M	7	16	No drugs reported	WM, Neuron
4848	16	M	7.6	15	No drugs reported	Neuron
5342	22	M	8.1	14	No drugs reported	WM
5079	33	M	7.3	16	Ethanol	WM
M3231M	37	M	7.4	24	No drugs reported	WM, Neuron
4337	8	M	8.4	16	No drugs reported	WM
MEAN	**20.38**		**7.64**	**19.14**		
SEM	**3.88**		**0.16**	**2.05**		
ASD						
AN04166	24	M	8.1	18.51	No drugs reported	WM, Neuron
AN02987	15	M	6.5	30.83	No drugs reported	WM
5144	7	M	8	3	No drugs reported	WM, Neuron
5302	16	M	6.6	20	Risperidone, Fluvoxamine, Clonidine, Insulin	Neuron
5027	37	M	7.7	26	Risperidone, Fluvoxamine	WM, Neuron, Astrocyte
4721	8	M	6.1	16	No drugs reported	WM
MEAN	**17.83**		**7.17**	**19.06**		
SEM	**4.59**		**0.35**	**3.90**		
P value[g]	**0.68**		**0.26**	**0.99**		

[a] RNA integrity number (index of RNA quality)
[b] Postmortem interval
[c]Results of a two-tailed independent t-test comparing control and ASD groups.
[d]White matter

Tissue Preparation and Laser Capture Microdissection

Superficial white matter was laser captured from BA24 brain sections (10 μm thickness) mounted on PEN membrane glass slides (Life Technologies, Grand Island,

NY). In order to identify cell types as well as key tissue structures and white or gray matter type, the tissue sections were stained using Histogene LCM Frozen Section Staining Kit (Life Technologies, Grand Island, NY) according to the manufacturer's instructions. Superficial white matter was defined as the white matter area directly adjacent to gray matter and within 3 mm of the white/gray matter border area. Multiple large circular areas were captured for each sample.

Pyramidal neurons and white matter astrocytes were stained and captured from BA24 cortical layer 3 using the methods previously described in Chapter 3. Enough cells were captured per samples to be able to prepare a RNA-Seq library (1000 neurons and 2000 astrocytes per subject) and to synthesize cDNA for PCR confirmation (500 neurons). Captured cells were incubated at 42°C for 30 min in the extraction buffer provided in the RNA isolation kit.

RNA-Seq Library Preparation

RNA was isolated from the captured samples using PicoPure RNA Isolation Kit (Life Technologies, Grand Island, NY) with the additional RNase-free DNase kit (Qiagen, Valencia, CA) step outlined in the manufacturer's protocol. RNA quality and quantity were assessed using the Agilent RNA 6000 Pico kit (Agilent Technologies, Santa Carla, CA). The Ovation Single Cell RNA-Seq System (NuGEN, San Carlos, CA) was used to generate RNA-Seq libraries from isolated RNA. An input amount of over 100 pg of starting RNA was used for each library sample. Two forms of library quality check were used before library pooling. Total quantity of library produced and fragment length was assessed using the Agilent High Sensitivity DNA Kit (Agilent Technologies,

Santa Carla, CA). This method quantified all library fragments produced. The KAPA Library Quantification Kit (KAPA Biosystems, Woburn, MA) was used to determine the amount of correctly made library that would be able to bind to the sequencing flow cell. This kit is a PCR based assay that determines the concentration of library using primer for the P5 and P7 sequencing adaptors for the Illumina platform. The assay included a six point serial dilution standard series that assisted in determining reaction efficiency and concentrations of samples.

Library Pooling

Each library created was uniquely barcoded with a unique sequence of DNA during the library preparation step. This barcode allows multiple samples to be sequenced within one flow cell. The generated data can then be sorted for individual samples based on this unique barcode sequence. Since there is no method for downstream normalization for library input amounts in a pooled sample, it is imperative that each individual library be equally represented by concentration in the pooled library. The sample concentrations determined by the KAPA PCR quantification assay were used to standardize input amounts.

RNA-Seq

Pooled libraries were sent to David H. Murdock Research Institute for sequencing. Prior to sequencing, another PCR based quantification was performed on the pooled library sample to ensure that cluster density on the flow cell would be optimal. A cBot instrument (Illumina, San Diego, CA) was used to perform cluster

amplification on the flow cell before sequencing. The HiSeq2500 instrument (Illumina, San Diego, CA) was used for 100 base paired reads with indexing sequencing using the instrument's high output sequencing run.

Bioinformatics Analysis

Following sequencing, base calling was performed with CASAVA (v1.8.2) (Illumina, San Diego, CA). Filtering and trimming of reads consisted of removal of Illumina Adapter Library and trimming using the following parameters (quality score limit: 0.05, trim ambiguous nucleotides: <2 and removed 15 bp from the 5' and 5 bp from the 3' end respectively) in the CLC Genomics Workbench 7.0.4 (Qiagen, Valencia, CA). The resulting read length averaged ~80 bp. Reads were then aligned to the human genome (latest version, hg38/GRCh38, assembled on December 2013, annotations updated in June 2014) using CLC Genomics Workbench 7.0.4 using the CLC's RNA-Seq package (Mismatch cost = 2, Insertion cost = 3, Deletion cost = 3, Length fraction = 0.8, Similarity fraction = 0.8). To determine differentially expressed genes, a Kal's Z-test (Kal et al., 1999) was performed for comparison within pairs. Baggerly Beta-binomial test (Baggerly, Deng, Morris, & Aldaz, 2003) was performed for group comparisons using the control donors as the reference. A false discovery rate (FDR) correction was used to further correct p-values achieved using the above proportion-based tests. We used both paired and unpaired statistical comparisons of control and autism gene expressions for these preliminary data understanding that with the small sample size, neither approach is likely to produce data with high statistical confidence.

PCR Confirmation

RNA was isolated from the captured samples using PicoPure RNA Isolation Kit (Life Technologies, Grand Island, NY) with the additional RNase-free DNase kit (Qiagen, Valencia, CA) step outlined in the manufacturer's protocol. RNA samples were reverse transcribed into cDNA using the Superscript III kit (Life Technologies; Grand Island, NY) that contained oligodT and random hexamer primers. Gene specific primers were purchased from a vendor (Qiagen; Valencia, CA). Gene primer sequences are shown in Appendix B. To quantify transcripts, endpoint PCR was used for RNA isolated from laser captured cells as previously described (Ordway et al., 2009; Xiang et al., 2008). Endpoint PCR data was computed as relative values generated from the ratios of amounts of target gene expression to a reference gene. Afterwards, endpoint PCR data were analyzed by the paired Student's t-test.

Results

Sequencing Quality Based on Phred Score

The first step in the analysis of sequencing is base-calling. This process consists of taking the multiple single nucleotide reads and composing the sequence of the fragment clusters. Using the Phred scoring methods, a cut-off score of around 30 is considered an acceptable quality for base-calling. A Phred score of 30 translates to a 1 in 1000 probability of an incorrect base-call or a 99.9% accuracy in sequence detection (B. Ewing, Hillier, Wendl, & Green, 1998; Brent Ewing & Green, 1998). The PHRED score for all samples (white matter, neuron, and astrocyte preparations) exceeded this cut-off by reaching an average score of 35 to 40. A score of 40 translates to a probability of 1

in 10,000 incorrect base-call or a 99.99% accuracy in detection.

Mapping and Alignment

Mapping Percent and Total Reads. The three types of sample preparations, white matter containing mixed populations of cells, pyramidal neurons, and GFAP-positive astrocytes, were compared to determine if there was a difference in mapping percentages based on sample type. There was no significant effect of sample type on the type of read produced by the samples (Figure 4.1). White matter and neuron samples were further analyzed to determine if there was a difference in the mapping between control and ASD subject samples. No difference was found between control and ASD samples for white matter (Figure 4.2A, $p = 0.64$) or neuron (Figure 4.2B, $p = 0.63$) preparations.

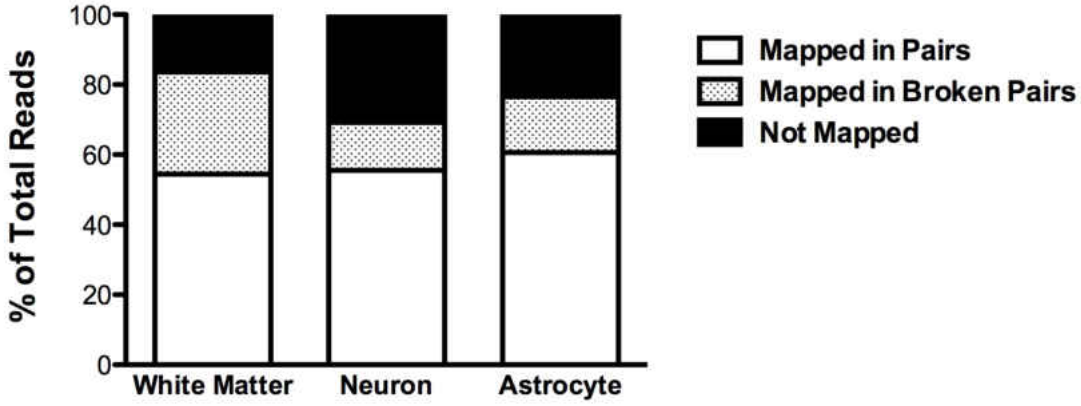

Figure 4.1. Division of read types of the white matter, neuron, and astrocyte RNA-Seq samples. The percent of reads mapped in pairs (white bars), mapped in broken pairs (shaded bars), and reads not mapped (black bars) were plotted as a percent of total

reads for all samples.

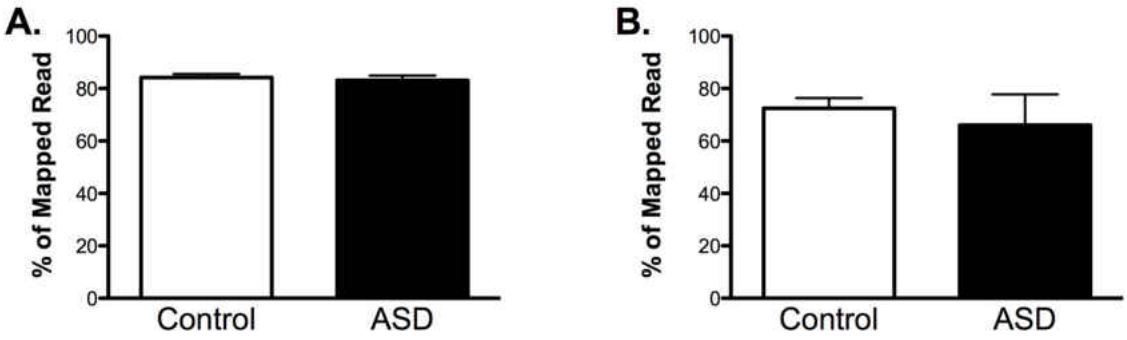

Figure 4.2. Comparison of read mapping between control and ASD samples for white matter (A) and neurons (B). The percentage of total mapped reads (mapped in pairs and broken pairs) of total reads was plotted. No significant difference was found between control and ASD samples for white matter or neuron samples.

Paired Read Mapping. For reads that were mapped as pairs, an analysis was done to investigate where those reads aligned (Figure 4.3). Approximately 75% of all mapped paired reads aligned to intron regions for all sample preparations. This was also the case when examining the alignment pattern between control and ASD samples for white matter (Figure 4.4A) and neuron (Figure 4.4B) sample preparations. To ensure that observed intronic read mapping was in agreement with previously reported brain sample RNA-Seq data, the percentage of intron reads was reported (Table 4.2) for known high intronic genes (Ameur et al., 2011). Each gene examined had a 52 to 100% intronic mapping percentage.

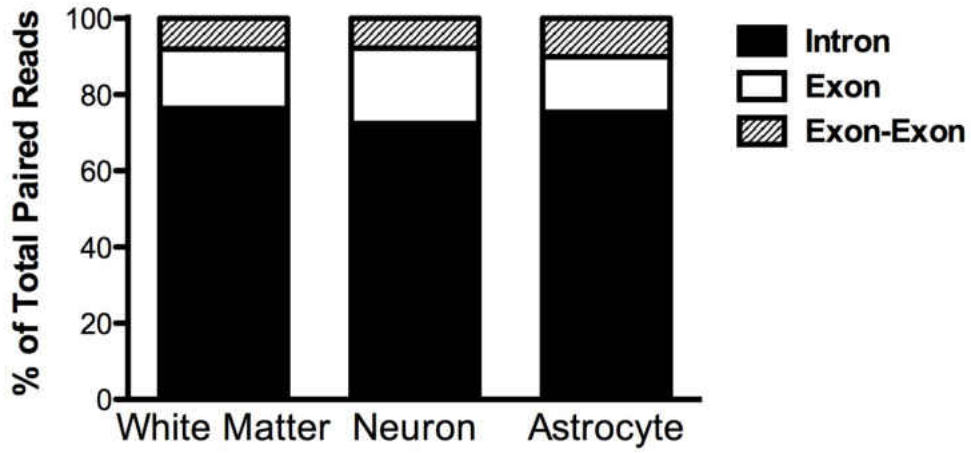

Figure 4.3. Comparison of read type for paired reads in white matter, neuron, and astrocyte samples. The percent of exon (white bar), exon-exon (shaded bar), and intron (black bar) reads of total paired reads were plotted.

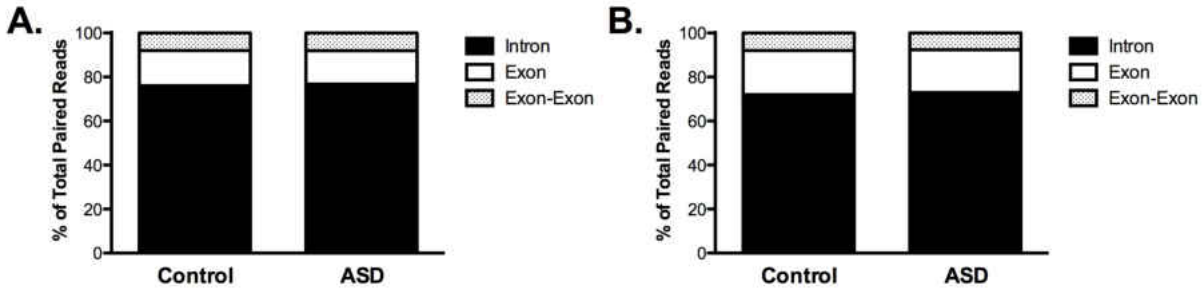

Figure 4.4. Comparison of read type for paired reads in control and ASD white matter (A) and neuron (B) samples. The percent of exon (white bar), exon-exon (shaded bar), and intron (black bar) reads of total paired reads were plotted for white matter and neuron control and ASD samples.

Table 4.2. Percentage of Intron Reads for Known High Intronic Genes.

Ameur et al. (Ameur et al., 2011) produced a ranking of genes in the adult and fetal brain that produce the highest amount of intronic reads using RNA-Seq. The top genes from those lists were examined in our data. The table below contains the mean percentage of intron reads for each of the genes listed for all white matter, neurons and astrocyte samples. For white matter and neurons samples, the mean percentage of intron reads is given for control and ASD subjects separately.

Gene Name	White Matter		Neurons		Astrocyte
	Control	ASD	Control	ASD	
PCDH9	85.69%	87.56%	91.38%	92.20%	82.50%
PCDH7	93.29%	83.84%	85.18%	87.38%	71.70%
QKI	57.90%	62.96%	66.95%	52.15%	69.90%
NRXN1	89.63%	92.92%	86.05%	88.33%	96.60%
KCNC2	72.24%	68.44%	88.93%	56.78%	100.00%
PID1	99.84%	99.98%	99.70%	99.70%	100.00%
KLF7	70.51%	69.28%	64.50%	70.98%	60.90%

Differentially Expressed Genes. A list of differentially expressed genes (DEGs) comparing control and ASD donor samples (Table 4.5) was produced for white matter and neuron samples preparations. The expression level of these genes was determined by the RPKM (reads per kilobase per million mapped reads) of exon mapping reads only. Two genes, *STX8* and *SSR3*, were selected for confirmation of DEGs in the BA24 pyramidal neuron samples. The expression of the two genes was not found to be different comparing the same control and ASD donors as was used for the RNA-Seq experiment (Figure 4.6).

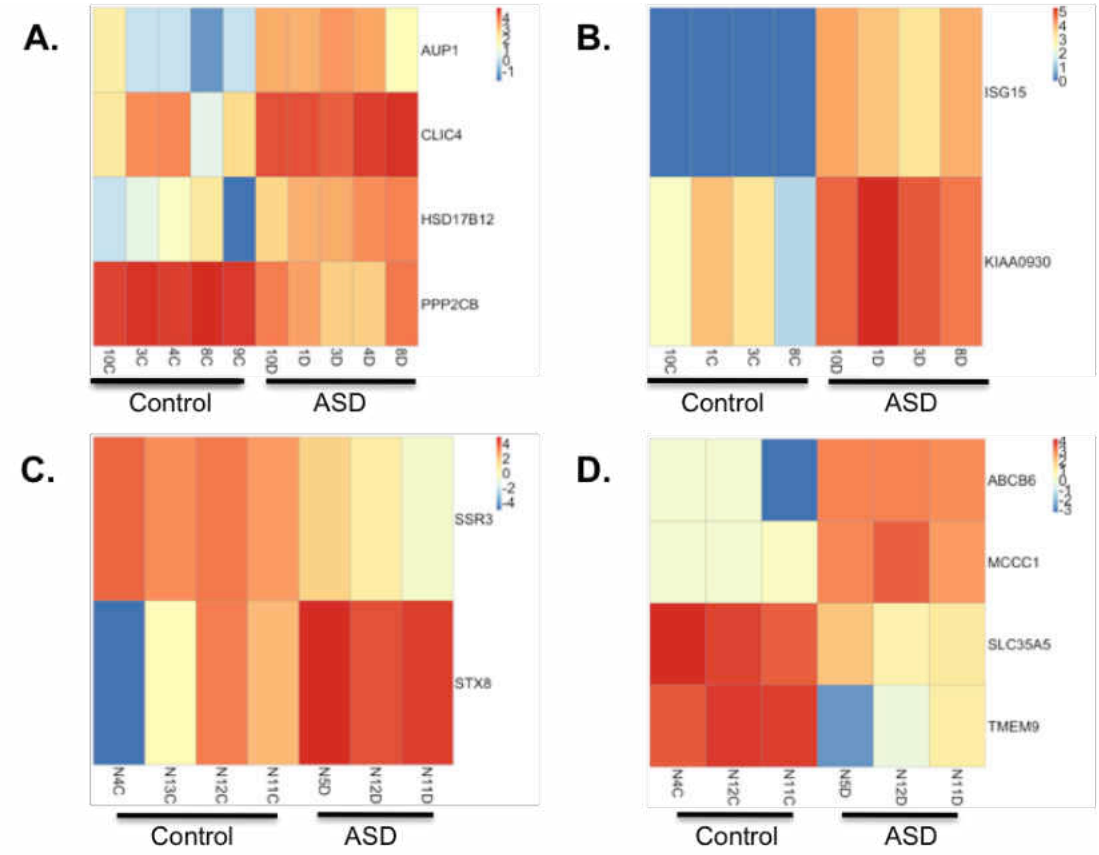

Figure 4.5. Differentially expressed genes in white matter and neuron samples. These heat maps represent the log2 transformed normalized expression value (RPKM) for each sample using a Baggerly beta-nominal test analysis. (A) white matter unpaired analysis (B) white matter paired analysis (C) neuron unpaired analysis (D) neuron paired analysis

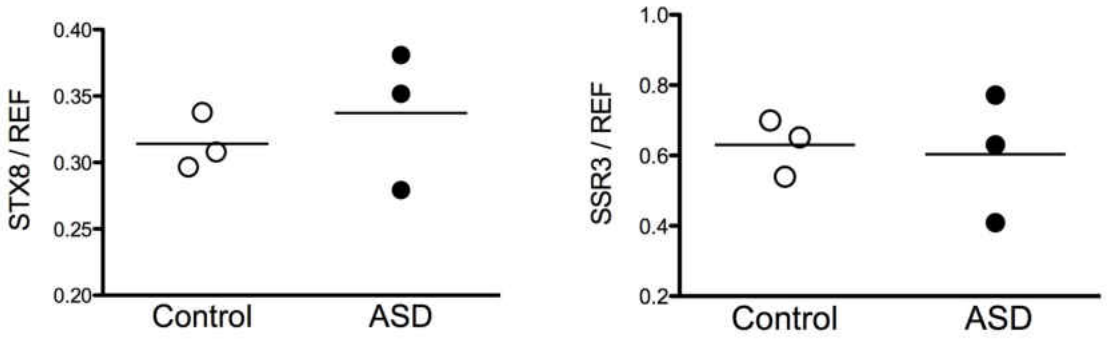

Figure 4.6. Levels of expression of *STX8* and *SSR3* in pyramidal neurons of BA24. Gene expression was measured in laser captured BA24 pyramidal neurons from typically developing control donors (open symbols) and ASD donors (closed symbols). Gene expression levels are normalized to *GAPDH* expression levels. Mean values are noted by horizontal lines. No statistically significant differences were observed.

Abnormalities in Intron Mapping in ASD. Because the majority of the mapped pair reads were aligned to intron regions, we examined the possibility that the percentage of intron reads might be predictive of an underlying pathological process in ASD. To start with, two genes found to be differentially expressed between control and ASD subjects using exon mapped reads were compared at the level of mapped introns. From RNA-Seq data of control and ASD donors, I compared the reads mapped to *STX8* and *HSD17B12* introns as a fraction of the total reads. Those genes were chosen to have a comparison of how intron reads mapped for one gene with altered exon expression in neurons and one with altered exon expression in white matter. The fraction of reads mapped to *STX8* introns was significantly lower in ASD donors in

neurons but not white matter. In contrast, the fraction of *HSD17B12* reads mapping to intronic regions was lower in white matter but not neurons comparing control and ASD donors (Figure 4.7).

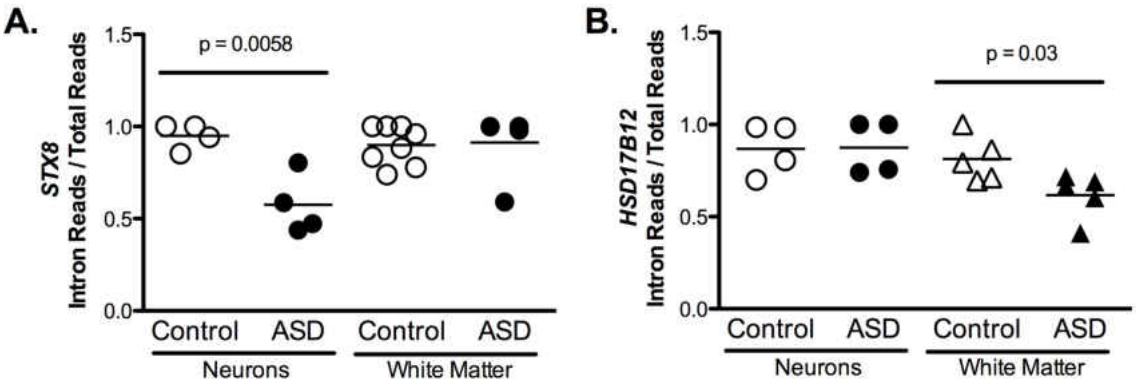

Figure 4.7. Comparison of intron reads for *STX8* and *HSD17B12* between control and ASD subject samples for neuron and white matter sample preparations. The ratio of intron reads to total reads for each gene is plotted for control (open symbols) and ASD (closed symbols) subjects for neurons and white matter samples. Statistical significance is noted in graph.

Discussion

The primary goal of this study was to establish the feasibility of using RNA-Seq to examine gene expression in brains cells captured by LCM. Three different LCM sampling methods were performed to determine which was suitable for this type of analysis. Overall, the quality of the sequencing data was high with a PHRED score that exceeded 35 and over 75% of all reads mapping to the reference genome for all sample preparation types (white matter, neuron, and astrocyte). There were also no observable

differences between samples from control and ASD subject in terms of the quality of the RNA-Seq data generated. Once the ability to sequence the prepared libraries and map those reads to a reference genome was confirmed, the next step was to determine what the mapped reads represented.

A secondary goal of this study was to utilize LCM/RNA-Seq to compare the gene expression profiles of brain neurons and glia from typically developing control and ASD donors. One obvious and major problem with this part of the study was a small sample size, and hence the low power of the statistical analyses of the comparison of the two study groups. During the sample preparation stage, there were more subject samples than those reflected in the final analysis above. However, due to various reasons such as poor RIN quality, low mapping rate, and low RNA-Seq library yield, samples from some subjects were eliminated prior to RNA-Seq analysis. For the few control-ASD pairs that we were able to analyze, we generated a list of differentially expressed genes for the RNA-Seq data for neuron and white matter samples (Figure 4.5). However, only two of the three pairs matched the RNA-Seq data by showing greater levels of *STX8* expression in ASD subjects compared to the controls using PCR confirmation (Figure 4.6). The small sample size could have been a cause for the inability to confirm the RNA-Seq finding with PCR. We are currently working to prepare more RNA-Seq libraries from additional paired subjects for analysis. For now, we assume that our inability to fully confirm existing RNA-Seq data is related to the small group sizes.

Within all the sample preparation types, a high percentage of intron mapping was observed. This is consistent with other RNA-Seq studies performed on brain tissue samples (Ameur et al., 2011; Kapranov et al., 2010). The high amount of intron reads

does not affect our ability to determine differential expressed genes since the RPKM or expression value is determined by exon mapping reads only. However, these intron reads and the differences therein between control and ASD samples suggest that other forms of transcriptional regulation in the brain may differentiate ASD from control subjects. There is evidence that genes involved in neuronal plasticity and synaptic regulation are stored in an unprocessed RNA form within cell (Ameur et al., 2011). This allows for another level of gene expression regulation within the dynamic cellular environment of the brain. Based on the results shown in Figure 4.7, the ratio of intron reads to total reads is significantly difference between control and ASD samples. This could reflect that the regulatory control in processing pre-mRNA to fully mature mRNA could be altered in ASD. This hypothesis will need to be confirmed using intron specific primers.

One of the disadvantages to using LCM collected samples is the small amount of material that can be obtained. When coupling LCM with the use of postmortem brain tissue, restrictions such as cost, time, and limited availability of tissue does not allow for the collection of sufficient amounts of input materials needed for many downstream applications. Due to the limited amount of sample that can be obtained from LCM, sample amplification is an unavoidable preparation step in the transcriptional analysis. The amplification step in sample preparation is a sensitive process that could introduce experimental artifact if not performed correctly or tailored to specific biological samples. Experiments were performed using both commercially available kits and LCM specialized protocols to determine the most effective and reliable method for sample amplification. The first strand synthesis step of RNA amplification is crucial since it

creates the basic template for amplification. Most methods are based on a 3' bias selection for this step of amplification. This selection technique is beneficial for reducing other RNA species such as rRNA and tRNA from the sample prior to mass amplification. This selection reduces potential bias toward more abundant RNAs since mRNA and non-coding RNA are significantly outnumbered by other RNA species in the samples. For samples collected from LCM, this 3' bias could reduce fidelity in amplification. Using frozen human tissue for these studies means that optimal RNA quality is never achieved because of decay that occurs during the brain collection process. A 3' bias selection could inadvertently exclude mRNAs that are susceptible to 3' degradation. Unlike other kits available on the market, the NuGEN amplification kits create a first strand using 3' and random primers giving better transcriptome coverage and reducing potential bias from degradation effects. This feature makes the kits ideal for LCM samples based on its tolerance for less than optimal RNA integrity and a small RNA input requirement of 100 picograms. However, the lack of ribosomal depletion or mRNA selection could have inadvertently biased our samples to pre-mRNA or intron containing transcripts. Intron spanning regions are larger than exon regions and would be more abundantly represented in the samples. It is still unclear if our samples produced enough exon based reads to truly reflect transcriptional changes at the mature mRNA level. Our samples might illustrate the regulation occurring between transcription and the finally mRNA product. More confirmation of the RNA-Seq data and more samples will be needed in order to fully answer this question.

Conclusion

When developing this method, efforts were made to circumvent the potential pitfalls associated with analyzing LCM samples. We were able to control for the limitations of these samples by selecting protocols suitable for sample type and putting in controls for the biological variances of human studies. There is still more work to be done to produce a full-scale analysis of transcription regulation underlying ASD brain pathology. In order to achieve that goal, there must first be a characterization of the type of transcriptional regulation reflected in our data whether it is exon or intron based. The data presented above suggest potential regulation at the pre-mRNA level in addition to that at the mature mRNA level. Further examination of intron based changes could reveal yet unknown transcriptional dysregulation associated with ASD brain pathology.

CHAPTER 5

SUMMARY AND CONCLUSIONS

The data in this dissertation provide evidence that autism pathology exists at the level of white matter astrocytes and glutamatergic pyramidal neurons in the ACC. Many past studies have shown gross anatomical differences between typically developing brains and those of autism patients. However, those findings have not lead to an understanding of the underlying cause of ASD brain abnormalities. By examining the pathology of autism and the cellular and molecular level as performed here, a more cogent understanding of autism neuropathology can be established. It is anticipated that with greater knowledge of the pathological process of autism, a strategy for developing biologically therapeutic interventions will be possible.

The studies present several different methods for the examination of ASD brain pathology at a cellular level. Chapter 2 used a combination of protein and gene expression analysis to determine the potential role of glial cell populations in ASD brain pathology. For a long time glial cell populations were thought of as merely support cells. In recent years glia have been found to play major roles in maintaining brain homeostasis. Glial dysfunction can be observed in a variety of brain pathologies. The study presented here revealed an increase in the glial marker GFAP in the ASD brain. This alteration was very specific to brain region (BA24 as opposed to BA10) and matter type (white matter as opposed to gray matter). This type of regional specificity of pathology reinforced the need to further explore ASD brain pathology at a higher anatomical resolution. For example, the abnormality of GFAP protein in ASD could

have gone undetected using a sample that contained both white and gray matters as typically are used in other postmortem ASD studies.

Chapter 3 explored pathology and a remarkably greater level of resolution, i.e. in two cell populations, neurons and astrocytes, from a discrete area of the brain (ACC). This work focused on key genes in the glutamate pathway because the type of neuron studied (pyramidal neuron) is known to use the neurotransmitter glutamate. Imbalances in this neurochemical pathway are theorized to contribute to ASD brain pathology and ASD behaviors. The genes investigated encode receptors, transmitters, and synaptic proteins. All of these proteins play a direct role in the release and termination of glutamate signaling. Gene expression differences were found comparing control and ASD subjects in ACC pyramidal neurons for genes such as *NTRK2* and *GRIP1*, but no changes were found for any genes in the astrocyte population. These neuronal gene changes were specific to BA24 neurons and were not found in BA10 neurons from the same subjects. These findings again speak to the specificity of cellular ASD pathology and provide a molecular basis for the excitatory and inhibitory imbalance that has been theorized to occur in ASD brain based on imaging studies. Collectively, the genes found to be reduced in ASD provided evidence that excess receptor signaling could be creating neuronal dysfunction. This type of dysfunction generally increases intercellular signaling pathways to the point that cell death occurs. The death of excitatory neurons would certainly change the overall excitatory and inhibitory balance. In future studies, we will focus on inhibitory cell populations to determine expression changes that might affect the overall balance of this system. These expression changes could help reveal the dysfunctional or compensatory mechanisms that characterize the brain pathology of

ASD.

Chapter 4 outlined the development of a protocol for a more in-depth analysis of transcription regulation in a disease state using laser captured samples. While Chapter 3 took a very targeted approach to exploring specific gene expressions in the ASD brain, work in Chapter 4 was designed to interrogate all gene expressions within a cell population of the ACC. This approach is often considered "unbiased" in that it is not assuming any particular abnormality but examining all possible abnormalities in gene expression. In terms of bioinformatics the data produced achieved high quality scores and mapping rates. However, the protocol used to amplify the small amount of RNA template could have introduced a possible bias towards more abundant fragments such as the intron portions of pre-mRNAs. This is evident in the high number of intronic mapped reads. More analysis will need to be performed to determine the transcription information provided from these data.

Overall, this research identified specific cellular pathologies that could contribute to ASD brain pathology and ultimately to ASD behaviors. In addition, preliminary data suggest that the it is possible to combine the methods of RNA-Seq and laser capture microdissection to perform whole transcriptome analysis of single cell types from the human brain, an approached that has not been previously achieved to date. The methods herein dramatically increase the anatomical and cellular resolution of the study of brain pathologies and greatly expand the amount of data that can be derived from postmortem brain samples. Ultimately these approaches provide a unique opportunity for the development of new theories regarding the pathogenesis and pathology of ASD. Future studies will include a deeper analysis of the pathways associated with the

differential expressed proteins and genes found in Chapters 2 and 3 as well as additional validation of the method developed in Chapter 4.

REFERENCES

Adrien, J. L., Faure, M., Perrot, A., Hameury, L., Garreau, B., Barthelemy, C., & Sauvage, D. (1991). Autism and family home movies: preliminary findings. *Journal of Autism and Developmental Disorders*, *21*(1), 43–9. Retrieved from http://www.ncbi.nlm.nih.gov/pubmed/2037548

Adrien, J. L., Perrot, A., Sauvage, D., Leddet, I., Larmande, C., Hameury, L., & Barthelemy, C. (1992). Early symptoms in autism from family home movies. Evaluation and comparison between 1st and 2nd year of life using I.B.S.E. scale. *Acta Paedopsychiatrica*, *55*(2), 71–5. Retrieved from http://www.ncbi.nlm.nih.gov/pubmed/1374996

Amaral, D. G., Schumann, C. M., & Nordahl, C. W. (2008). Neuroanatomy of autism. *Trends in Neurosciences*, *31*(3), 137–45. doi:10.1016/j.tins.2007.12.005

Ambrosini, A., Bresciani, L., Fracchia, S., Brunello, N., & Racagni, G. (1995). Metabotropic glutamate receptors negatively coupled to adenylate cyclase inhibit N-methyl-D-aspartate receptor activity and prevent neurotoxicity in mesencephalic neurons in vitro. *Molecular Pharmacology*, *47*(5), 1057–64. Retrieved from http://www.ncbi.nlm.nih.gov/pubmed/7746273

American Psychiatric Association. (2013). *Diagnostic and statistical manual of mental disorders* (5th ed.). Arlington, VA: American Psychiatric Publishing.

Ameur, A., Zaghlool, A., Halvardson, J., Wetterbom, A., Gyllensten, U., Cavelier, L., & Feuk, L. (2011). Total RNA sequencing reveals nascent transcription and

widespread co-transcriptional splicing in the human brain. *Nature Structural & Molecular Biology*, *18*(12), 1435–40. doi:10.1038/nsmb.2143

Angelidou, A., Asadi, S., Alysandratos, K.-D., Karagkouni, A., Kourembanas, S., & Theoharides, T. C. (2012). Perinatal stress, brain inflammation and risk of autism-review and proposal. *BMC Pediatrics*, *12*, 89. doi:10.1186/1471-2431-12-89

Angelucci, F., Mathé, A. A., & Aloe, L. (2000). Brain-derived neurotrophic factor and tyrosine kinase receptor TrkB in rat brain are significantly altered after haloperidol and risperidone administration. *Journal of Neuroscience Research*, *60*(6), 783–94. Retrieved from http://www.ncbi.nlm.nih.gov/pubmed/10861791

Auer, H., Lyianarachchi, S., Newsom, D., Klisovic, M. I., Marcucci, G., Marcucci, U., & Kornacker, K. (2003). Chipping away at the chip bias: RNA degradation in microarray analysis. *Nature Genetics*, *35*(4), 292–3. doi:10.1038/ng1203-292

Avino, T. A., & Hutsler, J. J. (2010). Abnormal cell patterning at the cortical gray-white matter boundary in autism spectrum disorders. *Brain Research*, *1360*, 138–46. doi:10.1016/j.brainres.2010.08.091

Baggerly, K. A., Deng, L., Morris, J. S., & Aldaz, C. M. (2003). Differential expression in SAGE: Accounting for normal between-library variation. *Bioinformatics (Oxford, England)*, *19*(12), 1477–83. Retrieved from http://www.ncbi.nlm.nih.gov/pubmed/12912827

Bailey, A. J. (2008). Postmortem studies of autism. *Autism Research : Official Journal of the International Society for Autism Research*, *1*(5), 265. doi:10.1002/aur.51

Baio, J. (2014). Prevalence of autism spectrum disorder among children aged 8 years — Autism and Developmental Disabilities Monitoring Network, 11 sites, United States, 2010. *MMWR*, *63*(2). Retrieved from http://www.cdc.gov/mmwr/preview/mmwrhtml/ss6302a1.htm?s_cid=ss6302a1_w

Baranek, G. T. (1999). Autism during infancy: a retrospective video analysis of sensory-motor and social behaviors at 9-12 months of age. *Journal of Autism and Developmental Disorders*, *29*(3), 213–24. Retrieved from http://www.ncbi.nlm.nih.gov/pubmed/10425584

Barnby, G., Abbott, A., Sykes, N., Morris, A., Weeks, D. E., Mott, R., … Monaco, A. P. (2005). Candidate-gene screening and association analysis at the autism-susceptibility locus on chromosome 16p: Evidence of association at GRIN2A and ABAT. *American Journal of Human Genetics*, *76*(6), 950–66. doi:10.1086/430454

Barton, M., & Volkmar, F. (1998). How commonly are known medical conditions associated with autism? *Journal of Autism and Developmental Disorders*, *28*(4), 273–8. Retrieved from http://www.ncbi.nlm.nih.gov/pubmed/9711483

Betancur, C. (2011). Etiological heterogeneity in autism spectrum disorders: More than 100 genetic and genomic disorders and still counting. *Brain Research*, *1380*, 42–77. doi:10.1016/j.brainres.2010.11.078

Bjorklund, G. (2013). The role of zinc and copper in autism spectrum disorders. *Acta Neurobiologiae Experimentalis*, *73*(2), 225–36. Retrieved from http://www.ncbi.nlm.nih.gov/pubmed/23823984

Blake, J., Hoyme, H. E., & Crotwell, P. L. (2013). A brief history of autism, the autism/vaccine hypothesis and a review of the genetic basis of autism spectrum disorders. *South Dakota Medicine : The Journal of the South Dakota State Medical Association*, *Spec no*, 58–65. Retrieved from http://www.ncbi.nlm.nih.gov/pubmed/23444593

Blankenship, K., Erickson, C., Stigler, K., Posey, D. J., & McDougle, C. J. (2010). Aripiprazole for irritability for associated with autistic disorder in children and adolescents aged 6-17 years. *Pediatric …*, *4*(4), 375–381. Retrieved from http://www.futuremedicine.com/doi/abs/10.2217/phe.10.45

Blumberg, S., Bramlett, M., Kogan, M. D., Schieve, L. A., Jones, J. R., & Lu, M. C. (2013). Changes in prevalence of parent-reported autism spectrum disorder in school-aged US children: 2007 to 2011–2012. *National Health Statistics Reports*, (65).

Bolivar, V. J., Walters, S. R., & Phoenix, J. L. (2007). Assessing autism-like behavior in mice: Variations in social interactions among inbred strains. *Behavioural Brain Research*, *176*(1), 21–6. doi:10.1016/j.bbr.2006.09.007

Boulle, F., Kenis, G., Cazorla, M., Hamon, M., Steinbusch, H. W. M., Lanfumey, L., & van den Hove, D. L. A. (2012). TrkB inhibition as a therapeutic target for CNS-

related disorders. *Progress in Neurobiology*, *98*(2), 197–206. doi:10.1016/j.pneurobio.2012.06.002

Browne, C. A., & Lucki, I. (2013). Antidepressant effects of ketamine: Mechanisms underlying fast-acting novel antidepressants. *Frontiers in Pharmacology*, *4*, 161. doi:10.3389/fphar.2013.00161

Bruining, H., Eijkemans, M. J., Kas, M. J., Curran, S. R., Vorstman, J. A., & Bolton, P. F. (2014). Behavioral signatures related to genetic disorders in autism. *Molecular Autism*, *5*(1), 11. doi:10.1186/2040-2392-5-11

Buchsbaum, M. S., Hollander, E., Mehmet Haznedar, M., Tang, C., Spiegel-Cohen, J., Wei, T.-C., … Mosovich, S. (2001). Effect of fluoxetine on regional cerebral metabolism in autistic spectrum disorders: a pilot study. *The International Journal of Neuropsychopharmacology*, *4*(02), 119–25. doi:10.1017/S1461145701002280

Buescher, A. V. S., Cidav, Z., Knapp, M., & Mandell, D. S. (2014). Costs of autism spectrum disorders in the United kingdom and the United States. *JAMA Pediatrics*, *168*(8), 721–8. doi:10.1001/jamapediatrics.2014.210

Butts, B. D., Houde, C., & Mehmet, H. (2008). Maturation-dependent sensitivity of oligodendrocyte lineage cells to apoptosis: Implications for normal development and disease. *Cell Death and Differentiation*, *15*(7), 1178–86. doi:10.1038/cdd.2008.70

Cao, C., Rioult-Pedotti, M. S., Migani, P., Yu, C. J., Tiwari, R., Parang, K., … Marshall, J. (2013). Impairment of TrkB-PSD-95 signaling in Angelman syndrome. *PLoS Biology*, *11*(2), e1001478. doi:10.1371/journal.pbio.1001478

Casanova, M., Buxhoeveden, D., Switala, A., & Roy, E. (2002). Neuronal density and architecture (Gray Level Index) in the brains of autistic patients. *Journal of Child Neurology*, *17*(7), 515–21. Retrieved from http://www.ncbi.nlm.nih.gov/pubmed/12269731

Casanova, M., & Trippe, J. (2009). Radial cytoarchitecture and patterns of cortical connectivity in autism. *Philosophical Transactions of the Royal Society of London. Series B, Biological Sciences*, *364*(1522), 1433–6. doi:10.1098/rstb.2008.0331

Chandley, M. J., Szebeni, K., Szebeni, A., Crawford, J., Stockmeier, C. A., Turecki, G., … Ordway, G. A. (2012). Gene expression deficits in pontine locus coeruleus astrocytes in men with major depressive disorder. *Journal of Psychiatry Neuroscience JPN*, *38*, 120110. doi:10.1503/jpn.120110

Connolly, A. M., Chez, M., Streif, E. M., Keeling, R. M., Golumbek, P. T., Kwon, J. M., … Deuel, R. M. K. (2006). Brain-derived neurotrophic factor and autoantibodies to neural antigens in sera of children with autistic spectrum disorders, Landau-Kleffner syndrome, and epilepsy. *Biological Psychiatry*, *59*(4), 354–63. doi:10.1016/j.biopsych.2005.07.004

Correia, C. T., Coutinho, a M., Sequeira, a F., Sousa, I. G., Lourenço Venda, L., Almeida, J. P., … Vicente, a M. (2010). Increased BDNF levels and NTRK2 gene

association suggest a disruption of BDNF/TrkB signaling in autism. *Genes, Brain, and Behavior*, *9*(7), 841–8. doi:10.1111/j.1601-183X.2010.00627.x

Courchesne, E., Karns, C., Davis, H., Ziccardi, R., Carper, R., Tigue, Z., … Courchesne, R. (2001). Unusual brain growth patterns in early life in patients with autistic disorder: an MRI study. *Neurology*, *57*(2), 245–54. Retrieved from http://www.ncbi.nlm.nih.gov/pubmed/11468308

Courchesne, E., Karns, C., Davis, H., Ziccardi, R., Carper, R., Tigue, Z., … Courchesne, R. (2011). Unusual brain growth patterns in early life in patients with autistic disorder: An MRI study. *Neurology*, *76*(24), 2111. doi:10.1212/01.wnl.0000399191.79091.28

Courchesne, E., Pierce, K., Schumann, C., Redcay, E., Buckwalter, J., Kennedy, D., & Morgan, J. (2007). Mapping early brain development in autism. *Neuron*, *56*(2), 399–413. doi:10.1016/j.neuron.2007.10.016

Devinsky, O., Morrell, M. J., & Vogt, B. A. (1995). Contributions of anterior cingulate cortex to behaviour. *Brain : A Journal of Neurology*, *118 (Pt 1*, 279–306. Retrieved from http://www.ncbi.nlm.nih.gov/pubmed/7895011

Devlin, B., & Scherer, S. W. (2012). Genetic architecture in autism spectrum disorder. *Current Opinion in Genetics & Development*, *22*(3), 229–37. doi:10.1016/j.gde.2012.03.002

Di Lieto, A., Rantamäki, T., Vesa, L., Yanpallewar, S., Antila, H., Lindholm, J., … Castrén, E. (2012). The responsiveness of TrkB to BDNF and antidepressant drugs is differentially regulated during mouse development. *PloS One*, *7*(3), e32869. doi:10.1371/journal.pone.0032869

Di Martino, A., Shehzad, Z., Kelly, C., Roy, A. K., Gee, D. G., Uddin, L. Q., … Milham, M. P. (2009). Relationship between cingulo-insular functional connectivity and autistic traits in neurotypical adults. *The American Journal of Psychiatry*, *166*(8), 891–9. doi:10.1176/appi.ajp.2009.08121894

Dölen, G., Osterweil, E., Rao, B. S. S., Smith, G. B., Auerbach, B. D., Chattarji, S., & Bear, M. F. (2007). Correction of fragile X syndrome in mice. *Neuron*, *56*(6), 955–62. doi:10.1016/j.neuron.2007.12.001

Ebert, D., & Greenberg, M. (2013). Activity-dependent neuronal signalling and autism spectrum disorder. *Nature*, *493*(7432), 327–337. doi:10.1038/nature11860.Activity-dependent

Ewing, B., & Green, P. (1998). Base-Calling of Automated Sequencer Traces Using Phred. II. Error Probabilities. *Genome Res.*, *8*(3), 186–194. Retrieved from http://genome.cshlp.org/content/8/3/186.long

Ewing, B., Hillier, L., Wendl, M. C., & Green, P. (1998). Base-Calling of Automated Sequencer Traces Using Phred. I. Accuracy Assessment. *Genome Research*, *8*(3), 175–185. doi:10.1101/gr.8.3.175

Gaetano, J. (2014). Holm-Bonferroni Sequential Correction: An EXCEL Calculator. Retrieved from http://www.researchgate.net/publication/236969037_Holm-Bonferroni_Sequential_Correction_An_EXCEL_Calculator

Gardener, H., Spiegelman, D., & Buka, S. L. (2009). Prenatal risk factors for autism: Comprehensive meta-analysis. *The British Journal of Psychiatry : The Journal of Mental Science*, *195*(1), 7–14. doi:10.1192/bjp.bp.108.051672

Gariépy, J.-F., Watson, K. K., Du, E., Xie, D. L., Erb, J., Amasino, D., & Platt, M. L. (2014). Social learning in humans and other animals. *Frontiers in Neuroscience*, *8*, 58. doi:10.3389/fnins.2014.00058

Ghanizadeh, A., Akhondzadeh, S., Hormozi, M., Makarem, A., Abotorabi-Zarchi, M., & Firoozabadi, A. (2012). Glutathione-related factors and oxidative stress in autism, a review. *Current Medicinal Chemistry*, *19*(23), 4000–5. Retrieved from http://www.ncbi.nlm.nih.gov/pubmed/22708999

Gidaya, N. B., Lee, B. K., Burstyn, I., Yudell, M., Mortensen, E. L., & Newschaffer, C. J. (2014). In utero exposure to selective serotonin reuptake inhibitors and risk for autism spectrum disorder. *Journal of Autism and Developmental Disorders*, *44*(10), 2558–67. doi:10.1007/s10803-014-2128-4

Ginsberg, S. D., Alldred, M. J., & Che, S. (2011). Gene expression levels assessed by CA1 pyramidal neuron and regional hippocampal dissections in Alzheimer's disease. *Neurobiology of Disease*, 1–9. doi:10.1016/j.nbd.2011.07.013

Ginsberg, S. D., & Che, S. (2005). Expression profile analysis within the human hippocampus: Comparison of CA1 and CA3 pyramidal neurons. *The Journal of Comparative Neurology*, *487*(1), 107–18. doi:10.1002/cne.20535

Ginsberg, S. D., Elarova, I., Ruben, M., Tan, F., Counts, S. E., Eberwine, J. H., … Che, S. (2004). Single-cell gene expression analysis: Implications for neurodegenerative and neuropsychiatric disorders. *Neurochemical Research*, *29*(6), 1053–64. Retrieved from http://www.ncbi.nlm.nih.gov/pubmed/15176463

Godlee, F., Smith, J., & Marcovitch, H. (2011). Wakefield's article linking MMR vaccine and autism was fraudulent. *BMJ (Clinical Research Ed.)*, *342*(January), c7452. doi:10.1136/bmj.c7452

Gozzi, M., Nielson, D. M., Lenroot, R. K., Ostuni, J. L., Luckenbaugh, D. A., Thurm, A. E., … Swedo, S. E. (2012). A magnetization transfer imaging study of corpus callosum myelination in young children with autism. *Biological Psychiatry*, *72*(3), 215–20. doi:10.1016/j.biopsych.2012.01.026

Groen, W. B., Buitelaar, J. K., van der Gaag, R. J., & Zwiers, M. P. (2011). Pervasive microstructural abnormalities in autism: A DTI study. *Journal of Psychiatry & Neuroscience : JPN*, *36*(1), 32–40. doi:10.1503/jpn.090100

Grubbs, F. (1950). Sample criteria for testing outlying oberservations. *The Annals of Mathematical Statistics*. Retrieved from http://www.jstor.org/stable/2236553

Hall, G. B. C., Szechtman, H., & Nahmias, C. (2003). Enhanced salience and emotion recognition in Autism: A PET study. *The American Journal of Psychiatry*, *160*(8), 1439–41. Retrieved from http://www.ncbi.nlm.nih.gov/pubmed/12900306

Hallmayer, J., Cleveland, S., Torres, A., Phillips, J., Cohen, B., Torigoe, T., … Risch, N. (2011). Genetic heritability and shared environmental factors among twin pairs with autism. *Archives of General Psychiatry*, *68*(11), 1095–102. doi:10.1001/archgenpsychiatry.2011.76

Harrington, R. A., Lee, L.-C., Crum, R. M., Zimmerman, A. W., & Hertz-Picciotto, I. (2013). Serotonin hypothesis of autism: Implications for selective serotonin reuptake inhibitor use during pregnancy. *Autism Research : Official Journal of the International Society for Autism Research*, *6*(3), 149–68. doi:10.1002/aur.1288

Hazlett, H. C., Poe, M. D., Gerig, G., Smith, R. G., & Piven, J. (2006). Cortical gray and white brain tissue volume in adolescents and adults with autism. *Biological Psychiatry*, *59*(1), 1–6. doi:10.1016/j.biopsych.2005.06.015

Hazlett, H. C., Poe, M., Gerig, G., Smith, R. G., Provenzale, J., Ross, A., … Piven, J. (2005). Magnetic resonance imaging and head circumference study of brain size in autism: Birth through age 2 years. *Archives of General Psychiatry*, *62*(12), 1366–76. doi:10.1001/archpsyc.62.12.1366

Herbert, M. R., Ziegler, D. A., Deutsch, C. K., O'Brien, L. M., Lange, N., Bakardjiev, A., … Caviness, V. S. (2003). Dissociations of cerebral cortex, subcortical and cerebral

white matter volumes in autistic boys. *Brain : A Journal of Neurology*, *126*(Pt 5), 1182–92. Retrieved from http://www.ncbi.nlm.nih.gov/pubmed/12690057

Holm, S. (1979). A simple sequentially rejective multiple test procedure. *Scandinavian Journal of Statistics*, *6*(2), 65–70. Retrieved from http://www.jstor.org/stable/4615733

Horlin, C., Falkmer, M., Parsons, R., Albrecht, M. A., & Falkmer, T. (2014). The cost of autism spectrum disorders. *PloS One*, *9*(9), e106552. doi:10.1371/journal.pone.0106552

Huttenlocher, P. R. (1970). Myelination and the development of function in immature pyramidal tract. *Experimental Neurology*, *29*(3), 405–15. Retrieved from http://www.ncbi.nlm.nih.gov/pubmed/5492915

Ingalhalikar, M., Parker, D., Bloy, L., Roberts, T. P. L., & Verma, R. (2011). Diffusion based abnormality markers of pathology: Toward learned diagnostic prediction of ASD. *NeuroImage*. doi:10.1016/j.neuroimage.2011.05.023

Jamain, S., Betancur, C., Quach, H., Philippe, A., Fellous, M., Giros, B., … Bourgeron, T. (2002). Linkage and association of the glutamate receptor 6 gene with autism. *Molecular Psychiatry*, *7*(3), 302–10. doi:10.1038/sj.mp.4000979

Jeste, S. S., & Geschwind, D. H. (2014). Disentangling the heterogeneity of autism spectrum disorder through genetic findings. *Nature Reviews. Neurology*, *10*(2), 74–81. doi:10.1038/nrneurol.2013.278

Kal, A. J., van Zonneveld, A. J., Benes, V., van den Berg, M., Koerkamp, M. G., Albermann, K., … Tabak, H. F. (1999). Dynamics of gene expression revealed by comparison of serial analysis of gene expression transcript profiles from yeast grown on two different carbon sources. *Molecular Biology of the Cell*, *10*(6), 1859–72. Retrieved from http://www.pubmedcentral.nih.gov/articlerender.fcgi?artid=25383&tool=pmcentrez&rendertype=abstract

Kanner, L. (1943). Autistic disturbances of affective contact. *Nervous Child*. Retrieved from http://neurodiversity.com/library_kanner_1943.pdf

Kapranov, P., St Laurent, G., Raz, T., Ozsolak, F., Reynolds, C. P., Sorensen, P. H. B., … Triche, T. J. (2010). The majority of total nuclear-encoded non-ribosomal RNA in a human cell is “dark matter” un-annotated RNA. *BMC Biology*, *8*(1), 149. doi:10.1186/1741-7007-8-149

Kennedy, D. P., & Courchesne, E. (2008). Functional abnormalities of the default network during self- and other-reflection in autism. *Social Cognitive and Affective Neuroscience*, *3*(2), 177–90. doi:10.1093/scan/nsn011

Kim, Y. S., Leventhal, B. L., Koh, Y.-J., Fombonne, E., Laska, E., Lim, E.-C., … Grinker, R. R. (2011). Prevalence of autism spectrum disorders in a total population sample. *The American Journal of Psychiatry*, *168*(9), 904–12. doi:10.1176/appi.ajp.2011.10101532

Kimelberg, H. K. (2010). Functions of mature mammalian astrocytes: A current view. *The Neuroscientist : A Review Journal Bringing Neurobiology, Neurology and Psychiatry*, *16*(1), 79–106. doi:10.1177/1073858409342593

Kirino, E. (2012). Efficacy and safety of aripiprazole in child and adolescent patients. *European Child & Adolescent Psychiatry*, *21*(7), 361–8. doi:10.1007/s00787-012-0270-0

Klein, R., Lamballe, F., Bryant, S., & Barbacid, M. (1992). The trkB tyrosine protein kinase is a receptor for neurotrophin-4. *Neuron*, *8*(5), 947–56. Retrieved from http://www.ncbi.nlm.nih.gov/pubmed/1375038

Klein, R., Nanduri, V., Jing, S. A., Lamballe, F., Tapley, P., Bryant, S., … Barbacid, M. (1991). The trkB tyrosine protein kinase is a receptor for brain-derived neurotrophic factor and neurotrophin-3. *Cell*, *66*(2), 395–403. Retrieved from http://www.pubmedcentral.nih.gov/articlerender.fcgi?artid=2710095&tool=pmcentrez&rendertype=abstract

Klein, R., Smeyne, R. J., Wurst, W., Long, L. K., Auerbach, B. A., Joyner, A. L., & Barbacid, M. (1993). Targeted disruption of the trkB neurotrophin receptor gene results in nervous system lesions and neonatal death. *Cell*, *75*(1), 113–22. Retrieved from http://www.ncbi.nlm.nih.gov/pubmed/8402890

Konstantareas, M. M., & Homatidis, S. (1999). Chromosomal abnormalities in a series of children with autistic disorder. *Journal of Autism and Developmental Disorders*, *29*(4), 275–85. Retrieved from http://www.ncbi.nlm.nih.gov/pubmed/10478727

Kral, T. V. E., Eriksen, W. T., Souders, M. C., & Pinto-Martin, J. A. (2013). Eating Behaviors, Diet Quality, and Gastrointestinal Symptoms in Children With Autism Spectrum Disorders: A Brief Review. *Journal of Pediatric Nursing*. doi:10.1016/j.pedn.2013.01.008

Laurence, J. A., & Fatemi, S. H. (2005). Glial fibrillary acidic protein is elevated in superior frontal, parietal and cerebellar cortices of autistic subjects. *Cerebellum (London, England)*, *4*(3), 206–10. doi:10.1080/14734220500208846

Le Couteur, A., Haden, G., Hammal, D., & McConachie, H. (2008). Diagnosing autism spectrum disorders in pre-school children using two standardised assessment instruments: The ADI-R and the ADOS. *Journal of Autism and Developmental Disorders*, *38*(2), 362–72. doi:10.1007/s10803-007-0403-3

Lee, B. K., Magnusson, C., Gardner, R. M., Blomström, S., Newschaffer, C. J., Burstyn, I., … Dalman, C. (2014). Maternal hospitalization with infection during pregnancy and risk of autism spectrum disorders. *Brain, Behavior, and Immunity*. doi:10.1016/j.bbi.2014.09.001

Levenson, D. (2013). Might diet play a role in autism? *The AJMG Sequence*. Retrieved from http://scholar.google.com/scholar?hl=en&btnG=Search&q=intitle:Might+Diet+Play+a+Role+in+Autism?#4

Leyfer, O. T., Folstein, S. E., Bacalman, S., Davis, N. O., Dinh, E., Morgan, J., … Lainhart, J. E. (2006). Comorbid psychiatric disorders in children with autism:

interview development and rates of disorders. *Journal of Autism and Developmental Disorders*, *36*(7), 849–61. doi:10.1007/s10803-006-0123-0

Leyfer, O. T., Tager-Flusberg, H., Dowd, M., Tomblin, J. B., & Folstein, S. E. (2008). Overlap between autism and specific language impairment: Comparison of Autism Diagnostic Interview and Autism Diagnostic Observation Schedule scores. *Autism Research : Official Journal of the International Society for Autism Research*, *1*(5), 284–96. doi:10.1002/aur.43

Liao, H.-M., Gau, S. S.-F., Tsai, W.-C., Fang, J.-S., Su, Y.-C., Chou, M.-C., … Chen, C.-H. (2013). Chromosomal abnormalities in patients with autism spectrum disorders from Taiwan. *American Journal of Medical Genetics. Part B, Neuropsychiatric Genetics : The Official Publication of the International Society of Psychiatric Genetics*, *162B*(7), 734–41. doi:10.1002/ajmg.b.32153

Lindholm, J. S. O., & Castrén, E. (2014). Mice with altered BDNF signaling as models for mood disorders and antidepressant effects. *Frontiers in Behavioral Neuroscience*, *8*, 143. doi:10.3389/fnbeh.2014.00143

Livak, K. J., & Schmittgen, T. D. (2001). Analysis of relative gene expression data using real-time quantitative PCR and the 2(-Delta Delta C(T)) Method. *Methods (San Diego, Calif.)*, *25*(4), 402–8. doi:10.1006/meth.2001.1262

Lofthouse, N., Hendren, R., Hurt, E., Arnold, L. E., & Butter, E. (2012). A review of complementary and alternative treatments for autism spectrum disorders. *Autism Research and Treatment*, *2012*. doi:10.1155/2012/870391

Lugo, J. N., Smith, G. D., Arbuckle, E. P., White, J., Holley, A. J., Floruta, C. M., … Okonkwo, O. (2014). Deletion of PTEN produces autism-like behavioral deficits and alterations in synaptic proteins. *Frontiers in Molecular Neuroscience*, *7*, 27. doi:10.3389/fnmol.2014.00027

Maestro, S., Casella, C., Milone, A., Muratori, F., & Palacio-Espasa, F. (1999). Study of the onset of autism through home movies. *Psychopathology*, *32*(6), 292–300. doi:29102

Marí-Bauset, S., Zazpe, I., Mari-Sanchis, A., Llopis-González, A., & Morales-Suárez-Varela, M. (2014). Evidence of the gluten-free and casein-free diet in autism spectrum disorders: A systematic review. *Journal of Child Neurology*. doi:10.1177/0883073814531330

Mars, A. E., Mauk, J. E., & Dowrick, P. W. (1998). Symptoms of pervasive developmental disorders as observed in prediagnostic home videos of infants and toddlers. *The Journal of Pediatrics*, *132*(3 Pt 1), 500–4. Retrieved from http://www.ncbi.nlm.nih.gov/pubmed/9544908

Massie, H. N. (1978). The early natural history of childhood psychosis. Ten cases studied by analysis of family home movies of the infancies of the children. *Journal of the American Academy of Child Psychiatry*, *17*(1), 29–45. Retrieved from http://www.ncbi.nlm.nih.gov/pubmed/632485

McFarlane, H. G., Kusek, G. K., Yang, M., Phoenix, J. L., Bolivar, V. J., & Crawley, J. N. (2008). Autism-like behavioral phenotypes in BTBR T+tf/J mice. *Genes, Brain, and Behavior*, *7*(2), 152–63. doi:10.1111/j.1601-183X.2007.00330.x

Meyza, K. Z., Defensor, E. B., Jensen, A. L., Corley, M. J., Pearson, B. L., Pobbe, R. L. H., … Blanchard, R. J. (2012). The BTBR T(+)tf/J mouse model for autism spectrum disorders-in search of biomarkers. *Behavioural Brain Research*, 1–10. doi:10.1016/j.bbr.2012.07.021

Minshew, N. J., & Williams, D. L. (2007). The new neurobiology of autism: Cortex, connectivity, and neuronal organization. *Archives of Neurology*, *64*(7), 945–50. doi:10.1001/archneur.64.7.945

Miyazaki, K., Narita, N., Sakuta, R., Miyahara, T., Naruse, H., Okado, N., & Narita, M. (2004). Serum neurotrophin concentrations in autism and mental retardation: A pilot study. *Brain & Development*, *26*(5), 292–5. doi:10.1016/S0387-7604(03)00168-2

Nagalakshmi, U., Waern, K., & Snyder, M. (2010). RNA-Seq: A method for comprehensive transcriptome analysis. *Current Protocols in Molecular Biology / Edited by Frederick M. Ausubel ... [et Al.]*, *Chapter 4*, Unit 4.11.1–13. doi:10.1002/0471142727.mb0411s89

Nakamura, K., Sekine, Y., Ouchi, Y., Tsujii, M., Yoshikawa, E., Futatsubashi, M., … Mori, N. (2010). Brain serotonin and dopamine transporter bindings in adults with high-functioning autism. *Archives of General Psychiatry*, *67*(1), 59–68. doi:10.1001/archgenpsychiatry.2009.137

Nelson, P. G., Kuddo, T., Song, E. Y., Dambrosia, J. M., Kohler, S., Satyanarayana, G., … Nelson, K. B. (2006). Selected neurotrophins, neuropeptides, and cytokines: developmental trajectory and concentrations in neonatal blood of children with autism or Down syndrome. *International Journal of Developmental Neuroscience : The Official Journal of the International Society for Developmental Neuroscience*, *24*(1), 73–80. doi:10.1016/j.ijdevneu.2005.10.003

Nibuya, M., Morinobu, S., & Duman, R. S. (1995). Regulation of BDNF and trkB mRNA in rat brain by chronic electroconvulsive seizure and antidepressant drug treatments. *The Journal of Neuroscience : The Official Journal of the Society for Neuroscience*, *15*(11), 7539–47. Retrieved from http://www.ncbi.nlm.nih.gov/pubmed/7472505

Noriuchi, M., Kikuchi, Y., Yoshiura, T., Kira, R., Shigeto, H., Hara, T., … Kamio, Y. (2010). Altered white matter fractional anisotropy and social impairment in children with autism spectrum disorder. *Brain Research*, *1362*, 141–9. doi:10.1016/j.brainres.2010.09.051

Oblak, A., Gibbs, T., & Blatt, G. (2009). Decreased GABAA receptors and benzodiazepine binding sites in the anterior cingulate cortex in autism. *Autism Research : Official Journal of the International Society for Autism Research*, *2*(4), 205–19. doi:10.1002/aur.88

Oblak, A., Gibbs, T., & Blatt, G. (2010). Decreased GABA(B) receptors in the cingulate cortex and fusiform gyrus in autism. *Journal of Neurochemistry*, *114*(5), 1414–23. doi:10.1111/j.1471-4159.2010.06858.x

Ordway, G., Szebeni, A., Duffourc, M. M., Dessus-Babus, S., & Szebeni, K. (2009). Gene expression analyses of neurons, astrocytes, and oligodendrocytes isolated by laser capture microdissection from human brain: Detrimental effects of laboratory humidity. *Journal of Neuroscience Research*, *87*(11), 2430–2438. doi:10.1002/jnr.22078.Gene

Osterling, J., & Dawson, G. (1994). Early recognition of children with autism: A study of first birthday home videotapes. *Journal of Autism and Developmental Disorders*, *24*(3), 247–57. Retrieved from http://www.ncbi.nlm.nih.gov/pubmed/8050980

Pardo, C. A., Vargas, D. L., & Zimmerman, A. W. (2005). Immunity, neuroglia and neuroinflammation in autism. *International Review of Psychiatry (Abingdon, England)*, *17*(6), 485–95. doi:10.1080/02646830500381930

Pekny, M., Wilhelmsson, U., & Pekna, M. (2014). The dual role of astrocyte activation and reactive gliosis. *Neuroscience Letters*. doi:10.1016/j.neulet.2013.12.071

Perry, E. K., Lee, M. L., Martin-Ruiz, C. M., Court, J. A., Volsen, S. G., Merrit, J., … Wenk, G. L. (2001). Cholinergic activity in autism: Abnormalities in the cerebral cortex and basal forebrain. *The American Journal of Psychiatry*, *158*(7), 1058–66. Retrieved from http://www.ncbi.nlm.nih.gov/pubmed/11431227

Pinto, D., Pagnamenta, A. T., Klei, L., Anney, R., Merico, D., Regan, R., … Betancur, C. (2010). Functional impact of global rare copy number variation in autism spectrum disorders. *Nature*, *466*(7304), 368–72. doi:10.1038/nature09146

Piras, I. S., Haapanen, L., Napolioni, V., Sacco, R., Van de Water, J., & Persico, A. M. (2014). Anti-brain antibodies are associated with more severe cognitive and behavioral profiles in Italian children with autism spectrum disorder. *Brain, Behavior, and Immunity*, *38*, 91–9. doi:10.1016/j.bbi.2013.12.020

Pizzarelli, R., & Cherubini, E. (2011). Alterations of GABAergic signaling in autism spectrum disorders. *Neural Plasticity*, *2011*, 297153. doi:10.1155/2011/297153

Poletaev, A. B., Poletaeva, A. A., Pukhalenko, A. I., Zamaleeva, R. S., Cherepanova, N. A., & Frizin, D. V. (2014). Adaptive maternal immune deviations as a ground for autism spectrum disorders development in children. *Folia Medica*, *56*(2), 73–80. Retrieved from http://www.ncbi.nlm.nih.gov/pubmed/25181843

Purcell, A. E., Jeon, O. H., Zimmerman, A. W., Blue, M. E., & Pevsner, J. (2001). Postmortem brain abnormalities of the glutamate neurotransmitter system in autism. *Neurology*, *57*(9), 1618–28. Retrieved from http://www.ncbi.nlm.nih.gov/pubmed/11706102

Radua, J., Via, E., Catani, M., & Mataix-Cols, D. (2010). Voxel-based meta-analysis of regional white-matter volume differences in autism spectrum disorder versus healthy controls. *Psychological Medicine*, 1–12. doi:10.1017/S0033291710002187

Rainey, L., & van der Walt, J. H. (1998). The anaesthetic management of autistic children. *Anaesthesia and Intensive Care*, *26*(6), 682–6. Retrieved from http://www.ncbi.nlm.nih.gov/pubmed/9876801

Robinson, S. J. (2012). Childhood epilepsy and autism spectrum disorders: Psychiatric problems, phenotypic expression, and anticonvulsants. *Neuropsychology Review*, *22*(3), 271–9. doi:10.1007/s11065-012-9212-3

Rohrer, B., Blanco, R., Marc, R. E., Lloyd, M. B., Bok, D., Schneeweis, D. M., & Reichardt, L. F. (2004). Functionally intact glutamate-mediated signaling in bipolar cells of the TRKB knockout mouse retina. *Visual Neuroscience*, *21*(5), 703–13. doi:10.1017/S095252380421505X

Ronald, A., & Hoekstra, R. A. (2011). Autism spectrum disorders and autistic traits: A decade of new twin studies. *American Journal of Medical Genetics. Part B, Neuropsychiatric Genetics : The Official Publication of the International Society of Psychiatric Genetics*, *156B*(3), 255–74. doi:10.1002/ajmg.b.31159

Rosenthal, J., Massie, H., & Wulff, K. (1980). A comparison of cognitive development in normal and psychotic children in the first two years of life from home movies. *Journal of Autism and Developmental Disorders*, *10*(4), 433–44. Retrieved from http://www.ncbi.nlm.nih.gov/pubmed/6927745

Santesso, D. L., Drmic, I. E., Jetha, M. K., Bryson, S. E., Goldberg, J. O., Hall, G. B., … Schmidt, L. A. (2010). An event-related source localization study of response

monitoring and social impairments in autism spectrum disorder. *Psychophysiology*. doi:10.1111/j.1469-8986.2010.01056.x

Sasaki, M., Nakagawa, E., Sugai, K., Shimizu, Y., Hattori, A., Nonoda, Y., & Sato, N. (2010). Brain perfusion SPECT and EEG findings in children with autism spectrum disorders and medically intractable epilepsy. *Brain & Development*, *32*(9), 776–82. doi:10.1016/j.braindev.2010.06.003

Savoy, M. (2014). Autism: 5 misconceptions that can complicate care. *The Journal of Family Practice*, *63*(6), 310–4. Retrieved from http://www.ncbi.nlm.nih.gov/pubmed/25061620

Scattoni, M. L., Martire, A., Cartocci, G., Ferrante, A., & Ricceri, L. (2013). Reduced social interaction, behavioural flexibility and BDNF signalling in the BTBR T+ tf/J strain, a mouse model of autism. *Behavioural Brain Research*, *251*, 35–40. doi:10.1016/j.bbr.2012.12.028

Simms, M. L., Kemper, T. L., Timbie, C. M., Bauman, M. L., & Blatt, G. J. (2009). The anterior cingulate cortex in autism: heterogeneity of qualitative and quantitative cytoarchitectonic features suggests possible subgroups. *Acta …*, *118*, 673–684. Retrieved from http://link.springer.com/article/10.1007/s00401-009-0568-2

Simonoff, E., Pickles, A., Charman, T., Chandler, S., Loucas, T., & Baird, G. (2008). Psychiatric disorders in children with autism spectrum disorders: Prevalence, comorbidity, and associated factors in a population-derived sample. *Journal of the*

American Academy of Child and Adolescent Psychiatry, *47*(8), 921–9. doi:10.1097/CHI.0b013e318179964f

Snijders, T. M., Milivojevic, B., & Kemner, C. (2013). Atypical excitation-inhibition balance in autism captured by the gamma response to contextual modulation. *NeuroImage. Clinical*, *3*, 65–72. doi:10.1016/j.nicl.2013.06.015

Sofroniew, M. V, & Vinters, H. V. (2010). Astrocytes: biology and pathology. *Acta Neuropathologica*, *119*(1), 7–35. doi:10.1007/s00401-009-0619-8

Sokhadze, E., Baruth, J., Tasman, A., Mansoor, M., Ramaswamy, R., Sears, L., … Casanova, M. F. (2010). Low-frequency repetitive transcranial magnetic stimulation (rTMS) affects event-related potential measures of novelty processing in autism. *Applied Psychophysiology and Biofeedback*, *35*(2), 147–61. doi:10.1007/s10484-009-9121-2

Stoner, R., Chow, M. L., Boyle, M. P., Sunkin, S. M., Mouton, P. R., Roy, S., … Courchesne, E. (2014). Patches of disorganization in the neocortex of children with autism. *The New England Journal of Medicine*, *370*(13), 1209–19. doi:10.1056/NEJMoa1307491

Suda, S., Iwata, K., Shimmura, C., Kameno, Y., Anitha, A., Thanseem, I., … Mori, N. (2011). Decreased expression of axon-guidance receptors in the anterior cingulate cortex in autism. *Molecular Autism*, *2*(1), 14. doi:10.1186/2040-2392-2-14

Sundaram, S. K., Kumar, A., Makki, M. I., Behen, M. E., Chugani, H. T., & Chugani, D. C. (2008). Diffusion tensor imaging of frontal lobe in autism spectrum disorder. *Cerebral Cortex (New York, N.Y. : 1991)*, *18*(11), 2659–65. doi:10.1093/cercor/bhn031

Tawfik, V. L., LaCroix-Fralish, M. L., Nutile-McMenemy, N., & DeLeo, J. A. (2005). Transcriptional and translational regulation of glial activation by morphine in a rodent model of neuropathic pain. *The Journal of Pharmacology and Experimental Therapeutics*, *313*(3), 1239–47. doi:10.1124/jpet.104.082420

Taylor, L. E., Swerdfeger, A. L., & Eslick, G. D. (2014). Vaccines are not associated with autism: An evidence-based meta-analysis of case-control and cohort studies. *Vaccine*, *32*(29), 3623–9. doi:10.1016/j.vaccine.2014.04.085

Tebartz van Elst, L., Maier, S., Fangmeier, T., Endres, D., Mueller, G. T., Nickel, K., … Perlov, E. (2014). Disturbed cingulate glutamate metabolism in adults with high-functioning autism spectrum disorder: Evidence in support of the excitatory/inhibitory imbalance hypothesis. *Molecular Psychiatry*. doi:10.1038/mp.2014.62

Thakkar, K. N., Polli, F. E., Joseph, R. M., Tuch, D. S., Hadjikhani, N., Barton, J. J. S., & Manoach, D. S. (2008). Response monitoring, repetitive behaviour and anterior cingulate abnormalities in autism spectrum disorders (ASD). *Brain : A Journal of Neurology*, *131*(Pt 9), 2464–78. doi:10.1093/brain/awn099

Thanseem, I., Nakamura, K., Miyachi, T., Toyota, T., Yamada, S., Tsujii, M., … Mori, N. (2010). Further evidence for the role of MET in autism susceptibility. *Neuroscience Research*, *68*(2), 137–41. doi:10.1016/j.neures.2010.06.014

Uutela, M., Lindholm, J., Rantamäki, T., Umemori, J., Hunter, K., Võikar, V., & Castrén, M. L. (2014). Distinctive behavioral and cellular responses to fluoxetine in the mouse model for Fragile X syndrome. *Frontiers in Cellular Neuroscience*, *8*, 150. doi:10.3389/fncel.2014.00150

Vargas, D. L., Nascimbene, C., Krishnan, C., Zimmerman, A. W., & Pardo, C. A. (2005). Neuroglial activation and neuroinflammation in the brain of patients with autism. *Annals of Neurology*, *57*(1), 67–81. doi:10.1002/ana.20315

Vlamings, P. H. J. M., Jonkman, L. M., Hoeksma, M. R., van Engeland, H., & Kemner, C. (2008). Reduced error monitoring in children with autism spectrum disorder: An ERP study. *The European Journal of Neuroscience*, *28*(2), 399–406. doi:10.1111/j.1460-9568.2008.06336.x

Wakefield, A. J., Murch, S. H., Anthony, A., Linnell, J., Casson, D. M., Malik, M., … Walker-Smith, J. A. (1998). Ileal-lymphoid-nodular hyperplasia, non-specific colitis, and pervasive developmental disorder in children. *Lancet*, *351*(9103), 637–41. Retrieved from http://www.ncbi.nlm.nih.gov/pubmed/9500320

Wang, Z., Gerstein, M., & Snyder, M. (2009). RNA-Seq: A revolutionary tool for transcriptomics. *Nature Reviews. Genetics*, *10*(1), 57–63. doi:10.1038/nrg2484

Wassink, T. H., Brzustowicz, L. M., Bartlett, C. W., & Szatmari, P. (2004). The search for autism disease genes. *Mental Retardation and Developmental Disabilities Research Reviews*, *10*(4), 272–83. doi:10.1002/mrdd.20041

Werner, E., Dawson, G., Osterling, J., & Dinno, N. (2000). Brief report: Recognition of autism spectrum disorder before one year of age: A retrospective study based on home videotapes. *Journal of Autism and Developmental Disorders*, *30*(2), 157–62. Retrieved from http://www.ncbi.nlm.nih.gov/pubmed/10832780

Whiteley, P., Shattock, P., Knivsberg, A.-M., Seim, A., Reichelt, K. L., Todd, L., … Hooper, M. (2012). Gluten- and casein-free dietary intervention for autism spectrum conditions. *Frontiers in Human Neuroscience*, *6*, 344. doi:10.3389/fnhum.2012.00344

Wilhelm, B. T., & Landry, J.-R. (2009). RNA-Seq-quantitative measurement of expression through massively parallel RNA-sequencing. *Methods (San Diego, Calif.)*, *48*(3), 249–57. doi:10.1016/j.ymeth.2009.03.016

Wink, L. K., Erickson, C. A., & McDougle, C. J. (2010). Pharmacologic treatment of behavioral symptoms associated with autism and other pervasive developmental disorders. *Current Treatment Options in Neurology*, *12*(6), 529–38. doi:10.1007/s11940-010-0091-8

Xiang, L., Szebeni, K., Szebeni, A., Klimek, V., Stockmeier, C. A., Karolewicz, B., … Ordway, G. A. (2008). Dopamine receptor gene expression in human amygdaloid

nuclei: elevated D4 receptor mRNA in major depression. *Brain Research*, *1207*, 214–24. doi:10.1016/j.brainres.2008.02.009

Zaccaria, K. J., Lagace, D. C., Eisch, A. J., & McCasland, J. S. (2010). Resistance to change and vulnerability to stress: Autistic-like features of GAP43-deficient mice. *Genes, Brain, and Behavior*, *9*(8), 985–96. doi:10.1111/j.1601-183X.2010.00638.x

Zakian, A., Malvy, J., Desombre, H., Roux, S., & Lenoir, P. (2000). [Early signs of autism and family films: A new study by informed evaluators and those unaware of the diagnosis]. *L'Encéphale*, *26*(2), 38–44. Retrieved from http://www.ncbi.nlm.nih.gov/pubmed/10858914

Zeidán-Chuliá, F., Salmina, A. B., Malinovskaya, N. A., Noda, M., Verkhratsky, A., & Moreira, J. C. F. (2014). The glial perspective of autism spectrum disorders. *Neuroscience and Biobehavioral Reviews*, *38*, 160–72. doi:10.1016/j.neubiorev.2013.11.008

Zerbo, O., Qian, Y., Yoshida, C., Grether, J. K., Van de Water, J., & Croen, L. A. (2013). Maternal infection during pregnancy and autism spectrum disorders. *Journal of Autism and Developmental Disorders*. doi:10.1007/s10803-013-2016-3

Zikopoulos, B., & Barbas, H. (2010). Changes in prefrontal axons may disrupt the network in autism. *The Journal of Neuroscience : The Official Journal of the Society for Neuroscience*, *30*(44), 14595–609. doi:10.1523/JNEUROSCI.2257-10.2010

Zikopoulos, B., & Barbas, H. (2013). Altered neural connectivity in excitatory and inhibitory cortical circuits in autism. *Frontiers in Human Neuroscience*, *7*, 609. doi:10.3389/fnhum.2013.00609

Zuker, M. (2003). Mfold web server for nucleic acid folding and hybridization prediction. *Nucleic Acids Research*, *31*(13), 3406–15. Retrieved from http://www.pubmedcentral.nih.gov/articlerender.fcgi?artid=169194&tool=pmcentrez&rendertype=abstract

Zwaigenbaum, L., Bryson, S., Rogers, T., Roberts, W., Brian, J., & Szatmari, P. (2005). Behavioral manifestations of autism in the first year of life. *International Journal of Developmental Neuroscience : The Official Journal of the International Society for Developmental Neuroscience*, *23*(2-3), 143–52. doi:10.1016/j.ijdevneu.2004.05.001

APPENDICES

APPENDIX A: Abbreviations and Definitions

Abbreviation	**Definition**
ABCB6	ATP-binding cassette sub-family B member 6
ACC	Anterior cingulate cortex
AD	Alzheimer Disease
ADI-R	Autism Diagnostic Interview Revised
ASD	Autism spectrum disorder
AUP1	Ancient ubiquitous protein
BA10	Brodmann area 10
BA24	Brodmann area 24
BDNF	Brain derived neurotrophic factor
CDC	Centers for Disease Control
CLIC4	Chloride intracellular channel 4
Ct	Cycle threshold
DEG	Differentially expressed genes
DSM-IV	Diagnostic and Statistical Manual of Mental Disorders IV
DSM-V	Diagnostic and Statistical Manual of Mental Disorders V
DTI	Diffusion tensor imaging
EEG	Electroencephalography
ERK	Extracellular signal-regulated kinases
FDA	Food and Drug Administration
GAPDH	Glyceraldehyde 3-phosphate dehydrogenase
GFAP	Glial fibrillary acidic protein
GM	Gray matter
GRIA1	Ionotropic glutamate receptor AMPA1
GRIK2	Ionotropic glutamate receptor kainate 2
GRIN1	NR1; Ionotropic glutamate receptor NMDA 1
GRIN2A	NR2A; Ionotropic glutamate receptor NMDA 2A
GRIN2B	NR2B; Ionotropic glutamate receptor NMDA 2B
GRIN2C	NR2C; Ionotropic glutamate receptor NMDA 2C
GRIN2D	NR2D; Ionotropic glutamate receptor NMDA 2D
GRIP1	Glutamate receptor interacting protein
GRM5	mGluR5; Metabotropic glutamate receptor 5
GRM8	mGluR8; Metabotropic glutamate receptor 8
HSD17B12	Hydroxysteriod 17-beta dehydrogenase 12

IR	Immunoreactivity
ISG15	Interferon, Alpha-Inducible Protein
KIAA0930	Uncharateristized protein C22orf9
KO	Knock out
LCM	Laser capture microdissection
MAPK	Mitogen-activated protein kinase
MCCC1	3-methylcrotonyl-CoA carboxylase
MMR	measles-mumps-rubella vaccine
MOG	Myelin oligodendrocyte glycoprotein
MTI	Magnetization transfer imaging
NICHD	National Institutes for Child Health and Development
NLGN	Neuroligin
NT-3	Neurotrophin-3
NT-4/5	Neurotrophin-4/5
NTRK2	Neurotrophic tyrosine kinase, receptor, type 2
PCR	Polymerase chain reaction
PDD-NOS	Pervasive developmental disorder-not otherwise specified
PET	Positron emission tomography
PI3	Phosphoinositide 3-kinase
PMI	Postmortem interval
PPP2CB	Protein phosphatase 2, catalytic subunit, beta isozyme
PTEN	Phosphatase and tensin homolog
Ribo18S	18S ribosomal RNA
RIN	RNA integrity number
RPKM	Reads Per Kilobase per Million mapped reads
RT-qPCR	Reverse transcription real-time polymerase chain reaction
SLC17A7	vGluT; vesicular glutamate transporter
SLC1A1	EAAT3; Neuronal/Epithelial High Affinity Glutamate Transporter, Member 1
SLC1A2	EAAT2; Glial High Affinity Glutamate Transporter, member 2
SLC1A3	EAAT1; Glial High Affinity Glutamate Transporter, member 3
SLC35A5	Sugar Transport Protein
SPECT	Single-photon emission computed tomography
SSR3	Signal sequence receptor, gamma
SSRI	Selective serotonin reuptake inhibitors
STX8	Syntaxin 8
TATA	TATA box

TBP	TATA binding protein
TMEM9	Transmembrane protein 9
TrkB	Tryosine kinase B
WM	White matter

APPENDIX B. Primer Sequences of Target and Reference Genes

Target or Reference	Genbank Accession Number	Primer Sequence	PCR Product Size (bp)
AQP4	NM_001650 NM_004028	(f) TCCAAACGGACTGATGTCACTGGCT (r) CAAAGGATCGGGCGGGATTCATGC	118
BDNF	NM_170735 NM_170732 NM_170731 NM_001709 NM_170733 NM_170734	(f) AGAGCCCTGTATCAACCCAGAAACACC (r) GCAATGCCAACTCCACATAGCCTCC	112
GAPDH	NM_002046	(f) TGCACCACCAACTGCTTAGC (r) GGCATGGACTGTGGTCATGAG	87
GFAP	NM_002055	(f) AAGCTGCTAGAGGGCGAGGAGAAC (r) TGACACAGACTTGGTGTCCAGGCT	99
GRIA1	NM_001200	(f) GTGCGCAGCTTCCACCATGAA (r) CTGAGGTGATAAACTCCTCCGTGGG	122
GRIK2	NM_000830 NM_175611	(f) ATTGACTCCAAAGGTTACGGAGTGGG (r) GCAGCTTCCCTTCTTCTTGGAGTTGA	100
GRIN1	NM_000832 NM_021569 NM_007327	(f) CCTGGAAGCAGAACGTCTCCCTGT (r) TGCTGCGCGAGTCACATTCCTGAT	108
GRIN2A	NM_001134407 NM_000833 NM_001134408	(f) TCGACCTGGCCTTGCTTCAGTTTGT (r) GCTGGCTGCTCATCACCTCGTTCTT	111
GRIN2B	NM_000834	(f) CCTCATCACCTTCATCTGCG (r) CATGGATGCAGCTGTAGATACC	125
GRIN2C	NM_000835	(f) TGGTGGCCATCACCGTCTTCAT (r) CCACACGGACTTGCCGATAGTGA	116
GRIN2D	NM_000836	(f) CTTCGTGGAGACCGGCATCAGCGTC (r) ACGAACATCATCACCCACACGGCGG	108

GRIP1	NM_021150 NM_001178074	(f) GCCACAGAAACTCTCTCTTCTCCACC (r) CACTCTGTCTCCAATCTGTAGCACCC	96
GRM5[a]	NM_000842	(f) GCCAGCAGATCCAGCAGCCTAGTCA (r) TCATTCTGGGCCCACGTGACGGATT	101
GRM5[b]	NM_000842 NM_001143831	Not available, purchased from Qiagen	125
GRM8	NM_000845 NM_001127323 NM_001127326 NR_028041	Not available-Purchased from Qiagen	78
MOG	NM_002433.3 NM_206809.2	(f) CCTGCTGGAAGATAACCCTGTTTG (r) CACTCAGAAGGGATTTCGTAGCTC	134
NTRK2	NM_006180 NM_001007097 NM_001018064 NM_001018065 NM_001018066	(f) TGTAGTGTGGCAGGTGATCCGGT (r) GGAGCCCTGTGTGTGGCTTGTTT	96
RNA18S1	NR_003286	(f) GTAACCCGTTGAACCCCATT (r) CCATCCAATCGGTAGTAGCG	131
SLC1A1[a]	NM_004170	Not available, purchased from Qiagen	110
SLC1A1[b]	NM_004170	(f) CCTGAAGTCAGTACGGTGGATGCC (r) GGGAGGCTTCACTTCTTCACGCTT	117
SLC1A3	NM_004172	(f) TGCAAGCACTCATCACCGCTCTGGG (r) ACGCGCTTGTCCACGCCATTGTTCT	100
SSR3	NM_007107	Not available, purchased from Qiagen	109
STX8	NM_004683 NR_033656	Not available, purchased from Qiagen	105
TATA	NM_003194	(f) CACTTCGTGCCCGAAACGCCGAAT (r) ATCAGTGCCGTGGTTCGTGGCTCT	88
UBC	NM_021009	(f) ATTTGGGTCGCGGTTCTTG (r) TGCCTTGACATTCTCGATGGT	133

VGlut1	NM_020309	(f) TCGGAGAGAGCGCGAAACTCAT (r) TGGCCACGATGATGGCATAGACT	99

[a] Denotes use in RT-PCR experiments
[b] Denotes use in Endpoint-PCR experiments

VITA

JESSICA D. CRAWFORD

Education:

B.S., Biology and Psychology, Averett University, Danville, Virginia 2008

Ph.D., Biomedical Sciences, East Tennessee State University, Johnson City, Tennessee 2014

Experience:

Graduate Assistant, Department of Biomedical Sciences, East Tennessee State University, 2009-2014

Student Researcher, Department of Psychology, Averett University, 2006-2008

Laboratory Assistant, Department of Biology, Averett University, 2004-2005

Publications:

Chandley MJ, Szebeni K, Szebeni A, **Crawford J,** Stockmeier C, Turecki G. Miguel Hidalgo J, Ordway GA. Gene Expression Deficits in Pontine Locus Coeruleus Astrocytes in Men with Major Depressive Disorder. *Journal of Psychiatry & Neuroscience.* Jul 2013; 38(4): 276–284

Szebeni A, Szebeni K, Diperi T, Chandley MJ, **Crawford JD**,

Stockmeier CA, Ordway GA. Shortened Telomere Length in White Matter Oligodendrocytes in Major Depression: Potential Role of Oxidative Stress. *International Journal of Neuropsychopharmacology.* Oct 2014; 17(10):1579-89

Chandley MJ, Szebeni A, Szebeni K, **Crawford JD**, Stockmeier C, Turecki G, Ordway GA. Elevated Gene Expression of Glutamate Receptors in Noradrenergic Neurons from the Locus Coeruleus in Major Depression. *International Journal of Neuropsychopharmacology.* Oct 2014; 17(10):1569-78

Crawford JD, Chandley MJ, Szebeni A, Szebeni K, Waters B, Ordway GA. Specific White Matter Pathology in the Anterior Cingulate Cortex from Males with Autism Spectrum Disorder. (In submission)

Chandley MJ, **Crawford JD**, Szebeni A, Szebeni K, Crawford J, Ordway GA. *NTRK2* Expression Deficit in Laser Captured Pyramidal Neurons from the Anterior Cingulate Cortex in Males with Autism Spectrum Disorder. (In preparation)